# DIOXYGEN AND PEROXIDE ACTIVATION BY AN UNNATURAL AMINO ACID INCORPORATED CYTOCHROME P450CAM AND P450 BM3

by

LETICIA LOREDO

Presented to the Faculty of the Graduate School of

The University of Texas at Arlington in Partial Fulfillment

of the Requirements

for the Degree of

DOCTOR OF PHILOSOPHY

THE UNIVERSITY OF TEXAS AT ARLINGTON

DECEMBER 2013

Acknowledgements

I would like to thank my research advisor Dr. Roshan Perera for providing me the opportunity to do research in his lab and for his guidance. I also would like to express my gratitude to Dr. Dias for allowing me to work in his lab.

Thanks to the members of my committee Dr. Kayunta Johnson-Winters and Prof. Frederick M. Macdonnell for their invaluable advice throughout these years.

I am indebt and thankful to Dr. Sridev Mohapatra for sharing his knowledge about molecular biology and for his kindly disposition to help, and to Dr. Sriparna Ray for her collaboration in the electorchemistry work, and for her valuable support in and out the lab

Thanks to my lab mates, especially to Sriparna, Subhash, Sriyani, and Sridev. It has been a great pleasure meeting you all.

I would like to thank the staff in the Chemistry Department; special thanks to the people who have provided instrumentation training.

Thanks to my friends who have been there for me always.

I want to dedicate this research to my parents for their love, their unconditional support, and their patience through all these years, and to my sisters, my brothers, and my grandma for their love and motivation.

November 25, 2013

Abstract

DIOXYGEN AND PEROXIDE ACTIVATION BY AN UNNATURAL AMINO ACID INCORPORATED CYTOCHROME P450CAM AND P450 BM3

Leticia Loredo, PhD

The University of Texas at Arlington, 2013

Supervising Professor: Roshan Perera

This study focuses on the process development for a nanobioreactor for the oxidation of aliphatic C-H bond by the dependent activation of molecular oxygen and hydrogen peroxide dependent catalysis of cytochrome P450cam and P450 BM3 and their genetically encoded 3-$NH_2$ tyrosine mutant enzymes.

Oxidation of aliphatic carbons is an enormous challenge in classical synthesis due to their inert nature. However, it is significant in the production of fine chemicals and commodity products, which are precursors for the production of other valuable compounds.

Among these reactions is the conversion of cyclohexane to cyclohexanol which is an intermediate in the production of nylon 6,6, a compound in high demand worldwide. Current industrial methods to carry out these reactions are energy intensive and suffer from low selectivity. In this context, industrial cyclohexanol production uses heavy metals like cobalt and manganese, requires pressures around 12 bar, and temperatures over 140 °C resulting in quite low yields (4-10%). These processes are inefficient and produce high amounts of toxic waste. Thus, there is clearly a need for a more efficient and greener technology. The direct biooxidation of hydrocarbons would change drastically the current chemical catalysis due to a number of advantages, such as the direct use of

hydrocarbons for the synthesis of valuable intermediates, the reduction of the steps required to reach the final product, hence reduction of waste generation, etc. However, several major challenges exist in biocatalytic processes. Among them, denaturation of catalyst, difficulty in attaching the catalyst on the surface, low solubility of the substrate in water, etc. Cytochrome P450s (CYP) are heme metalloenzymes capable of selectively activating aliphatic C-H bonds and oxidizing them by inserting an oxygen atom under very mild conditions. Among these P450s is P450cam, a water soluble protein that enables the selective and efficient conversion of cyclohexane to cyclohexanol, utilizing $H_2O_2$ as the oxidant at ambient temperatures producing water as the only by-product. Therefore, the use of CYP proteins to carry out hydrocarbon oxidation reactions is promising in this field. Therefore, chapters 2 and 3 discuss the cloning and expression of P450cam as well as P450 BM3 proteins. Furthermore, attempts to prepare solid phase bioreactors for catalysis have faced enormous challenges due to the non-availability of a good protein immobilization technique where denaturation of the protein during the immobilization process is common. In this investigation, we have developed a method for nanoparticle-bound cytochrome P450. It involves covalent attachment of the protein to the support via a benzoxazine ring formation through a Diels–Alder reaction in water and a genetically encoded 3-$NH_2$Tyr amino acid through site directed mutagenesis as discussed in chapter 3, 4, and 5. The method produces a homogeneous monolayer with retention of the protein conformation, and the site of the mutation dictates the orientation. Consequently, the mutation was strategically introduced in a specific site to control protein orientation. The immobilized protein was found to retain its inherent activity. As a result, fully functional protein microarrays, with monolayer arrangements and complete control over their orientations, were generated using this strategy. Iron oxide magnetic nanoparticles and silica nanoparticles have been synthesized and functionalized for site-

oriented protein attachment. Other supports such as glass, polypropylene and gold electrodes have been successfully used for that purpose. In this research we also investigated the random immobilization of WT P450cam via EDC bioconjugation for its use in cyclohexane oxidation.

In chapter 6, we have successfully used P450cam bound nano-particles as a recyclable catalyst for the oxidation of cyclohexane to cyclohexanol with 30% conversion in the presence of hydrogen peroxide at room temperature. Our by-product was water, and hence it is a greener process. This also provides a strategy for cost effective production of valuable chemicals on a larger scale. Furthermore, the genetically encoded 3-$NH_2$Tyr amino acid has not only served as an anchor point for the protein to control its orientation, but it has also incorporated redox properties to the protein that may play an important role during electron transfer processes. It is noteworthy that in the case of the mutated Q343(3-$NH_2$Tyr) P450cam protein, it has shown a four fold increase in the activity over the WT for camphor oxidation. The 3-$NH_2$Tyr moiety may facilitate the electron transfer from the putidaredoxin to the P450cam protein as it is probably in the electron transfer pathway of these proteins. Similar immobilization techniques have been used to immobilize P450 BM3, to produce a promising protein microarray for the field of bioreactors for alcohol generation as well as P450 assay platform for drugs during drug discovery process.

Table of Contents

List of Illustrations

List of Tables

Chapter 1

# Introduction to Hydrocarbon Oxidation Chemistry

## 1.1 Introduction

### *1.1.1 Hydrocarbon Oxidation*

The activation (i.e. oxidation) of $sp^3$ hybridized C-H bonds is very challenging due to their inert character. Hence, it has represented a challenge for the utilization of less reactive, saturated and cheap products such as petroleum, for the synthesis of more reactive or more synthetically useful compounds.[1,2] The activation of hydrocarbons via oxidation leads to the production of more valuable compounds, such as alcohols, epoxides, ketones, aldehydes etc. The difficulties associated with this type of activation lie on the great stability of these C-H bonds and in the selectivity to activate a desired C-H bond as hydrocarbons have many saturated C-H bonds, with bond dissociation energy (BDE) of about 97 kcal/mol for cyclohexane.[3]

The work on saturated hydrocarbon activation has been recently focused in the use of transition metal complexes to achieve this goal.[2,4] However, these methods usually results in poor selectivity when C-H bonds with similar energy can react equally producing a mixture of products, or the selectivity is mainly directed to the weakest C-H bond.[4]

The other challenge is the inherent higher reactivity of the product compared to the reagent molecule. The activated molecule can react further and more easily than the inactivated form, the parent molecule, resulting in a mixture of by products. This lowers the yield significantly in these processes.

Hence, methods employed to directly hydroxylate aliphatic or aromatic compounds is still poor in terms of stereoselectivity and yield.[5] Nevertheless, it is certain that an effective direct activation of inactivated C-H bonds would have a tremendous impact in organic synthesis. The activation of hydrocarbons is a potential for the exploitation of these compounds and their functionalization will provide starting materials for the synthesis of more complex and fine molecules.[6] It will mean reduction of multistep processes, and protection-deprotection requirements.

One of the most important reactions of hydrocarbon activations is the oxidation of cyclohexane to cyclohexanol. This is because cyclohexanol has been used in the production of highly demanded

and valuable compounds such as nylon-6,6. This product is formed from the reaction between adipic acid and hexamethylene diamine and its synthesis has been attributed to Wallace, H Carothers in 1935. DuPont has commercialized it since then. Therefore, one of the most important industrial processes regarding C-H activation involves the oxidation of cyclohexane to cyclohexanol (and cyclohexanone) (Figure 1-1), which is the central process for the production of nylon 6,6 (worldwide production of which exceeds 5100 million tons/year) and other important industrial materials. Industrial processes for cyclohexanol production include the catalytic oxidation of cyclohexane with manganese or cobalt salts. The drawbacks of this method include harsh conditions with median temperature and pressure requirements of 140°C and 12 bar respectively, but results in low yield with about 10% conversion to prevent overoxidation.[7]

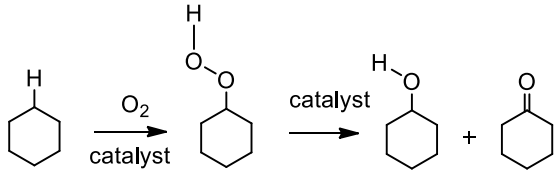


Figure 1-1 Common industrial routes to cyclohexanol

Phenol is another important commodity chemical used in the manufacture of polycarbonates, various resins, aspirin, and adipic acid. It has an annual worldwide demand of over 9 million tons. There are a variety of important chemicals obtained via simple C-H oxidation of inert hydrocarbons (e.g., *n*-paraffins to alcohols, toluene to benzoic acid).[7] Most of these processes, like the cyclohexanol and phenol manufacturing chemistry, require harsh conditions and require high-energy consumption. Furthermore, these reactions generate large amounts of hazardous waste.

It is of high importance to find new alternatives that provide greener processes for these oxidation reactions. Nature provides a viable solution to this challenging task. There are some natural enzymes (P450cam and horseradish peroxidase), which can be designed to carry out stereoselective activation of hydrocarbons under mild conditions and are superior to synthetic

catalysts, due to the higher selectivity and no byproducts. However, these enzymes may face another set of troubles in industrial usage that require further development. Most of the enzymes are sensitive to organic solvents, and possible denaturation may result in the presence of a large volume of organic substrate.

*1.1.2 Enzymes*

Metabolic processes are coupled with life sciences, as these processes provide the energy sources, supply building blocks, and can generate the required substances for the organism to maintain life. Enzymes are fundamentally important for the metabolic processes to take place, endowing them the reputation of highly efficient and selective catalysts. After all, they are the ones involved in catalyzing a variety of biochemical reactions that otherwise will not take place at ambient temperature, rendering life impossible. Enzymes accelerate the rate of chemical reactions by lowering the activation energy. This is due to the fact that the protein is capable of stabilizing the transition state. In this way, enzymes bind the substrate, catalyze the reaction on them, and release the product without being consumed in the process. Once the substrate binds, the protein induces a different configuration to fit the substrate in the active site, a process known as induced fit, which help in making the substrate more labile for reaction.[8,9] All proteins are synthesized from 20 L-amino acids, and it is the order in which these amino acids are arranged in the primary structure the responsible for the unique tridimensional shape of each protein giving an “infinite” number of different possibilities and particular properties to each of them. At the same time, the chiral nature of the protein renders it highly specific and able to discriminate among enantiomers and diastereomers. They are chemoselective as they can discriminate between non-equivalent similar functional groups and also regioselective. Stereospecificity is provided by the interactions of the residues in the active site with the substrate, positioning it in such a way that the reaction takes place at a particular site even when there may be similar groups in the substrate, which may facilitate an equal reaction opportunity during catalysis. Therefore, nature

protein scaffold provides the best platform for the catalysis and can carry out a plethora of reactions with high efficiency and specificity.

1.1.2.1 Cytochrome P450s

CYP enzymes catalyze a broad range of reactions that do not have an equivalent in synthetic catalyst reactions. As mentioned earlier, hydrocarbon oxidation of aliphatic compounds falls within this category, where cytochrome P450 proteins have the proper mechanism to carry out these types of reactions.

CYP P450s belong to a family of heme thiolate proteins prominent in all kingdoms of life. The name was derived from their electronic absorption at 450 nm when bound to carbon monoxide in the ferrous state of iron. They have protoheme IX as prosthetic group with the iron ligated to a cysteinate sulfur of the protein. These metalloenzymes activate molecular oxygen and insert one of the oxygen atoms between the C-H bond of the hydrocarbon, whereas the other oxygen is reduced to water (Rxn 1).

$$R_3C\text{-}H + O_2 + 2H^+ + 2e^- \rightarrow R_3C\text{-}OH + H_2O \quad \text{(Rxn I)}$$

CYP proteins have been categorized into three different classes. Class I P450s work in a three-component system where an FAD containing reductase accepts two electrons from NAD(P)H and transfers them to ferredoxin one at a time, In a similar way the ferredoxin transfers the electrons to the cytochrome. In this class fall most bacterial P450s and the eukaryotic mitochondrial P450s. Class II P450s constitute a two-component system with electron transfer from NADPH by a FAD and FMN containing reductase to the cytochrome. This category includes eukaryotic microsomal P450s. Class III P450 enzymes include P450 BM3. The system contains a FAD and FMN containing reductase domain and the cytochrome center, which are fused in a single polypeptide.[10] Class II CYPs catalyze a great variety of reactions. In humans, they catalyze the oxidation of steroids, prostaglandins, drugs, and other xenobiotics, especially in the liver. These have also been implicated in the activation of precarcinogens.

P450cam from *Pseudomonas putida* is one of the most studied P450s. The studies on this protein has allowed for a better understanding of the structure and function of other P450s. The isolation and study of microsomal P450 proteins has found difficulties due to the fact that these are membrane bound proteins. However, bacterial P450s are soluble and can be overexpressed. These characteristics have made it possible to study bacterial P450s, to characterize them, and use them as models for P450s in general.[11] Consequently, bacterial P450s have been the best choice among researchers.

*1.1.3 Biocatalysis*

Nature has created enzymes not only to lower the energy of activation for reactions to take place but also to make an efficient use of the resources available in vivo environment minimizing or eliminating waste production. It provides the best examples of catalysts that carry out a plethora of reactions in a highly effective way. For similar reasons, it is desirable to use catalysts in synthesis, especially in the production of fine chemicals where otherwise the synthesis is generally carried out with stoichiometric amounts of reactants generating large quantities of toxic waste. Therefore, catalysts can be used for fine chemical synthesis if reusability, stability, and conversion efficiency can be introduced in the production process. Certainly, biocatalysts provide the cost effective synthesis due to the ability to overexpress them in *E. coli* cells.

Enzyme denaturation is one aspect that may limit its application in industrial scale. Furthermore isolation of a pure enzyme is sometimes laborious and the yield is generally reduced in multiple purification steps. Cofactor requirements add up to the limited use of enzymes in industry. These cofactors are expensive, and although in some instances they have been made catalytic by use of regenerating systems like other enzymes or replaced with electrodes in the case of oxidoreductases. Efficiency can be introduced to these systems by the proper design of a reactor system. Another factor that has to be taken into consideration is the instability of the proteins outside the cell as they are no longer in their natural environment and are sensitive to

factors in the new environment that can alter their shape and conformation, as well as activity thereby their activities. Nevertheless, immobilization of cheap, overexpressing bacterial proteins on solid support can eliminate some of these drawbacks.

### *1.1.4 Nanobioreactor*

Biocatalysis has the potential to fulfill these requirements if enzymes can be recovered after the reaction has taken place, if it remains active, and if cost of production is not compromised, in other words, if it can achieve repeatability.

Enzymes show stereospecificity and selectivity due to their 3D chiral scaffold conformation, where the substrate may have various interactions with different residues in the active site of the protein at a given time. These interactions position the substrate in a specific way where the catalytic reaction takes place at a particular site on the substrate. This may be a very important reason behind the failures of enzyme mimics, because these different interactions are lost.

#### 1.1.4.1 Enzyme Immobilization

There are important aspects to be taken into consideration for development of functional enzyme arrays on solid supports. There must be a permanent linkage (covalent) between the protein and the substrate to avoid leaching of the enzyme from the solid support. Additionally, the attachment of the protein to the solid support should be uniform (monolayer) to prevent coagulation of unbound proteins and possible obstruction of the active site. The orientation of the immobilized protein is essential so that the active site is available for the substrate. Equally important is the retention of the native conformation so that the protein is stable and activity being preserved after immobilization on the surface.[2] However, this is a challenging task, but if the requirements are met, the result will provide a fully active, stable and recyclable catalyst bound to the surface of a nanoparticle, or other surface.

Immobilized enzymes are defined as 'enzymes physically confined or localized in a certain defined region of space with retention of their catalytic activities, and which can be used repeatedly and continuously.[12] Different techniques have been used to immobilize proteins on supports. These encompass physical and chemical methods.[13]

1.1.4.1.1 Adsorption

Proteins generally get adsorbed when they are in contact with a solid surface.[14] Hence, physical adsorption takes place when the protein is incubated with the adsorbent under appropriate conditions due to interactions between the protein and the surface of the support including H-bonding and mainly hydrophobic[15, 16] and electrostatic effects[15] which are maximized when the support and the protein contain opposite charges or when the ionic strength is low. An increase in entropy is the main driving force in protein adsorption [17-19]

The extent of protein adsorption depends on the identity of the protein as well as that of the substrate where the nature of the interactions of one kind of protein with the support will differ for those that another type of protein can have as well as pH, ionic strength, temperature, concentration. [15] Time is a crucial factor to maximize the contact of the proteins with the support and allow for adsorption. [13]

One of the drawbacks of this method is the weak attachment of the protein to the support, which causes leaching of the protein from the surface and results in very low loads of protein. Changes in the environment of the adsorbed protein may cause its desorption from the support. Conformational changes have been observed in the protein upon adsorption.[20-22] These changes can be less pronounced in stable proteins classified as hard and they adsorb only if electrostatic forces are present, or more pronounced in proteins with lower stability classified as soft .[23,24] Some of these disadvantages can be addressed with covalent binding of the protein to the support.

1.1.4.1.2 Covalent Binding

The process comprises the chemical reaction of the functional groups on the surface of the protein provided by the side chain of the amino acids with an appropriate functional group on the surface of the support to form covalent linkage.

Reactive amino side chains include $NH_2$ in lysine and arginine, the SH group of cysteine, the COOH of aspartic and glutamic acids, and the OH groups in serine and threonine, and these can react with different functionalities on the surface of a support like carboxylic acid, maleimide, amine, and epoxy respectively among other functional groups[25] This type of immobilization provides a permanent bonding between protein and support . Protein load is high with very low leakage.

Disadvantages include equal or similar reactivity of residues on the surface of the protein providing different orientations, and reduced activity due to possible interaction with residues involved in the activity of the protein. However, the orientation problem can be alleviated by covalent immobilization with site-specifically incorporated active groups. [26-28]

1.1.4.1.3 Cross-linking

Cross-linking involves the generation of a polymer with a protein unit and the linking agent, which is a bi or multifunctional molecule. Factors like heat, and alkaline conditions promote crosslinking. [29] The process can be mediated by a variety of enzymes [30] or chemically done with a diversity of crosslinking agents [31] among which glutaraldehyde is widely used in crosslinking processes.[32]

Drawbacks of this method include the modification that a protein may suffer in terms of structure and function.[33] The product is not homogeneous as it may consists of different products. For example, both ends of the crosslinking unit may not react as one of the ends may be hydrolyzed stopping the polymerization, the crosslinking unit may bind the protein in two of its residues or it may bind two peptides.[34] Furthermore, the cross linking unit can react with different residues other than the intended ones, making it a random process.

1.1.4.1.4 Entrapment

Entrapment involves the confinement of the protein inside the support. Disadvantages include denaturation of the protein during entrapment and leakage of the protein if the conditions promote an increase in the pore of the support. Mass transfer is another problem.

In protein immobilization, the support plays a main role. The importance regarding the nature of the support lies in its biocompatibility as the proteins have to be immobilized on it. Therefore, it is crucial that the support does not have any detrimental effect on the protein. Equally important, is the stability and inertness of the support under the reaction conditions used namely solvent, pH, temperature, pressure, etc. Furthermore, the quality of the support to be recovered and to remain intact after the reaction is necessary for recyclability. Glass beads can be isolated from the medium by decanting or filtering the reaction mixture or by removing the beads from it. In the same way, polypropylene can be removed from the reaction mixture. This quality is important as it nullifies the contamination of the reaction with the catalyst making it easier for the purification process.

Silica and iron oxide magnetic nanoparticles (NPs) are chemically stable for the conditions used. They are biocompatible, and can be easily isolated from the reaction at the end of the reaction, either by centrifugation or filtration in the case of silica nanoparticles (Si-NPs) and by magnetization with a magnet in the case of the magnetic particles (MNPs).

Even though the substrate range of the P450cam and P450 BM3 proteins may not be as broad as desired, bioengineering of these proteins offers the possibilities to prepare them to fulfill certain characteristics required during immobilization. Furthermore, the stability of the proteins in organic solvents, at a different temperature and pH to those of the natural conditions of the native protein, can be improved by genetically modifying them.

Proper Immobilization of these proteins on solid supports can lead to bioreactors for industrial applications. However, this process requires an innovative approach and its development is the focus of this study. The method consists in the covalent attachment of water

soluble monooxygenase P450cam protein to a solid support via a hetero Diels-Alder reaction between a 3-$NH_2$Tyr unnatural amino acid incorporated protein (which can be converted into an *o*-imino-quinone) and an acryloyl group present on the support. The amino acid is incorporated via site directed mutagenesis at position Q343 in cytochrome P450cam.[3] The hetero Diels-Alder bioconjugation reaction takes place in the presence of sodium periodate as an oxidant.[4] Fully active and covalently immobilized enzymes with unprecedented control over their orientation can be attained by developing this method.

### *1.1.5 Thesis Aims*

Therefore, The focus of this thesis pursues the development of new methods for the proper immobilization of proteins for preparation of bioreactors. It involves the generation and functionalization of silica and magnetic iron NPs for site-specific immobilization of proteins via covalent linkages. The work described herein aims to develop silica and magnetic iron NP-bound CYP P450cam arrays using a hetero Diels-Alder bioconjugation reaction in water and to investigate the ability of protein arrays to perform hydrocarbon oxidation minimizing waste and providing a greener alternative to current classical chemistry oxidation methods. Another aim of this study is the expansion of these concepts to CYP P450 BM3 to generate a microarray to serve as a new drug discovery tool and its future implementation in the production of drug metabolites.

Chapter 2

# Cloning and Expressing Cytochrome P40cam and P450 BM3 from *Pseudomonas Putida* and *Bacillus Megaterium*

All the experiments in this chapter were done by Leticia Loredo in the laboratory of Dr. Roshan Perera.

## 2.1 Introduction

P450cam is a 45 kDa water-soluble heme dependent monooxygenase from *Pseudomonas putida*. It catalyzes the stereospecific oxidation of camphor to 5-exohydroxycamphor by the incorporation of an oxygen atom from molecular oxygen to the unreactive C-H bond, as a carbon source for *Pseudomonas putida*. [35] To carry out its catalytic activity, the protein requires a two one-electron reduction at different stages of the catalytic cycle. The electrons are provided by NADH via redox partners, a 43.5 kDa flavoprotein FAD reductase, putida redoxin reductase (PdR), and a 12 kDa iron-sulfide redox Putidaredoxin (Pdx) that transfer the electrons from the reductase to the cytochrome. [36-38] These proteins form the methylene camphor oxidase system of *Pseudomonas putida*. Isolation of each gene for protein expression has been advantageous for the purification of each enzyme. In this chapter, the isolation of each gene, *camC* coding for P450cam, *camA* coding for PdR, and *camB* coding for Pdx, from *Pseudomonas putida* and further recombination into pBAD and transformation into *Escherichia coli* (*E.coli*) host system is described. Another bacterial cytochrome P450 used in this study is cytochrome P450 BM3, a 118 kDa holoenzyme isolated from *Bacillus megaterium* involved in long chain fatty acid oxidation. It consists of a catalytic heme containing domain and a FADH FMN reductase domain. In this study, the P450 BM3 protein has been isolated from *Bacillus megaterium* and has been recombined and transformed for protein expression.

## 2.2 Experimental Section

### *2.2.1 Chemicals*

Chemicals used were of analytical grade or higher quality, and were used as received unless stated otherwise. Lysogeny broth (LB) contained 10 g tryptone, 5 g yeast extract, and 10 g sodium chloride per liter. The broth was sterilized by autoclaving and the corresponding antibiotic was added just before using it. Agarose was obtained from Fisher Scientific. LB agar (Fisher Scientific) contained 10 g tryptone10 g, 5 g yeast extract, 10 g sodium chloride, and agar 15 g per liter. The agar was sterilized by autoclaving, and before solidifying the corresponding antibiotic

was added and poured in a petri dish. 2x Yeast extract and Tryptone broth (2XYT Broth, Fisher Scient) contained 16 g tryptone, 10 g yeast extract, 5 g sodium chloride, and the corresponding antibiotic. Primers were obtained from Sigma Aldrich.

*2.2.2. Cloning of camC Gene*

2.2.2.1. *CamC* Gene Isolation

Bacterial colonies of *Pseudomonas putida* containing plasmid pUS200 were grown for 15 h in an agar plate supplemented with ampicillin at 37 °C. A pre-culture was prepared by inoculating with a bacterial colony 10 mL of LB supplemented with ampicillin. The pre-culture cells were harvested at 5000 rpm for 3 minutes. The plasmid was isolated with QIAprep Spin Miniprep Kit (QIAGEN) according to manufacturer's procedure. 1% (w/v) agarose gel electrophoresis was used to analyze the DNA extract.

2.2.2.2 Agarose Gel Electrophoresis

Agarose was dissolved in 1X TAE buffer by heating the mixture. The resulting solution was cooled down to about 50 °C and 3 µL of ethidium bromide solution were added. The mixture was poured into a cast gel and allowed to solidify. For the sample preparation, the DNA sample was mixed with blue juice gel loading buffer. 1Kb DNA ladder (Promega) was used for DNA size estimation. Electrophoresis was carried at 125 V for 45 minutes. The DNA bands were visualized in a UV transilluminator.

2.2.2.3 *CamC* Gene Amplification

The *camC* gene was amplified by polymerase chain reaction (PCR). The following primers were used to introduce *Kpn*I and *Nco*I restriction sites as well as a C-terminal hexahistidine tag into the gene, forward 5'-ATACGCTCACCATGGGGATGACGACTGAA ACCATACAAAGCAACG-3', and reverse 5'-CCAGTTGGTACCTCAATGGTGATGGTGATGATGTACCGCTTTGGTAGTCGCCGGAT-3'. PCR

samples were prepared using Phusion High-Fidelity PCR kit (New England Bio Labs) following the conditions in Table 2.1 PCR was carried out in an MJ Mini thermal cycler (Bio-Rad) using the PCR program in Table 2.2. The PCR product was purified using MinElute PCR purification kit (QIAGEN) following manufacturer's instructions.

Table 2.1 Conditions for PCR gene amplification sample preparation

| Component | Amount |
|---|---|
| 5x Phusion HF | 5 (1X) |
| 10 mM dNTPs | 1 µL (200 µM each) |
| 10 µM Forward primer | 1 µL (0.2 µM) |
| 10 µM Reverse primer | 1 µL (0.2 µM) |
| Template DNA | 1 µL (250 ng) |
| Phusion DNA polymerase | 0.5 µL (1 unit) |
| Ultra pure nuclease-free water | to 50 µL final volume |

Table 2.2 PCR program conditions for gene amplification

| Step | Temperature (°C) | Time (min) |
|---|---|---|
| 1 Initial denaturation | 95 | 3 |
| 2 Denaturation | 95 | 0.5 |
| 3 Annealing | 55 | 0.5 |
| 4 Extension | 72 | 2 |
| 5 Number of cycles | Go to step 2 29 cycles | |
| 6 Final extension | 72 | 5 |
| 7 End | 4 | Forever |

2.2.2.4 *CamC* Gene Digestion

The purified PCR product of the *camC* gene was digested with *Nco*I and *Kpn*I restriction enzymes (New England Bio Labs) following the conditions mentioned in Table 2.3 by incubating at 37 °C for 2 h. The digested product was purified as mentioned above using the MinElute PCR purification kit (QIAGEN) following manufacturer's instructions. 1% (w/v) agarose gel electrophoresis was used to analyze the DNA extract.

Table 2.3 Conditions for digestion of *camC* gene and pBAD

| Component | Amount |
|---|---|
| 10X NEB I | 5 µL (1X) |
| BSA | 0.5 µL |
| Template DNA | 1 µg |
| *Nco*I | 1 µL |
| *Kpn*I | 1 µL |
| Ultra pure nuclease free water | to 50 µL final volume |

2.2.2.5 Vector Preparation: pBAD Restricted Digestion

A pre-culture of bacterial cells containing pBAD plasmid with ampicillin resistance marker in LB supplemented with ampicillin was grown overnight at 37 °C. The pre-culture cells were harvested at 5000 rpm for 3 minutes. The plasmid was isolated with QIAprep Spin Miniprep Kit (QIAGEN) according to manufacturer's procedure. The plasmid was digested with *Nco*I and *Kpn*I restriction enzymes (New England Bio Labs) following the conditions in Table 2.3 with incubation at 37 °C for 2 h. Gel electrophoresis was carried out in a 0.6% agarose gel as previously discussed in order to isolate the pBAD vector. The correct band of the gel was cut and the DNA was extracted using MinElute Gel Extraction Kit (QIAGEN).

2.2.2.6 Recombinant Plasmid

Ligation of the digested and purified gene and the pBAD vector was done by T4 DNA ligase using a 1:3 ratio of vector to insert in 10X ligase buffer. The ligation mixture was incubated for 1 h at room temperature. The ligated mixture was subjected to PCR purification prior to transformation into *E. coli* DH10B cells.

2.2.2.7 Transformation of the Recombinant Plasmid

The recombinant plasmid was transformed into electrocompetent *E. coli* DH10B expression host. 3 µL of the recombinant plasmid were added to a 50 µL aliquot of the electrocompetent *E. coli* DH10B cells which was previously thawed on ice. The mixture was transferred to a pre-chilled MicroPulser electroporation cuvette (Bio-Rad). Electroporation of the sample was carried out in a MicroPulser electroporator (Bio-Rad). The cells were recovered in 300 µL of freshly prepared S.O.C. medium with shaking for 1 h at 37 °C. Transformed cells were plated in LB agar medium supplemented with ampicillin. After 12 h incubation at 37 °C, bacterial colonies were screened by PCR following the conditions for sample preparation given in Table 2.4 using pBAD primers. With the exception of the template, all other reagents were added into a PCR tube and mixed thoroughly on ice. This mixture was inoculated with sample from the bacterial colony to be screened, mixed thoroughly and incubated for 1 min. PCR was run using the conditions in Table 2.2 with annealing temperature modified to 39 °C and extension time to 2.5 minutes. 1% (w/v) agarose gel electrophoresis was used to analyze the PCR product as described previously. Desired colonies were used to inoculate pre-cultures for plasmid isolation.

Table 2.4 Conditions for colony PCR sample preparation

| Component | Amount |
|---|---|
| 5x Taq buffer | 5 (1X) |
| 10 mM dNTPs | 1 µL (200 µM each) |
| 10 µM Forward primer | 1 µL (0.2 µM) |
| 10 µM Reverse primer | 1 µL (0.2 µM) |
| Template DNA | n/a |
| Taq polymerase | 0.5 µL |
| Ultra pure nuclease free water | to 50 µL final volume |

Table 2.5 SOB and SOC medium protocol

| **SOB** | Amount |
|---|---|
| Tryptone | 20 g |
| Yeast extract | 5.0 g |
| MgSO4 | 2.4 g |
| NaCl | 0.5 g |
| KCl | 0.186 g |
| Milli-Q water sterilized | 1L |
| **SOC** | Amount |
| Glucose | 3.6 g |
| Sterilized SOB | 1L |

2.2.2.8. *E. coli* DH10B Electrocompetent Cells Propagation

Electrocompetent cells were propagated by inoculating LB broth either with a stock or a single colony of electrocompetent *E. coli* DH10B (Invitrogen). The culture was incubated at 37 °C until $OD_{600}$ reached ~0.5 but not higher. The culture was cooled down on ice and transferred to pre-chilled centrifuge tubes. Cells were harvested by centrifugation at 5000 rpm for 10 min. at 4 °C in a Beckman centrifuge. The supernatant was decanted and the cells were resuspended in sterilized ice-cold water. Cell resuspension with ice cold water was repeated one more time, followed by two successive resuspension processes with ice-cold sterilized 10% glycerol in water (v/v). Every resuspension was followed by centrifugation with the conditions mentioned above. Finally the cells were resuspended with a small amount of ice-cold sterilized 10% glycerol to make 50 µL aliquots in pre-chilled sterilized microcentrifuge tubes on dry ice. These aliquots were stored at -80 °C until further use.

*2.2.3 Clonning of CamA Gene: Isolation of CamA Gene (His-tagged)*

The *camA* gene was isolated from live *Pseudomonas putida* using genomic DNA. The following primers were used to introduce *Kpn*I and *Nco*I restriction sites as well as a C-terminal hexahistidine tag into the gene by polymerase chain reaction (PCR), forward 5'-GACCTGACTATGCGACGGTAATTCCCCATCACCTA3' and reverse 5'-GCACTAGGTACCTCAATGGTGATGGTGATGATGGGCACTACTCAGTTCAGCTTTGGCG-3'. Digestion of the genomic DNA with *Kpn*I and *Nco*I resulted in the isolation of the *camA* gene. The fragment was inserted into a pBAD vector, which carries the ampicillin resistant marker, by T4 DNA ligase. The recombinant plasmid was used to transform *E. coli* DH10B electrocompetent cells, which were recovered in S.O.C. for 1 h. Transformed cells were plated in agar medium supplemented with ampicillin. After 15 h incubation at 37 °C, a colony was selected and grown in LB broth. The generated pBAD-P450cam plasmid was isolated and analyzed.

*2.2.4 CamA Gene Non-His-tagged*

The *camA* gene was isolated from live *Pseudomonas putida* using genomic DNA. The following primers were used to introduce *Kpn*I and *Nco*I restriction sites into the gene by polymerase chain reaction (PCR), forward 5'-GACCTGACTATGCGACGGTAATTCCCCATCACCTA-3' and reverse 5'-GCACTTGGTACCTTCAGGCACTACTCAGTTCAGCTTTGGCG-3'. Digestion of the genomic DNA with *Kpn*I and *Nco*I resulted in the isolation of the *camA* gene. The fragment was inserted into a pBAD vector, which carries the ampicillin resistant marker, by T4 DNA ligase. The recombinant plasmid was used to transform *E. coli* DH10B electrocompetent cells, which were recovered in S.O.C. for 1 h. Transformed cells were plated in agar medium supplemented with ampicillin. After 15 h incubation at 37 °C, a colony was selected and grown in LB-broth.

*2.2.5 Cloning of CamB Gene: Isolation of CamB Gene (His-tagged)*

The *camB* gene was isolated from live *Pseudomonas putida* using genomic DNA. The following primers were used to introduce *Kpn*I and *Nco*I restriction sites as well as a C-terminal hexahistidine tag into the gene by polymerase chain reaction (PCR), forward 5'-ATACGCTCACCATGGGGATGTCTAAAGTAGTGTATGTGTCACATGAT-3' and reverse 5'-CAGAGTAGGTACCTTAATGGTGATGGTGATGATGCCATTGCCTATCGGGAACATCGAC-3'. Digestion of the genomic DNA with *Kpn*I and *Nco*I resulted in the isolation of the *camB* gene. The fragment was inserted into a pBAD vector, which carries the ampicillin resistant marker, by T4 DNA ligase. The recombinant plasmid was used to transform *E. coli* DH10B electrocompetent cells, which were recovered in S.O.C. for 1 h. Transformed cells were plated in agar medium supplemented with ampicillin. After 15 h incubation at 37 °C, a colony was selected and grown in LB broth. The generated pBAD-P450cam plasmid was isolated and analyzed.

*2.2.6 CamB Gene Non-His-tagged*

The *camB* gene was isolated from live *Pseudomonas putida* using genomic DNA. The following primers were used to introduce *Kpn*I and *Nco*I restriction sites into the gene by polymerase chain reaction (PCR), forward 5'-ATACGCTCACCATGGGGATGTCTAAAGTAGTGTATGTGTCACATGAT-3' and reverse 5'-CAGAGTTGGTACCTTCACCATTGCCTATCGGGAACATCGAC-3'. Digestion of the genomic DNA with *Kpn*I and *Nco*I resulted in the isolation of the *camB* gene. The fragment was inserted into a pBAD vector, which carries the ampicillin resistant marker, by T4 DNA ligase. The recombinant plasmid was used to transform *E. coli* DH10B electrocompetent cells, which were recovered in S.O.C. for 1 h. Transformed cells were plated in agar medium supplemented with ampicillin. After 15 h incubation at 37 °C, a colony was selected and grown in LB broth.

*2.2.7 Cloning of CYP102A1 Gene: Isolation of the CYP102A1 Gene*

A pre-culture was prepared by inoculating with *Bacillus megaterium cells* (American Type Culture Collection [ATCC] cat. No. 14581) 10 mL of LB supplemented with ampicillin. The pre-culture cells were harvested at 5000rpm for 3 minutes. The plasmid was isolated with QIAprep Spin Miniprep Kit (QIAGEN) according to manufacturer's procedure. 1% (w/v) agarose gel electrophoresis was used to analyze the DNA extract.

2.2.7.1 *CYP102A1* Gene Amplification

The *CYP102A1* gene was amplified by polymerase chain reaction (PCR). The following primers were used to introduce *Kpn*I and *Nco*I restriction sites as well as a C-terminal hexahistidine tag into the gene, forward 5' AATCACACCATGGGGACAATTAAAG AAATGCCTCAGCCAAAAAC-3', and reverse 5'-CCTATGGGTACCTCAGTGATGGTGATGGTGATGCCCAGCCCACACGTCTTTTGC-3'. PCR samples were prepared using Phusion High-Fidelity PCR kit (New England Bio Labs) following the conditions in Table 2.1 PCR was carried out in an MJ Mini thermal cycler (Bio-Rad)

using the PCR program in Table 2.2. with the exception of the elongation time, which was increased to 4 min. The PCR product was purified using MinElute PCR purification kit (QIAGEN) following manufacturer's instructions.

*2.2.7.2 CYP102A1* Gene Digestion

The purified PCR product of the *CYP102A1* gene was digested with *Nco*I and *Kpn*I restriction enzymes (New England Bio Labs) following the conditions mentioned in Table 2.3 by incubating at 37 °C for 2 h. The digested product was purified as mentioned above using the MinElute PCR purification kit (QIAGEN) following manufacturer's instructions.

Recombinant Plasmid pBAD-*CYP102A1*

2.2.7.3 *CYP102A1* Gene Ligation

Ligation of the digested and purified gene and the pBAD vector was done by T4 DNA ligase using a 1:3 ratio of vector to insert in 10X ligase buffer. The ligation mixture was incubated for 1 h at room temperature. The ligated mixture was subjected to PCR purification prior to transformation into *E. coli* DH10B cells.

2.2.7.4 Transformation of the Recombinant Plasmid pBAD-*CYP102A1*

Transformation of the pBAD-*CYP102A1* plasmid was done following the same process as for pBAD-*camC* recombinant plasmid.

## 2.3 Results and Discussion

The project started with the isolation of the genes from *Pseudomonas putida*. Figure 2-1 shows the method followed for the isolation and recombinant cloning of the *camC* gene. This was achieved by genomic DNA isolation from *Pseudomonas putida* (Figure 2-2 A) followed by PCR amplification with primers containing *Kpn*I and *Nco*I restriction sites as well as a hexahistidine tag

at the carboxyl terminal to simplify the protein purification process. The DNA was successfully digested with *Kpn*I and *Nco*I restriction enzymes as can be seen in Figure 2-2 B, which clearly shows a DNA band with the expected size. The digested DNA was inserted by T4 DNA ligase into a pBAD vector containing *Kpn*I and *Nco*I sticky ends, which have been produced by digestion of the pBAD plasmid with the respective restriction enzymes.

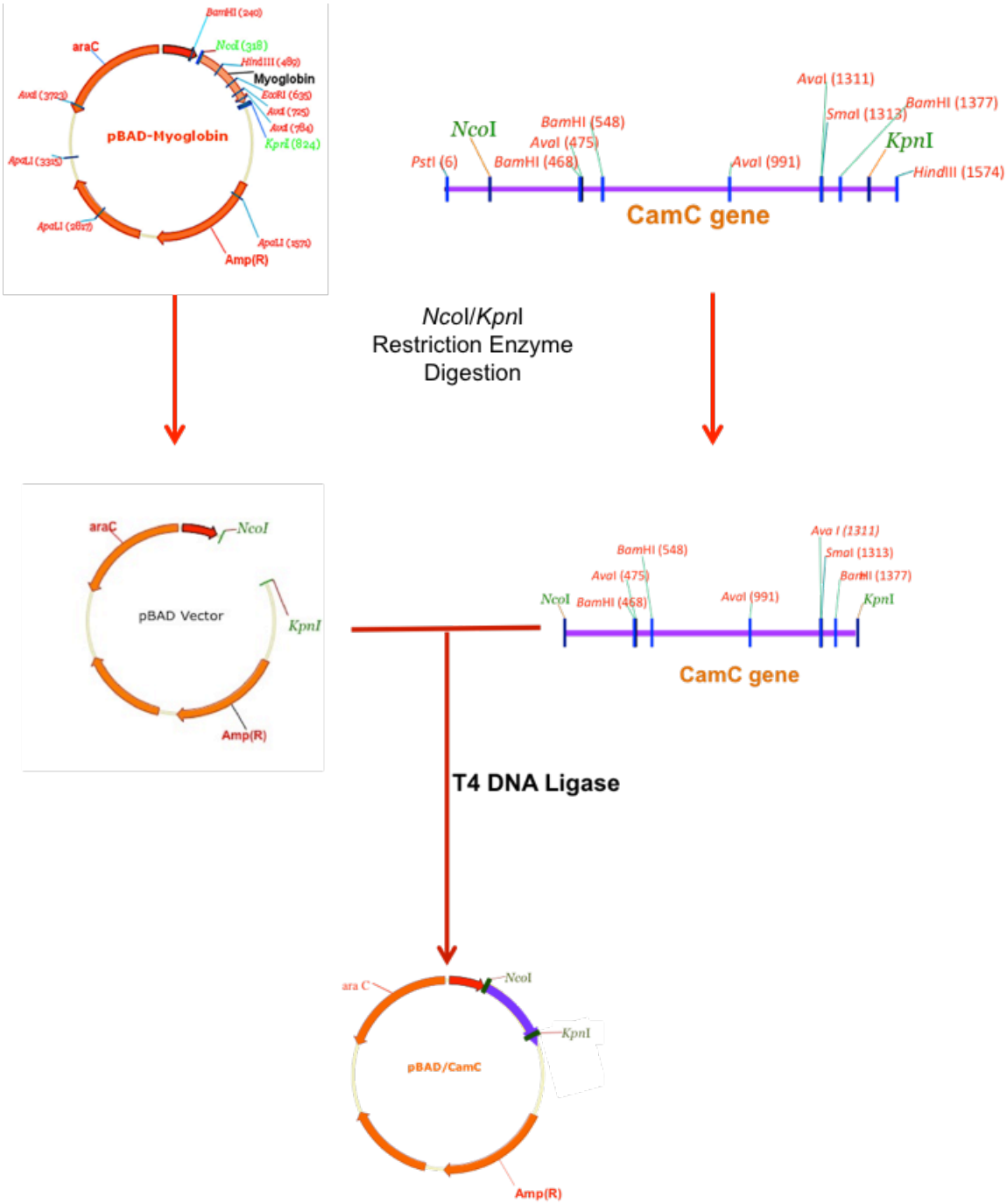


Figure 2-1 Method used to generate DNA recombinant plasmid containing the *camC* gene. Depiction of the plasmid carrying the vector and the isolated *camC* gene.

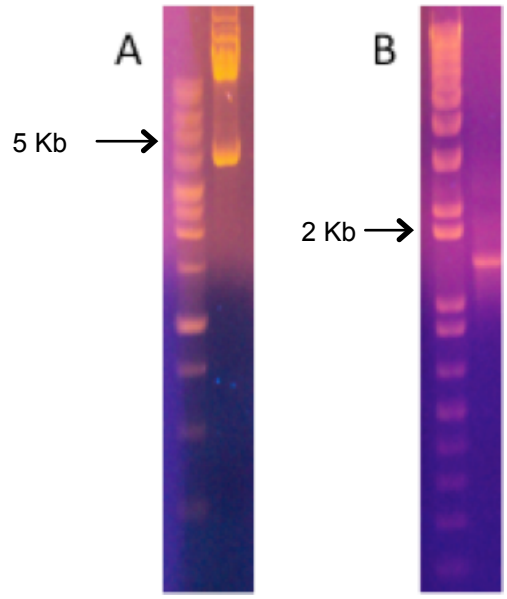


Figure 2-2 Agarose DNA gel analysis of *camC* gene. (**A**) DNA isolated from *Pseudomona putida*. (***B***) *Nco*I and *Kpn*I digested *camC* gene.

Transformation was done into *E. coli* DH10B expression host by electroporation. The cells were recovered in S.O.C media and subjected to selection in ampicillin containing LB agar plates. Bacterial clones containing the camC gene grew. This process is depicted in Figure 2-3.

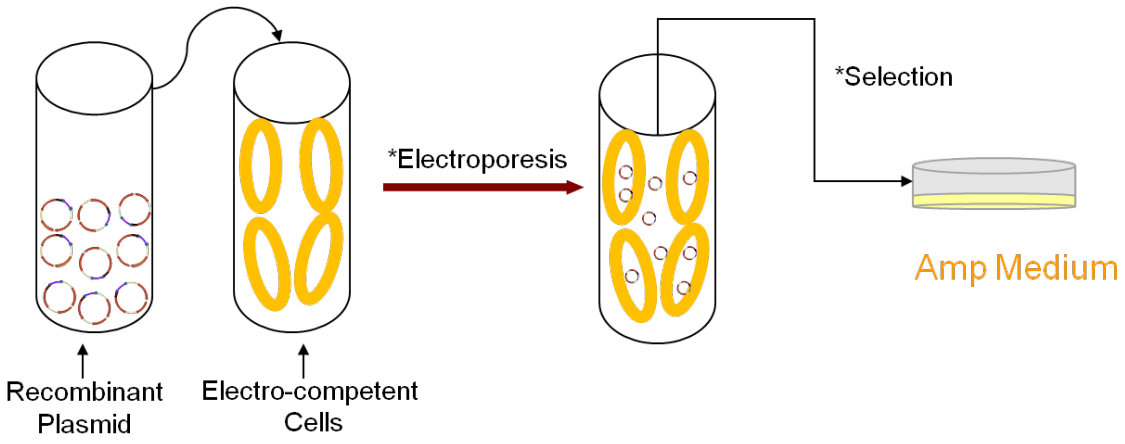


Figure 2-3 Transformation of recombinant plasmid carrying the *camC* gene.

Colonies were screened for plasmids carrying the *camC* gene, and analyzed in 1% (w/v) agarose gel electrophoresis. Figure 2-4 shows a DNA band in the agarose gel with the correct size for the recombinant plasmid carrying the *camC* gene.

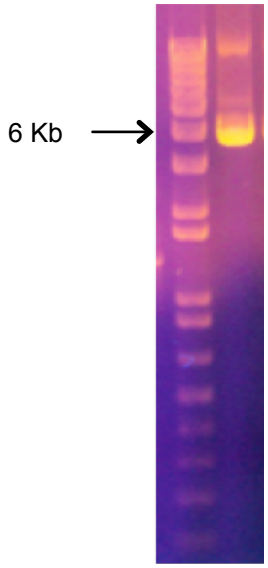


Figure 2-4 Agarose DNA gel analysis of recombinant plasmid carrying the *camC* gene coding for P450cam.

*CamA* gene and *camB* gene were initially isolated from *Pseudomonas putida* by using primers containing *Nco*I and *Kpn*I restriction sites as well as a hexahistidine tag. Each gene was inserted into pBAD vector and transformed into E-coli electrocompetent cells in the same way as for P450cam. Pdx and PdR containing the hexahistidine tag appeared to have reduced activity in subsequent experiments. A possible reason could have been the hexahistidine tags causing some negative interactions in the reconstituted system of P450cam during catalysis. Therefore, *camA* and *camB* genes were isolated from *Pseudomonas putida* with primers lacking the hexahistidine tag. Figure 2-5 shows the DNA gel analysis of the digested PdR and Pdx genes, leaving *Nco*I and *Kpn*I digested ends to be ligated to the digested *Nco*I and *Kpn*I ends of the pBAD vector.

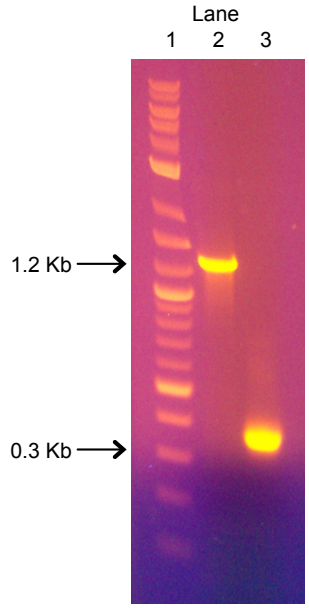


Figure 2-5 Agarose DNA gel. Line 1: ladder; lane 2: digested *camA* gene; line 3, digested *camB* gene.

After ligation and transformation of the recombinant plasmids, colonies were screened. Figure 2-6 shows the recombinant non-His tag pBAD-*camB* plasmid from a screened colony.

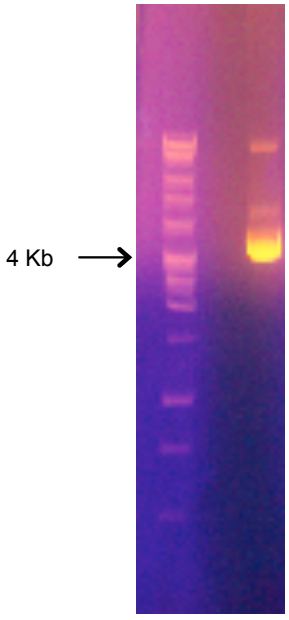


Figure 2-6 Recombinant non-His tag pBAD-*camB* DNA plasmid

*CYP102A1* was isolated from *Bacillus megaterium* in a similar way to the isolation of *CamC* gene. The isolated DNA was subjected to PCR amplification for the incorporation of *Kpn*I and *Nco*I restriction sites as well as a hexahistidine tag. Upon restriction enzyme digestion of the gene, a recombinant plasmid was obtained by ligation to the digested pBAD vector. The recombinant plasmid was transformed into *E.coli* electrocompetent cells and screened for the recombinant plasmid carrying the *CYP102A1* gene.

## 2.4 Conclusion

In this chapter, the isolation of the genes *camC*, *camA*, *camB*, and *CYP102A1* from their natural source has been successfully achieved and recombined into pBAD vector. The recombinant plasmids were transformed in heterologous *E.coli* host cells. This will allow for over expression of proteins and constitutes a reliable expression host system for prokaryotic proteins. Furthermore, the isolation of each gene, *camC*, *camA*, *camB*, and the future protein expression as described in the next chapter may simplify the purification process to obtain proteins in pure form without coenzyme contamination.

# Chapter 3

## Unnatural Amino Acid Incorporated

## Cytochrome P450cam and P450 BM3

All the experiments in this chapter were done by Leticia Loredo in the laboratory of Dr. Roshan Perera.

## 3.1 Introduction

The machinery of protein synthesis in the cell consists of a ribosome where translation of the messenger RNA (mRNA) takes place, transfer RNAs (tRNA) that transport amino acids to the ribosome where they are paired to the complementary codon in mRNA, and the aminoacyl-tRNA synthetase (aaRS) that recognizes the anticodon in the tRNA and charges it with the correct amino acid. Proteins are synthesized using the 20 natural amino acids, and during synthesis of the polypeptide, the codons UAG (amber), UAA (ochre) and UGA (opal), are used to signal the termination of the synthesis. The amber codon (UAG) has been conveniently and efficiently used to incorporate unnatural amino acids into proteins by using an orthogonal tRNATyr /TyrRS pairs from *Methanococcus jannaschii (Mj)* .[39-42] This has allowed the diversification of the genetic code and the system has been improved to perform the introduction of unnatural amino acids into proteins in vivo. [39,43] Other researchers have designed codons as quadruplet with engineering tRNAs with quadruplet anticodons for introduction of unnatural amino acids.[44,45]

The arrangement of the amino acids in the backbone of the protein polypeptide provides unique conformational structure to the protein, thereby rendering its unique properties. The ability to incorporate new amino acids with a particular functionality in vivo during the natural mechanism of protein synthesis is a powerful biotechnical tool.[45] This biotechnology allows substitution of an amino acid by another at a particular position. In the present study, the biotechnological tool of genetically encoding the unnatural amino acid has been used to genetically introduce the unnatural amino acid 3-$NH_2$Tyr via site-directed mutagenesis at the position Q343 in CYP 450cam and T366 P450 BM3. Incorporation of 3-$NH_2$Tyr into CYP 450cam and P450 BM3 provides a new functionality to the proteins in an assigned position that can be used for future applications. The idea is to take advantage of the reactivity of this group and use it to anchor the protein covalently and to control its orientation onto a support as will be described in chapter 5.

The focus of this chapter is the genetic incorporation of the unnatural amino acid (3-$NH_2$Tyr) by site-directed mutagenesis at the position Q343 in CYP 450cam and T366 P450 BM3, as well as the expression and purification of these metalloenzymes. The genetic incorporation of the 3-$NH_2$Tyr amino acid into proteins can be achieved using the tyrosyl-tRNA synthetase (*mj*TyrRS derived from *Methanococcus jannaschii* ) and *mj*tRNA$^{Tyr}_{CUA}$ pair which is selectively evolved to recognize the 3-$NH_2$Tyr substrate in *E. coli* expression strains.[45,46] The incorporation of the unnatural amino acid takes place during protein synthesis therefore using the natural machinery for protein synthesis inside the cell. By employing this method, fully functional proteins with a unique reactivity acquired with the incorporated unnatural amino acid could be site-specifically bound to supports as will be described in chapter 5.

## 3.2 Experimental Section

### *3.2.1 Chemicals*

Lysogeny broth (LB) contained 10 g tryptone, 5 g yeast extract, 10 g sodium chloride per liter. The broth was sterilized by autoclaving and the corresponding antibiotic was added just before using it. Agar plates (LB agar contained 10 g casein, 5 g yeast extract, 10 g sodium chloride, and 12 g agar per liter. The LB agar was sterilized by autoclaving, and before solidifying the corresponding antibiotic was added and poured into a petri dish.) M9 Media contained $MgSO_4$ (1 mmol), $CaCl_2$ ( 0.1 mmol), NaCl (86 mmol), M9 salts (200 mL of 5X) biotin (1 mL of stock (5 mg/ mL in 50% ethanol)), glycerol (1%) thiamine (5 mg ), trace metals (1 mL of stock ), per liter, and the corresponding antibiotics. Agarose, M9 Minimal Salts 5x, Biotin, Imidazole, and Ribonuclease A bovine pancreas were ordered from Fisher Scientific; Thiamine Hydrochloride, Calcium chloride, anhydrous powder, Magnesium chloride, Calcium chloride L-Leucine were purchased from Acros Organics, Novex, tris-Acetate SDS running Buffer 20X was from Invitrogen; Deoxyribonuclease I, Lysozyme, and (1R)-(+)-Camphor were from Sigma Chemical Company; Ethidium Bromide Potassium Phosphate, Dibasic, Potassium Phosphate Monobasic, and Magnesium Sulfate were from JT Baker; L-(+)-Arabinose was from Alfa Aesar; Nickel

nitrilotriacetic acid resin Ni-NTA was obtained from Qiagen. Trace metals stock contained $MoNa_2SO_4$ (500 mg ), $CoCl_2$ (250 mg), $CuSO_4.5H_20$ (175 mg), $MnSO_4.H_2O$ (1 g), $MgSO_4.7H_2O$ (8.75 g), $ZnSO_4.7H_2O$ (1.25 g), $FeCl_2.4H_2O$ (1.25 g), $CaCl_2.2H_2O$ (2.5 g), $H_3BO_3$ (1 g), 1 M HCl, Per liter

*3.2.2 Instrumentation*

UV–Vis spectroscopic measurements were conducted on a Cary 50 Bio UV-visible spectrophotometer.

*3.2.3 Preparation of Q343(3-$NH_2$Tyr) P450cam*

The *camC* gene was mutated at the Q343 position with the amber (TAG) codon by PCR mutagenesis using Phusion Site-Directed Mutagenesis Kit (NEB) using the following primers: forward 5'-TCGACTTCAGTCGCTAGAAGGTTTCACACA-3' and reverse 5'-CGTGCATCGGGCAGGCGTTTT-3' to generate pBAD-p450cam (Q343TAG). Conditions used are given in Table 3.1 and Table 3.2 for sample preparation and PCR program respectively. The product was circularized using the Quick Ligation Kit (NEB) where the DNA sample was incubated with Quick T4 DNA ligase in 2X Quick ligation buffer at room temperature for 5 minutes then, it was chilled on ice for 15 minutes. The ligated mixture was subjected to a PCR purification prior to transformation into *E. coli* DH10B electrocompetent cells and selection following the procedure described above. Gene mutation was confirmed by DNA sequencing.

Table 3.1 PCR conditions for mutation sample preparation

| Component | Amount |
|---|---|
| 5x HF buffer | 10 (1X) |
| 10 mM dNTPs | 1 μL (200 μM each) |
| 10 μM Forward primer | 2.5 μL (0.5 μM) |
| 10 μM Reverse primer | 2.5 μL (0.5 μM) |
| Template DNA | 2 ng |
| DNA polymerase | 0.5 μL |
| Nuclease free water | up to 50 μL |

Table 3.2 PCR program conditions for mutation

| Step | Temperature (°C) | Time (min) |
|---|---|---|
| 1 Initial denaturation | 98 | 3 |
| 2 Denaturation | 98 | 0.5 |
| 3 Annealing | 55 | 0.5 |
| 4 Extension | 72 | 7 |
| 5 Number of cycles | Go to step 2 29 cycles | |
| 6 Final extension | 72 | 20 |
| 7 End | 4 | Forever |

Electrocompetent *E. coli* DH10B cells were co-transformed with the Q343(3-$NH_2$Tyr) mutant P450cam gene plasmid and PAC-3-$NH_2$TyrRS-6tRNA synthetase plasmid carrying the genes encoding for transfer RNA mjtRNA tyr CUA, and tyrosyl-tRNA synthetase, with tetracycline resistance marker, following the procedure described above. Transformed cells were plated in agar medium supplemented with ampicillin and tetracycline and incubated at 37 °C. Colonies were selected and used to prepare pre-culture and cell stocks.

*3.2.4 Preparation of T365(3-$NH_2$Tyr) P450 BM3*

The *CYP102A1* gene was mutated at position T365 with the amber (TAG) codon by PCR mutagenesis using Phusion site-directed mutagenesis kit (NEB) the (TAG) mutation was introduced into the WT gene sequence in the T365(TAG) position using the following primers: forward 5'-TTCACCGTGATAAATAGATTTGGGGAGAC-3', and reverse 5'-GCTGAGGAATCAGAAC CATTAGTTCGTC-3' The conditions for sample preparation are given in Table 3.1. The conditions for PCR follow those in Table 3.2 with the exception of the elongation time, which was increased to 11 min. The product was circularized using the Quick Ligation Kit (NEB) where the DNA sample was incubated with Quick T4 DNA ligase in 2X Quick ligation buffer at room temperature for 5 minutes. Then, it was chilled on ice for 15 minutes. The ligated mixture was subjected to a PCR purification prior to transformation into *E. coli* DH10B electrocompetent cells and selection following the procedure described above. Gene mutation was confirmed by DNA sequencing. Samples were prepared following the protocol, preparation for DNA sequencing, described above.

*3.2.5 Expression of WT Cytochrome P450cam*

A pre-culture grown from a colony containing the pBAD-*camC* plasmid was used to inoculate LB broth supplemented with ampicillin and D-(+)-camphor. The culture was incubated at 37 °C with shaking to achieve an optical density ($OD_{600}$) of 0.5, at which protein expression was

induced with 0.2% arabinose. Incubation temperature was decreased to 30 °C, and the culture was incubated for 12 h. Cells were harvested by centrifugation.

*3.2.6 Expression of P450cam Redox Coenzymes*

His-tagged and non-His tagged putidaredoxin reductase and putidaredoxin were expressed following the same method.

3.2.6.1 Putidaredoxin Reductase Expression

Putidaredoxin Reductase : A pre-culture with PdR expressing *E. coli* freeze stock in 2xYT (2x Yeast extract and Tryptone) broth was grown to an $OD_{600}$ of 0.6. 1 L of 2xYT was inoculated with 10 mL pre-culture and incubated at 37 °C at 120 rpm until $OD_{600}$ reached 0.5. At this point, protein expression was induced by adding 0.2% arabinose. Incubation temperature was decreased to 30 °C, and the culture was incubated for 12 h.

3.2.6.2 Putidaredoxin Expression

Pd was expressed in 2xYT following the same protocol as for PdR.

*3.2.7 Expression of Q343(3-$NH_2$Tyr) P450cam*

A pre-culture inoculated with a selected bacterial colony containing the TAG mutated *camC* gene recombinant plasmid and the *Mj* PAC-3-$NH_2$Tyr RS-6tRNA synthetase plasmid was used to grow a culture in glycerol minimal medium (GMML medium) supplemented with ampicillin, tetracycline, and d-camphor. The culture was incubated at 37 °C with shaking until $OD_{600}$ reached 0.5. At this point, 3-$NH_2$Tyr (1 mM) was added to the culture followed by protein expression induction with 0.2% arabinose. Incubation temperature was decreased to 30 °C, and the culture was incubated for 12 h.

*3.2.8 Expression of WT P450 BM3*

A pre-culture grown from a colony containing the pBAD-*CYP102A1* plasmid was used to inoculate LB broth supplemented with ampicillin. The culture was incubated at 37 °C with shaking to achieve an optical density ($OD_{600}$) of 0.5, at which protein expression was induced with 0.2% arabinose. Incubation temperature was decreased to 30 °C, and the culture was incubated for 12 h. Cells were harvested by centrifugation.

*3.2.9 Expression of T365(3-$NH_2$Tyr) P450 BM3*

A pre-culture inoculated with a selected bacterial colony containing the TAG mutated *CYP102A1* gene recombinant plasmid and the PAC-3-$NH_2$Tyr RS-6tRNA synthetase plasmid was used to grow a culture in glycerol minimal medium (GMML medium) supplemented with ampicillin and tetracycline. The culture was incubated at 37 °C with shaking until $OD_{600}$ reached 0.5. At this point, 3-$NH_2$Tyr (1 mM) was added to the culture followed by protein expression induction with 0.2% arabinose. Incubation temperature was decreased to 30 °C, and the culture was incubated for 12 h.

*3.2.10 Purification WT Cytochrome P450cam*

The WT cytochrome P450cam protein was purified both as a substrate bound protein (for which case the buffers used during the purification process contained 500 μM) or as camphor free protein, where the D-(+)-camphor was omitted in the buffers used for purification and storage; otherwise, the buffers have the same composition and the purification process was carried out in the same way. The cells were lysed in lysis buffer (50 mM Tris and 100 mM NaCl, pH 8.0) with 150 μL of lysozyme (100 mg/mL), 50 μL of DNase I (5 mg/mL), and 50 μL of RNase A (100 mg/mL) under stirring conditions for 30 min at room temperature followed by three freeze (liq. $N_2$) - thaw (37 °C) cycles, and sonication on ice (3 x 1-minute intervals). Cell debris was removed by centrifugation at 5000 rpm for 40 min and the His-tagged protein was purified using nickel nitrilo-triacetic acid Ni-NTA resin (QIAGEN). The resin bound protein was subjected to a

column, and protein was eluted with imidazole containing buffer (300 mM NaCl, 250 mM imidazole, 50 mM phosphate buffer, pH 8.0). Analysis was done using sodium dodecyl sulfate-polyacrylamide gel electrophoresis (SDS-PAGE) in a precast gel (Novex Tris-Glycine). The purified protein was dialyzed to remove imidazole, flash frozen, and stored at -80 °C in potassium phosphate buffer (100 mM, 500 μM D-(+)-camphor, pH 7.4) until further use. The amount of expressed P450cam was determined by UV-Vis with $\varepsilon_{417}$ = 115 $mM^{-1}\cdot cm^{-1}$ for camphor free protein or $\varepsilon_{391}$ = 102 $mM^{-1}\cdot cm^{-1}$ for camphor bound protein.[47]

*3.2.11 Cam Redox Coenzymes Purification*

His-tagged and non-His tagged putidaredoxin reductase and putidaredoxin were purified following the same method.

3.2.11.1 Putidaredoxin Reductase Purification

Cells were harvested at 8000 rpm for 15 min. The cell paste was dissolved in 50 mM phosphate buffer (KPi) pH 7.0 containing 1mM EDTA, 150 μL of Lysozyme (100 mg/mL), 50 μL of DNase I (5 mg/mL), and 50 μL of RNase A (100 mg/mL) under stirring conditions for 30 min at room temperature followed by three freeze (liq. $N_2$) - thaw (37 °C) cycles, and sonication on ice (3 x 1-minute intervals). Cell debris was removed by centrifugation at 5000 rpm for 40 min The supernatant was immediately loaded onto a DE52 column followed by a P100 column purification.

3.2.11.2 Putidaredoxin Purification

Pdx was lysed in the same way as PdR. After cell debris removal, the supernatant was subjected to two consecutive salt cuts: 0 - 30% $(NH_4)_2SO_4$ (saved supernatant) and 30 - 60% $(NH_4)_2SO_4$ (saved precipitant). The final precipitate was dissolved in buffer and loaded onto a DE52 (Whatman DE52 Pharmacia) column. Elution was done with a 0.5 M salt gradient. The fractions with $A_{325}/A_{280}$ > 0.30 were concentrated and subjected to a P100 column purification. Fractions with $A_{325}/A_{280}$ > 0.63 were concentrated, flash frozen and stored at -80 °C.

*3.2.12 Purification of Q343(3-$NH_2$Tyr) P450cam*

Protein isolation and purification followed the same protocol as that for the WT P450cam. After dialysis, the protein was reconstituted with hemin (10 mg/mL in .1 M NaOH). Aliquots of the fully reconstituted protein were flash frozen, and stored at -80 °C in potassium phosphate buffer (100 mM, 500 μM D-(+)-camphor, pH 7.4) until further use.

*3.2.13 Purification of P450 BM3 Proteins*

Two methods were used for the purification of WT and T365(3-$NH_2$Tyr) P450 BM3 proteins. One of these methods comprised the protocol followed for isolation and purification of WT P450cam, using buffers supplemented with 3% glycerol without camphor The protein was dialyzed, flash frozen, and stored at -80 °C in potassium phosphate buffer (100 mM, 20% glycerol, pH 7.4) until further use. The other method involved the use of different buffers for the purification process.[48] In this case, protein isolation was achieved following the same protocol as that for the WT P450cam. For the purification process, Ni-NTA resin bound protein was washed successively with buffer 1 (50 mM KPi, 800 mM NaCl, pH 6.2) and buffer 2 (50 mM KPi, 800 mM NaCl, 25 mM glycine, pH 7.5). The protein was eluted with L-histidine buffer (50 mM KPi, 80 mM L-histidine, pH 7.5). The protein was dialyzed, flash frozen, and stored at -80 °C in potassium phosphate buffer (100 mM, 20% glycerol, pH 7.4) until further use.

## 3.3 Results and Discussion

TAG amber codon was introduced into the *camC* gene via site directed mutagenesis using primers containing the mutation. After circularization of the recombinant DNA carrying the mutation, transformation into *E. coli* DH10B electrocompetent cells, and selection, DNA gel analysis of the mutated *camC* gene revealed a DNA band of size corresponding to the size of of the recombinant *camC* gene as can be seen in Figure 3-1. Sequencing was done to confirm the incorporation of the TAG codon, and it proved that mutation was successful.

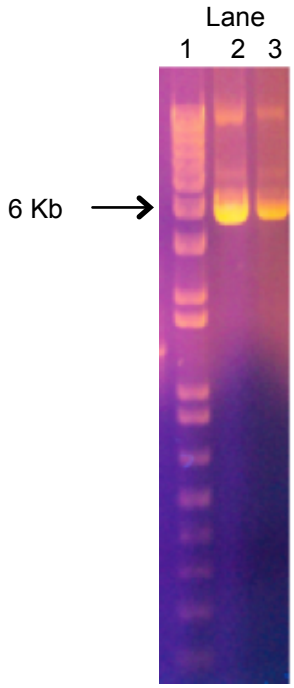


Figure 3-1 Agarose DNA gel analysis of recombinant plasmid carrying the *camC* gene. Lane 1: DNA ladder; lane 2: recombinant plasmid carrying the *camC* gene coding for the WT P450cam; lane 3: recombinant plasmid carrying the *camC* gene coding for Q343(3-$NH_2$Tyr) mutant P450cam.

The target was to generate a P450cam protein containing the unnatural amino acid 3-$NH_2$Tyr. In order for the mutated gene to be successfully expressed, the plasmid containing the mutated *camC* gene had to be co-transformed with PAC-3-$NH_2$TyrRS-6tRNA synthetase plasmid encoding for the orthogonal $tRNA_{CUA}$/aminoacyl-tRNAsynthetase pair from *Methanococcus Jannaschi* (*Mj*) tyrosyl/aminoacyl- tRNA synthetase pair which recognize and is specific for the 3-$NH_2$Tyr substrate in *E. coli* expression strains.[39,41]

The *Mj* PAC-3-$NH_2$TyrRS-6tRNA synthetase plasmid carries a tetracycline resistant marker, which allows for clone selection. The co-transformed cells were selected in ampicillin-tetracycline containing medium. The amber codon resulted in the incorporation of 3-$NH_2$Tyr in place of Q343 during protein expression producing the Q343(3-$NH_2$Tyr) mutant P450cam. This process is illustrated in Figure 3-2.

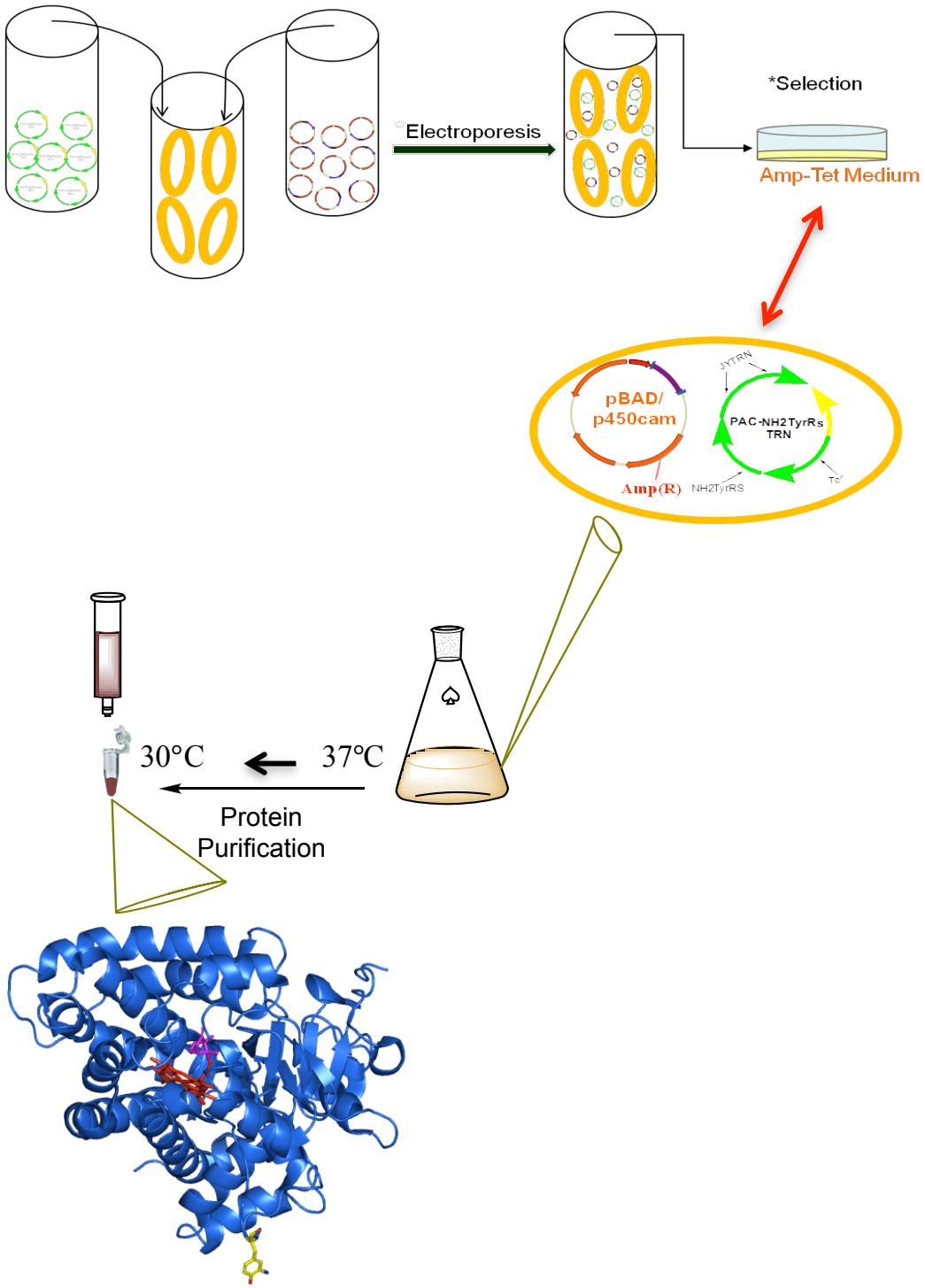


Figure 3-2 Diagram for co-transformation of recombinant plasmid to generate a functional cell for the production of Q343(3-$NH_2$Tyr) mutant P450cam during protein expression.

Mutant Q343(3-$NH_2$Tyr) P450cam was successfully expressed in GMML. During protein expression process, the medium has 3-$NH_2$Tyr that the incorporated tRNACUA/aminoacyl-tRNAsynthetase pair uptakes and inserts at the specified 343 TAG (amber codon) position during the peptide growth. Therefore, at the end of protein synthesis, the folded protein has an incorporated 3-$NH_2$Tyr which has replaced a glutamine residue at position 343 of the WT protein. The resulting mutant protein required hemin reconstitution as it was obtained mostly as apoprotein. Protein analysis was done using SDS-PAGE and visualized by staining it with Coomassie Brilliant blue.

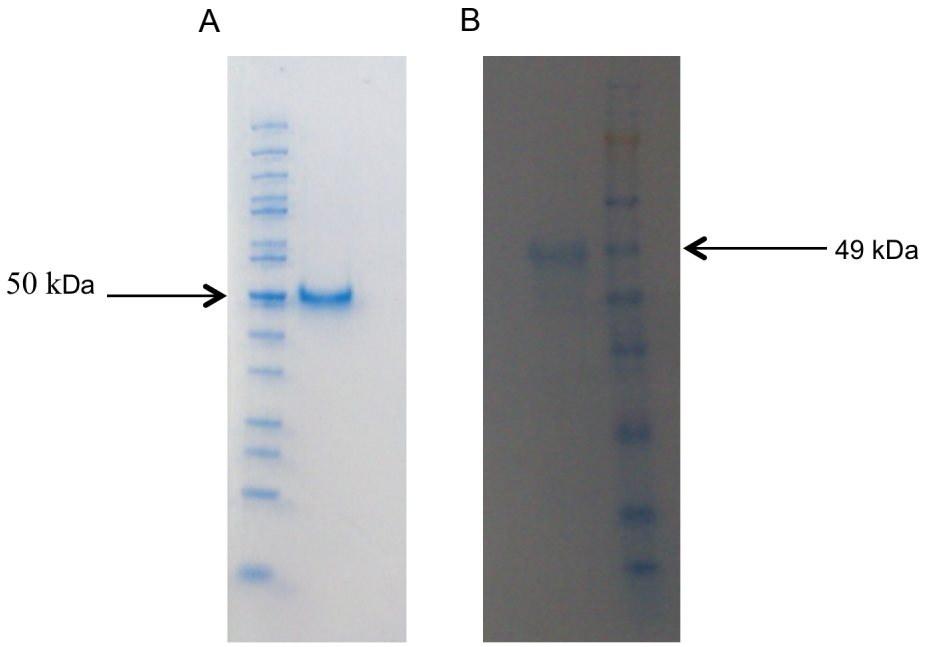


Figure 3-3 Coomassie-stained SDS-PAGE of P450cam protein. (A) WT P450cam. (B) Q343(3-$NH_2$Tyr) P450cam.

SDS PAGE protein gel [Figure 3-3 (A)] shows a band corresponding to WT P450cam which migrated along the 50 kDa marker and is in agreement with the molecular weight of the protein 4600 Da. In a similar way, Q343(3-$NH_2$Tyr) P450cam migrated along the 49 kDa marker of the ladder [Figure 3-3 (B)]. Also, it can be concluded from the gels that the expressed proteins are highly pure.

Figure 3-4 shows the DSD –PAGE analysis of the PdR (A) and Pdx (B) redox proteins. PdR is below the 49 kDa marker which is in agreement with the expected size of 43.5 kDa. In a similar manner, Pdx is below the 14 kDa marker and it is in agreement with the expected 12 kDa of the protein

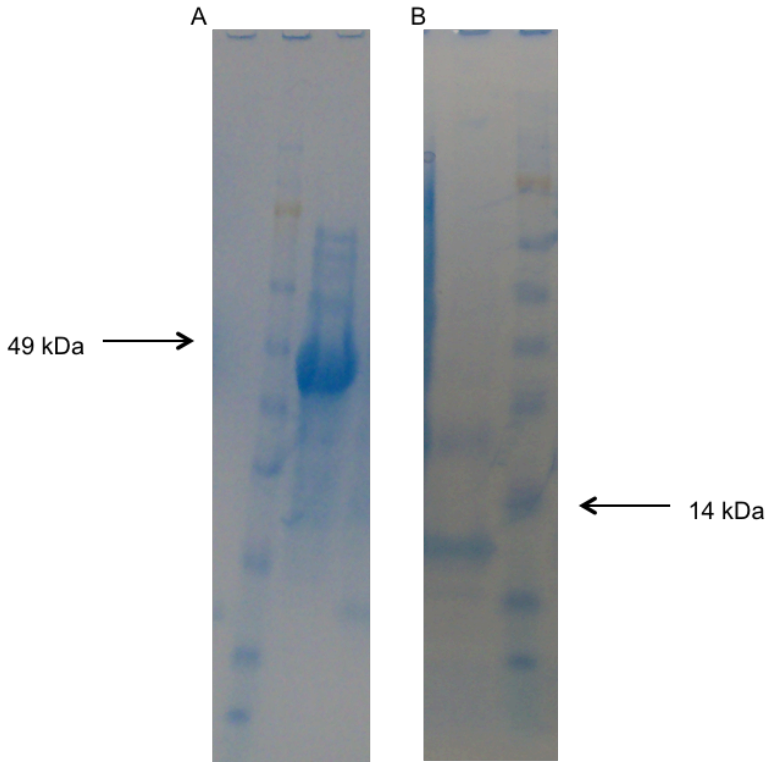


Figure 3-4 Coomassie-stained SDS-PAGE of P450cam redox partners: PdR (A), PdX (B).

TAG amber codon was introduced into the *CYP102A1* gene via site-directed mutagenesis using primers containing the mutation. Sequence analysis proved a successful mutation. As discussed for Q343 (3-$NH_2$Tyr) P450cam, T365(3-$NH_2$Tyr) P450 BM3 was co expressed with the PAC-3-$NH_2$Tyr RS-6tRNA synthetase plasmid encoding for $tRNA_{CUA}$/aminoacyl-tRNAsynthetase pair in order to incorporate the unnatural amino acid during protein expression. T365(3-$NH_2$Tyr) P450 BM3 was successfully expressed in GMML supplemented with 3-$NH_2$Tyr The process taking place is that described for Q343(3-$NH_2$Tyr)

P450cam. The resulting T365(3-$NH_2$Tyr) P450 BM3 was obtained as a holoenzyme where hemin reconstitution was not required.

Protein analysis was done using SDS-PAGE and visualized by staining it with Coomassie Brilliant blue Figure 3-5. There are two blue bands migrating the same distance, which lay near the 120 kDa marker of the ladder, and this is in agreement with the molecular weight of the P450 BM3 of 118.5 kDa. It can be concluded from the gel that the expressed proteins are highly pure.

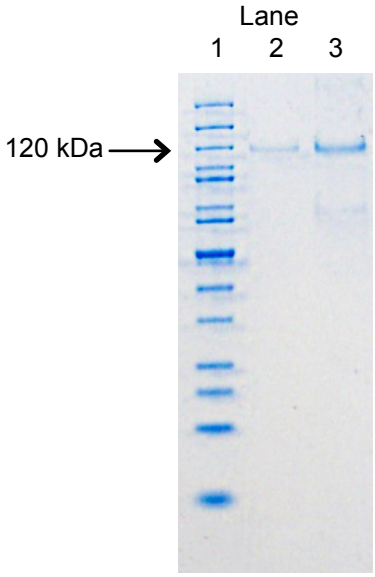


Figure 3-5 Coomassie-stained SDS-PAGE of P450 BM3 proteins. Lane 1: molecular weight standards; lane 2: WT P450 BM3. Lane 3 T365(3-$NH_2$Tyr) P450 BM3

Initially, purification of WT P450 BM3 was achieved following the same protocol as that for the WT P450cam, using buffers without camphor and supplemented with 3% glycerol. It was found that higher concentration of glycerol interfered with binding of the protein to Ni-NTA resin. The protein was dialyzed and supplemented with 10% glycerol. It was flash frozen, and stored at -80 °C in potassium phosphate buffer (100 mM, pH 7.4) until further use. Nevertheless, the protein activity in subsequent experiments was found to be highly diminished. This brought in the possibility of inactivation during the purification process where imidazole could be a factor. In fact,

Maurer *et. al.* have reported this observation and they used L-His for elution of P450 BM3.[48] Following this elution condition, the protein recovered was found to be in active form.

Figure 3-6 shows the electronic absorption spectra of WT and Q343(3-$NH_2$Tyr) P450cam proteins. The UV-Vis spectrum of the purified WT P450cam in the ferric state showed absorptions at 356, 536 and 569 nm due to the δ, β and α bands respectively with the soret peak at 417 nm for camphor free protein. These characteristic absorptions are in full agreement with reported values.[49] However, the mutant P450cam protein presents a 2-nm blue shift in the soret. Furthermore, the α band is smaller than the β band as opposed to the WT protein. From these observations, it can be recognized that the mutation may have slightly perturbed the conformation of the protein.

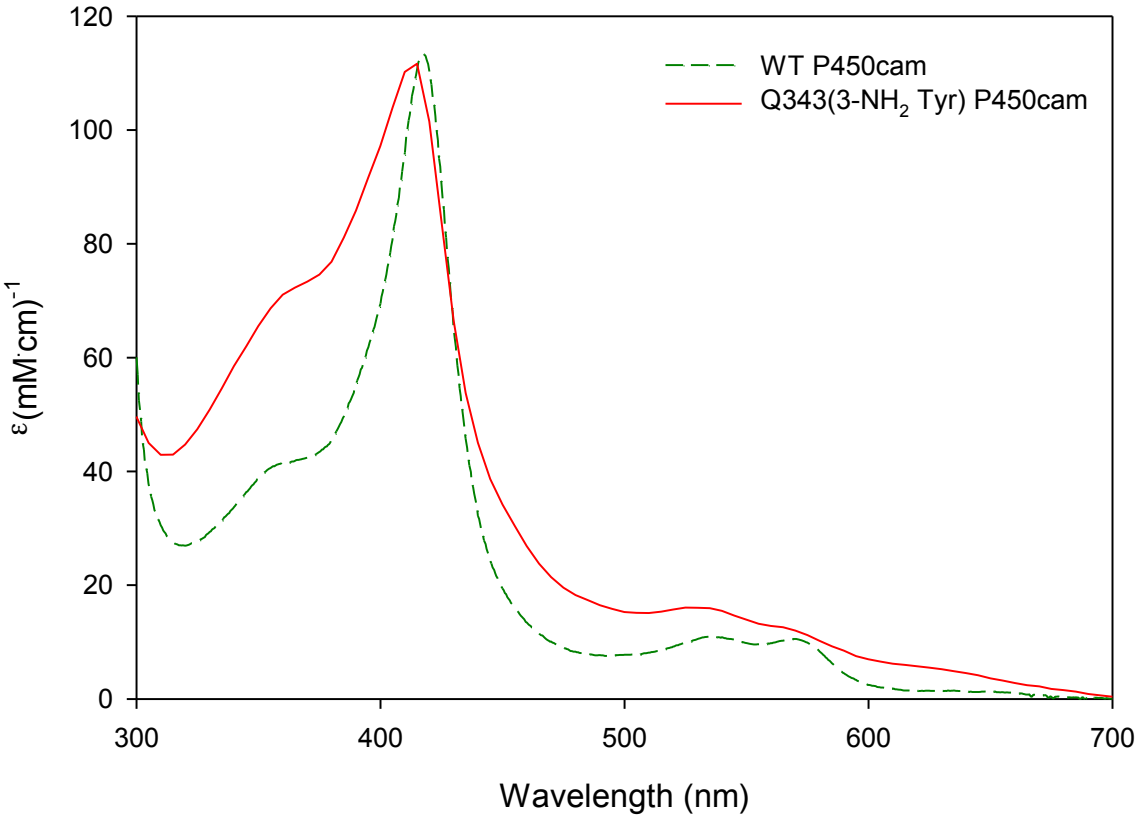


Figure 3-6 UV-Vis absorption spectra of WT P450cam (dotted line) and Q343(3-$NH_2$Tyr) P450cam (solid line).

PdR is a 43.5 kDa flavin containing protein. It shows the following peaks as seen in Figure 3-7: 380 nm, 455 nm, and 480 nm.

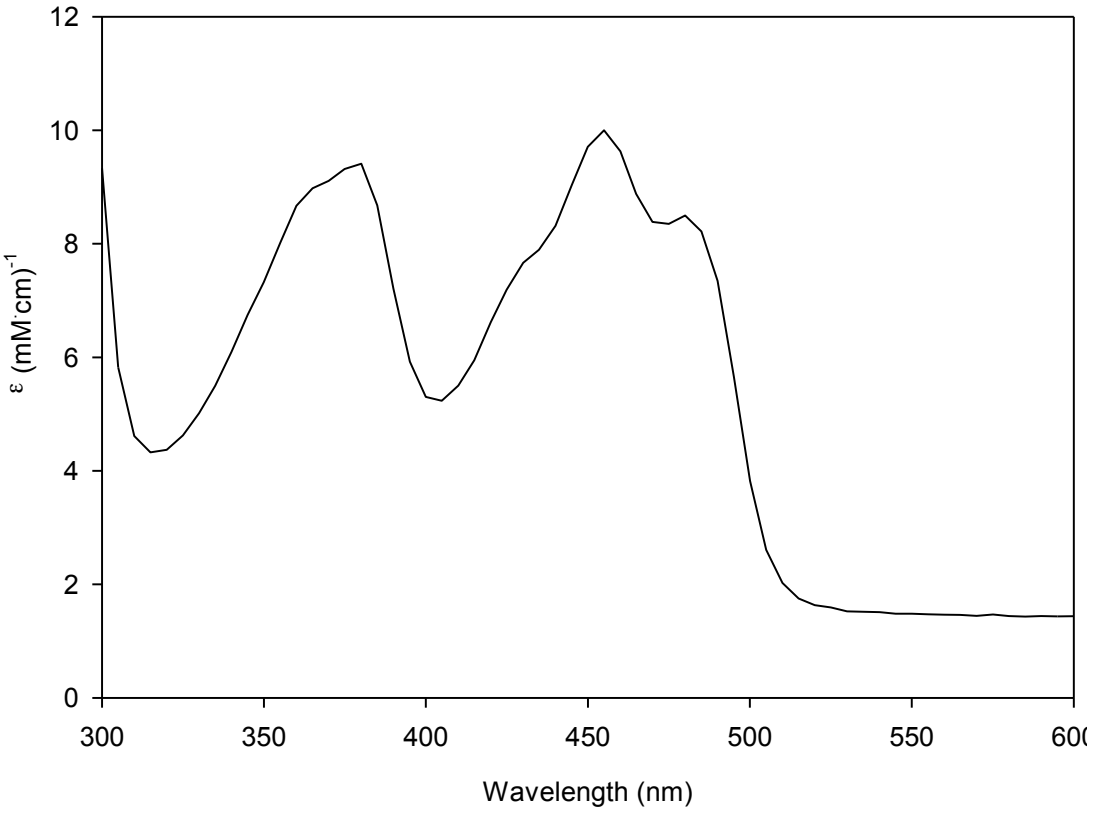


Figure 3-7 UV-Vis absorption spectra of PdR

Figure 3-8 shows the spectra of the 12 KDa iron sulfur Pdx. It presents the following peaks: 340 nm, 415 nm, and 455nm.

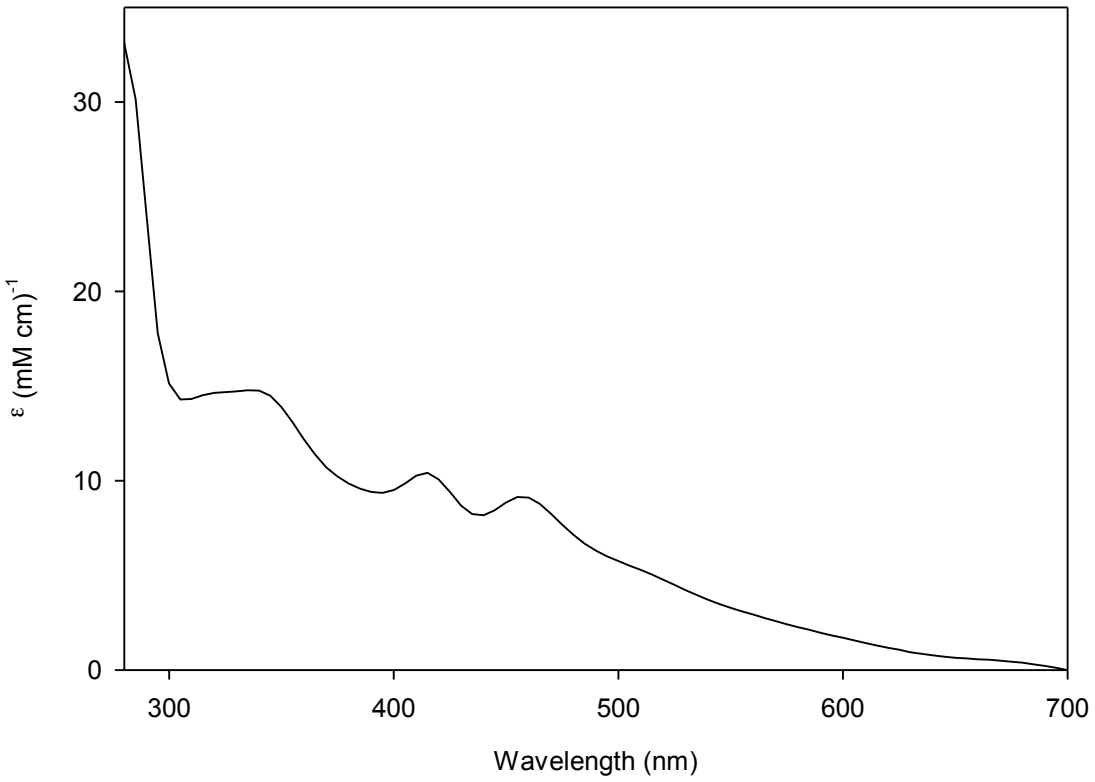


Figure 3-8 UV-Vis absorption spectra of Pdx

Figure 3-9 shows the electronic absorption spectra of WT P450 BM3 (dotted line) and T365(3-$NH_2$Tyr) P450 BM3 (solid line). The electronic absorption features of the mutant P450 BM3 proteins are coincidental to those of WT P450 BM3 except for the β band at 535 nm that looks absent in the mutant. The soret absorption for both proteins falls in the 418.5 nm region, and a shoulder at 365 nm. The α band falls in the 568 nm region which is in agreement with reported values.[50] These results indicate that the conformation of the protein may not be significantly influenced by the 3-$NH_2$Tyr mutation at position T365 of the P450 BM3.

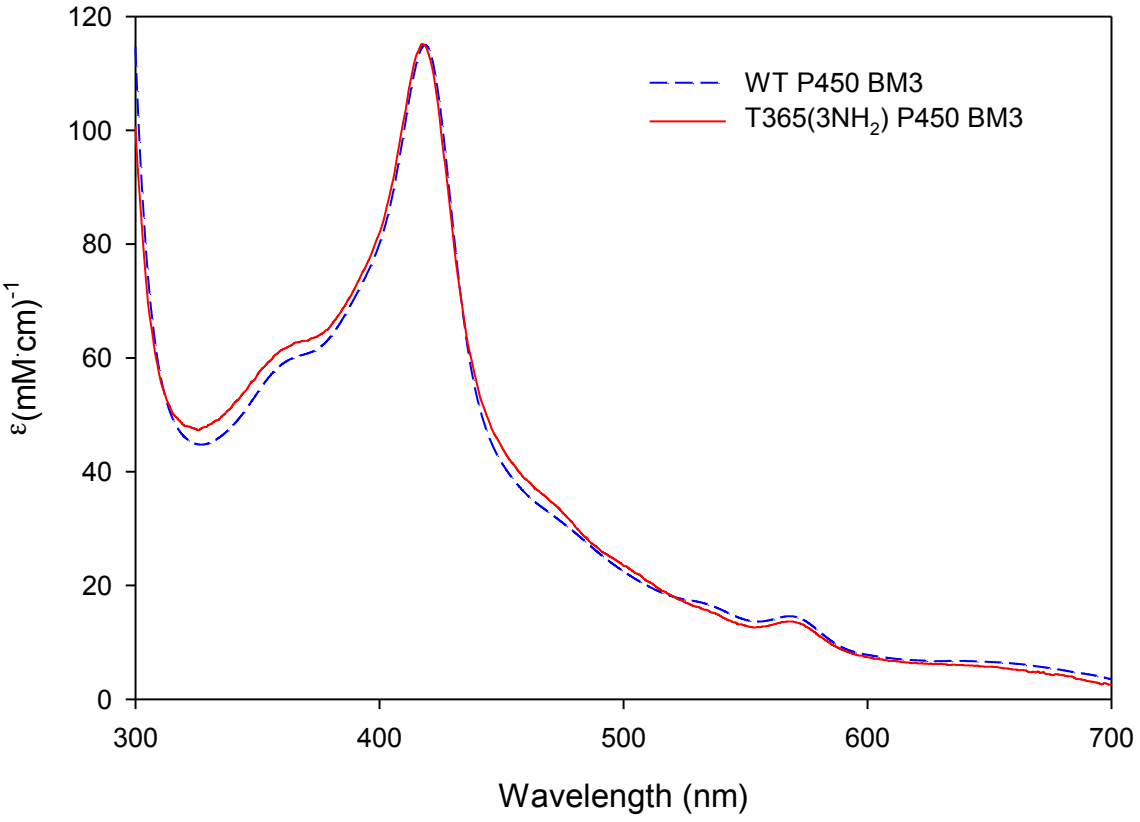


Figure 3-9 UV-Vis absorption spectra of WT P450 BM3 (dotted line) and T365 (3-$NH_2$Tyr) P450 BM3 (solid line).

## 3.4 Conclusion

Incorporation of the unnatural amino acid 3-$NH_2$Tyr in cytochromes P450cam and P450 BM3 was accomplished by genetically encoding the unnatural amino acid. The process involved the introduction of TAG codon into the *camC* and the *CYP102A1* genes that code for P450cam and P450 BM3 respectively, which were confirmed by DNA sequencing, and the incorporation of tyrosyl-tRNA synthetase (mjTyrRS derived from *Methanococcus jannaschii* ) and mjtRNATyrCUA pair that recognize the 3-$NH_2$Tyr substrate in *E. coli* expression host.[45,46]. Using this method, Q343(3-$NH_2$Tyr) P450cam and T365(3-$NH_2$Tyr) P450 BM3 have been effectively expressed. The purification processes used have been efficient to obtain highly pure, active, and native mutated proteins. The unnatural amino acid in the genetically modified proteins provides a new reactive functionality. Subsequent experiments have proved that the unnatural amino acid has the desired properties to use it as an anchor point. Furthermore, during the surface attachment experiment, the mutations have not had shown detrimental effects on the activity of the proteins. The redox partners of P450cam Pdx and PdR have been successfully expressed and purified. These proteins will be used for reconstituted P450cam system hydroxylation reactions as described in chapter 6.

# Chapter 4

## Synthesis of Nanoparticles and Surface Derivatization

All the experiments in this chapter were done by Leticia Loredo in the laboratory of Dr. Roshan Perera.

## 4.1 Introduction

Proper immobilization of proteins on solid supports such as nanoparticles, glass beads, polypropylene, etc. can lead to the generation of cost effective bioreactors for industrial applications since these can be easily isolated after the reaction and reused again. However, this process requires an innovative approach. Metalloenzymes can be immobilized on supports like silica or magnetic iron oxide-silica core-shell nanoparticles (NPs).[51-55] This type of immobilization is promising to produce a reusable biocatalyst. The catalyst can be recovered from the reaction medium by simple filtration in the case of silica nanoparticles (Si-NPs) or by magnetization with an external magnet in the case of MNPs. Considerations have to be taken regarding the MNPs as there is the possibility for the development of the unfavorable Fenton chemistry in the presence of hydrogen peroxide.[56,57] This possibility can be minimized by encapsulating the iron oxide NP with silica coating and further protected by a layer of polyethylene glycol (PEG).[58] Therefore, it is crucial to achieve proper functionalization of the support, as it will provide the protein microenvironment. Many proteins are unstable *in vitro*, and the proper immobilization methods are required in order to satisfy those requirements.[58,59]

In this study, synthesis and functionalization of different supports have been carried out. Preparation of functionalized NPs is important to assemble supports with covalently immobilized active protein via the Diels Alder bioconjugation reaction in water.[60] Towards this end, we have functionalized the NPs with acryloyl end groups. Different methods are available for synthesis of stable silica and iron oxide MNPs, which can be used to generate homogeneous suspension of dispersible homogeneous bio-nanoparticles during their use as surfaces for biocatalyst attachment in reactions. Consequently, we have based our approach for synthesis and functionalization on those previous reports with slight modifications.

Silica NPs have been synthesized based on the sol-gel method developed by Stober *et al*.[63] The synthesis consists of the hydrolysis of tetraethoxysilane (TEOS) and its subsequent condensation in a water/ethanol solution with ammonia as a catalyst. Characteristics of the particle like size and monodispersity are dependent on the reaction parameters such as water

and ammonia concentration which can be adjusted to manipulate the said features.[61] Iron oxide MNPs have been prepared by the co-precipitation method (Reaction 4.1),[53] in which iron (II) and iron (III) salts react in presence of a base (NaOH and $NH_4OH$) under inert atmospheric conditions, resulting in particles with characteristics such as size and shape, dependent on reaction conditions like pH, temperature, ionic strength, nature of the salts and their ratio.[52]

$$Fe^{2+} + 2Fe^{3+} + 8OH^- \longrightarrow Fe_3O_4 + 4H_2O \quad \text{(Reaction 4.1)}$$

The iron oxide MNPs have been further stabilized with oleic acid. Oleic acid can be exchanged with a variety of other reagents. Silica and iron oxide NPs have been silanized with (3-aminopropyl)triethoxysilane (APTES) and further derivatized with acryloyl functional group.

## 4.2 Experimental Section

### *4.2.1 Chemicals.*

Chemicals used were of analytical grade or higher quality, and were used as received unless stated otherwise. Iron (III) chloride hexahydrate and Acryloyl Chloride were obtained from Alfa Aesar; Tetraethylene Glycol Diacrylate was from TCI America; Iron (II) sulfate hepta-hydrate, Tetraethyl Orthosilicate, N,N-Diisopropylethylamine, and (3-Aminopropyl)triethoxysilane were from Sigma-Aldrich; Ammonium Hydroxide was from Bdh Lab Supplies.

### *4.2.2 Instrumentation*

TEM images were taken on an ultra high resolution transmission electron microscopy Hitachi H-9500 at an accelerating voltage of 300 kV. Samples dispersed were cast onto a carbon-coated copper grid.

### *4.2.3 Synthesis of Oleate Coated Iron Oxide Magnetic Nanoparticles*

Iron oxide MNPs stabilized with oleic acid were synthesized following a reported method.[53] In short, $FeSO_4.7H_2O$ (2.35 g) and $FeCl_3.6H_2O$ (4.1 g) were dissolved in deoxygenated Milli-Q water (100 mL) under vigorous mechanical stirring. $NH_4OH$ (25% w/w , 25 mL) was added

as fast as possible. The mixture was heated at 80 °C and oleic acid (1 mL) was added over a one hour period. The procedure was carried out under nitrogen atmosphere. The particles were extracted into toluene by adding a saturated NaCl solution.

*4.2.4 Amino Functionalization of Magnetic Iron Oxide Nanoparticles*

(3-aminopropyl)triethoxysilane (APTES) (2 mL) and triethyl amine (1.12 mL) were added to a dispersion of oleate coated MNPs (200 mg) in toluene under a nitrogen atmosphere. The reaction mixture was stirred for 8 h at room temperature. The NPs were precipitated with petroleum ether, isolated and dried in a vacuum. MNPs were dispersed into acetone and re-precipitated with petroleum ether five times.

*4.2.5 Acryloyl Functionalization of Magnetic Iron Oxide Nanoparticles*

To obtain the acryloyl surface, a mixture of acryloyl chloride (1 mmol), *N*,*N*-di-iso-propyl-ethylamine (DIPEA) (1 mmol) and anhydrous dichloromethane (30 mL) was prepared in a polypropylene container, previously flushed with nitrogen, followed by addition of the MNPs containing $NH_2$ functionality. The reaction was allowed to take place for 2 h at room temperature on an orbital shaker. The supports were washed thoroughly with dichloromethane, isolated with a magnet and dried with a flow of nitrogen.

*4.2.6 Silica Encapsulation of Magnetic Iron Oxide Nanoparticles*

Encapsulation of the MNPs was achieved following a literature procedure.[62] Briefly, amino-functionalized MNPs were dispersed in ethanol. Tetraethoxysilane (TEOS) was added to the dispersion and the mixture was stirred continuously while adding water (10 mL). The mixture was stirred for 3 h. Particles were isolated with a magnet and washed thoroughly with ethanol. The resulting particles will be called silica encapsulated magnetic nanoparticles (Si-MNPs).

*4.2.7 Amino Functionalization of Si-MNPs*

The silanol groups of the silica coat of the Si-MNPs were activated following a literature method.[63] In short, Si-MNPs (100 mg) in a solution of 6 M HCl (5 mL) for a period of two hours. The mixture was filtered, and the activated Si-MNPs were washed with water (3 x 5 mL) followed by methanol (3 x 5 mL). The particles were dried in an oven overnight. The dry activated Si-MNPs were mixed with 5 mL of toluene under anhydrous conditions. To this mixture, 500 µL of APTES were added. The mixture was refluxed for 7 h. The particles were isolated by filtration and washed successively with toluene, methanol and diethyl ether. The amino-functionalized NPs were dried overnight in the oven.

*4.2.8 Synthesis of Silica Nanoparticles with Amine Functionality*

Si-NPs were synthesized following a reported method.[64] TEOS (3.8 mL) was mixed with a solution of aqueous ammonium hydroxide (5.7 mL) in ethanol (114 mL) and stirred overnight at room temperature. To the reacted mixture, APTES was added under vigorous stirring and the reaction was allowed to take place for 24 h. The functionalized silica NPs were centrifuged and washed by re-dispersing in ethanol three times. The amino-functionalized NPs were dried overnight in the oven.

*4.2.9 Amino Functionalization of Commercial Silica Nanoparticles*

Alternatively, commercial Si-NPs were functionalized following a literature method.[63] The silanol groups of the Si-NPs were activated by refluxing 10 g of Si-NPs in 50 mL of 6 M HCl for a period of two hours. The mixture was filtered, and the activated silica was washed with water (25 mL x 3) followed by methanol (25 mL x 3). The particles were dried in the oven overnight. Under anhydrous conditions, 5 g of the dry activated Si-NPs were mixed with 20 mL of toluene. To this mixture, 5 mL of APTES were added. The mixture was refluxed for 7 h. The particles were isolated by filtration and washed successively with toluene, methanol and diethyl ether. The amino-functionalized nanoparticles were dried overnight in the oven.

*4.2.10 Amino Functionalization of Glass Surfaces*

The process used for functionalization of glass slides and porous and non-porous glass beads, was based on a reported protocol with slight modifications.[65] Briefly, a glass support was etched by completely immersing it in a solution of 10% NaOH overnight with gentle shaking. The support was subsequently washed with water, 1% (v/v) HCl solution, water, and methanol. The next step was surface silanization by immersing the support in a solution of 3% (w/v) APTES in 95 % (v/v) methanol and sonicating this mixture for 15 minutes or stirring for 1 h. The support was subsequently washed with methanol, water, dried, and baked for 15 minutes at 110 °C.

*4.2.11 Acryloyl Functionalization of Glass Surfaces*

To obtain the acryloyl surface, a mixture of acryloyl chloride (1 mmol), DIPEA (1 mmol) and anhydrous dichloromethane (30 mL) was prepared in a polypropylene container, previously flushed with nitrogen, followed by addition of the support. The reaction was allowed to take place for 2 h at room temperature on an orbital shaker. The supports were washed thoroughly with dichloromethane and dried with a stream of nitrogen.

For AFM analysis, slides were further washed with water and dried under a gentle stream of nitrogen.

*4.2.12 Derivatization of Gold Electrode:*

4.2.12.1 Au/Cysteamine

The pretreated gold electrode was immediately immersed in a 400 mM ethanolic solution of cysteamine hydrochloride for 8h. It was washed thoroughly.

4.2.12.2 Au/Cysteamine/TEGDA

The pretreated gold electrode was immediately immersed in a 400 mM aqueous solution of cysteamine hydrochloride for 8 h. It was washed thoroughly with ethanol and immersed in 20 mM DIPEA in dimethylformamide. To this solution, 10 mM tetraethylene glycol diacrylate

(TEGDA) was added and the electrode was kept in it for 3 h. The chemically modified gold electrode was washed thoroughly to remove the traces of unreacted molecules

## 4.3 Results and Discussion

Iron oxide MNPs and silica NPs were synthesized and functionalized with organosilanes and further derivatized to provide a surface with acryloyl end groups. Other materials such as glass slides, glass beads, polypropylene chips and gold electrodes have been derivatized as well in this study.

### *4.3.1 Functionalization of Glass Surface*

The first step in functionalization of the support was the cleaning and the etching of the glass slides to produce OH groups on the surface. This was followed by silanation with APTES resulting in an amino functionalized surface that was activated with acryloyl chloride or elongated further with a PEG-like linker tetra(ethylene glycol) diacrylate where the amine reacts with the unsaturated acryloyl group. In either case, the surface was left with a terminal acrylate functional group as shown in Figure 4-1.

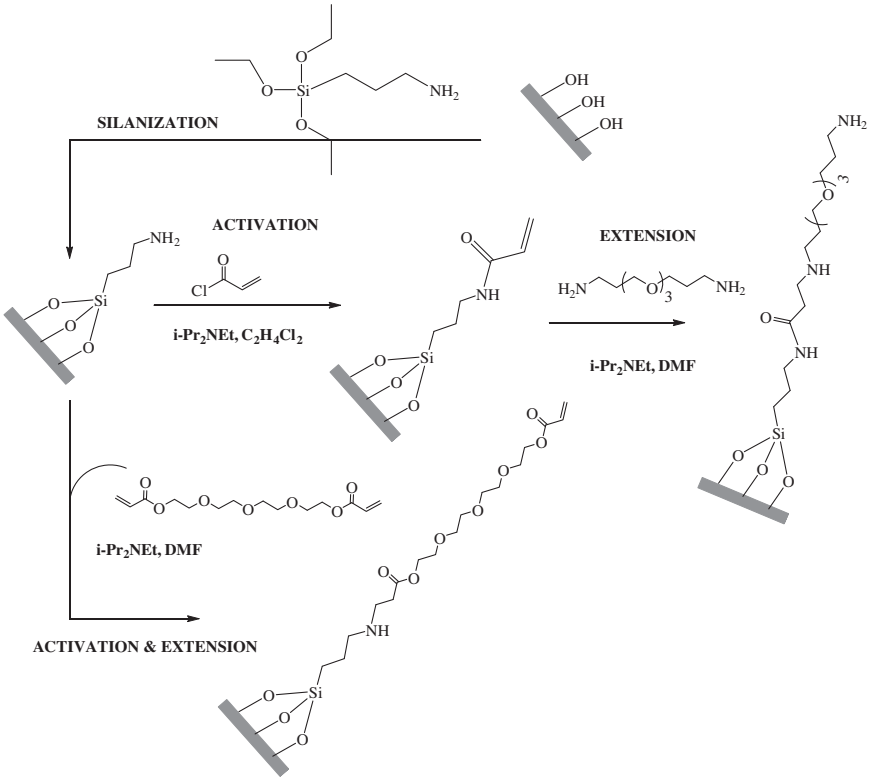


Figure 4-1 Representation of the methods used in this study for support derivatization and extension of the linker with PEG containing chains.

*4.3.2 Oleate Coated Iron Oxide Magnetic Nanoparticles*

As previously mentioned, iron oxide MNPs have been prepared by the co-precipitation method (Reaction 4.1). The synthesis of iron oxide MNPs is illustrated in Figure 4-2. The particles were prepared by mixing $FeCl_3$ and $FeSO_4$ in presence of ammonium hydroxide, and oleic acid as a surfactant. The particles were extracted into toluene by precipitating them with a NaCl saturated solution.

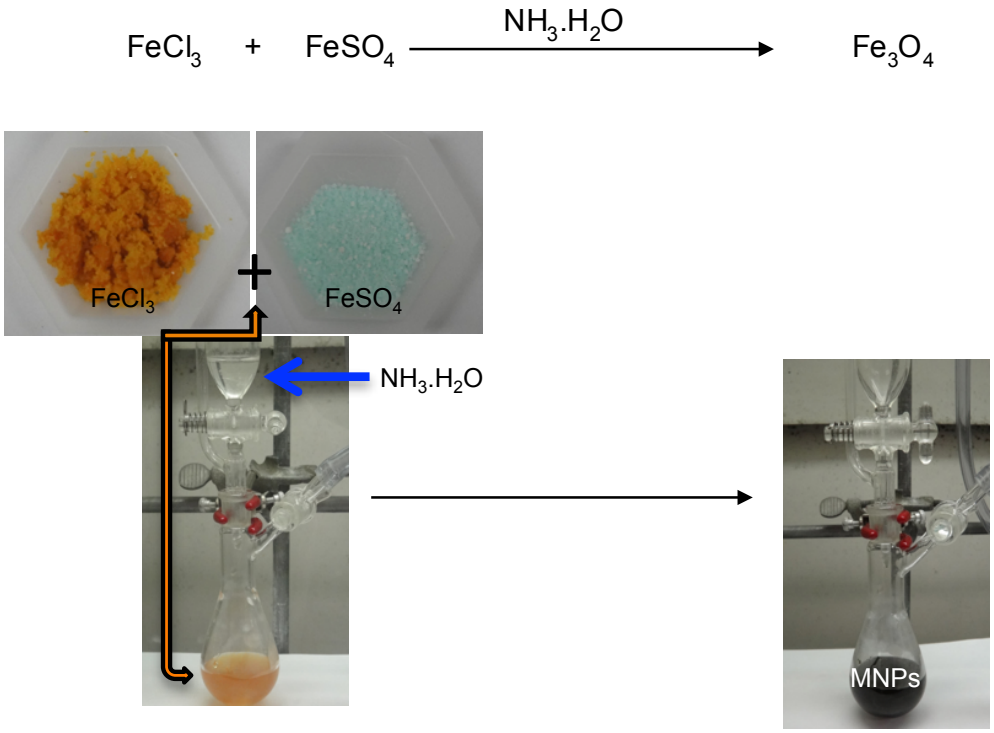


Figure 4-2 Picture depiction of preparation of iron MNPs.

The oleate coated MNPs were reacted with APTES to provide the amino functionality that has the potential to react further and therefore allows for further derivatization of the support. In this case, the amino-functionalized particles were reacted with acryloyl chloride in presence of DIPEA. These particles were analyzed by TEM (Figure 4-3 A) and were found to have sizes within 8-14 nm range. MNPs have the potential to be easily separated in the presence of a magnet while they regain dispersability once the magnet is removed, as can be seen in Figure 4-3 B. Therefore, immobilized P450cam on MNPs can be used for hydrocarbon oxidation catalysis, which can be easily isolated from the reaction mixture at the end of the reaction, eliminating contamination of the products with catalyst and reducing the purification requirements. At the same time, these characteristics provide recyclability of the catalyst.

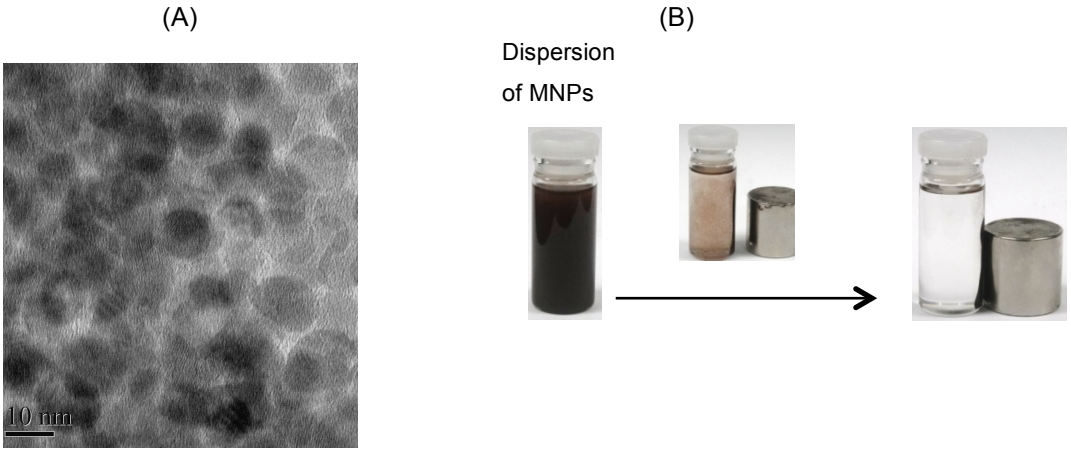


Figure 4-3 MNPs (A) Transmission electron micrograph image of MNPs functionalized with acryloyl end group. (B) Response of MNPs to magnetic field.

The choice of the method to prepare the MNPs was the relative small nanometric size of the particle and the stability provided by the oleate coating, which allow the easy replacement of the oleate by alkoxysilanes. The oleate provides dispersability to the particles preventing their agreggation.[51]

The exchange of the oleate coating of the MNPs with APTES leaves the particles ready for further derivatization, including the option to encapsulate the MNPs in silica and/or further functionalization with acryloyl chloride in presence of diisopropylethylamine (DIPEA) to produce a surface with acryloyl end groups. Coating of the iron MNPs was necessary as they were prepared to be used as supports for protein immobilization, as mentioned before, and their further employment in reactions containing hydrogen peroxide, therefore, to prevent Fenton chemistry. MNPs can be directly coated with silica; however, researchers have found that direct encapsulation of MNPs pushes the particle to one side.[62] This is not a desired feature since the objective is to keep the particle as isolated as possible from the reaction medium. A different type of NPs we used consisted of silica, and although they are not magnetic, they can be used as supports for the generation of recyclable biocatalysts.

*4.3.4 Synthesis of Amine-Functionalized Silica Nanoparticles*

The synthesis of silica NPs was achieved using the sol-gel method developed by Stober *et al.*[16] The Si-NPs were prepared by adding tetraethyl ortho silicate (TEOS) in a solution of ethanol and ammonium hydroxide. At the end of the NPs synthesis, APTES was added to incorporate the amine functionality on the support. The reaction was monitored by the Kaiser Test, where NPs were treated with ninhydrin at the end of the reaction producing the deep purple color known as Ruhemann's purple, as expected for a primary amines (Figure 4-4).

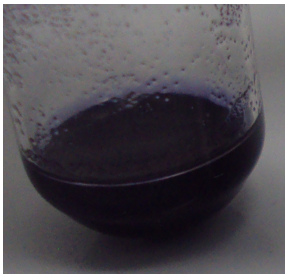

Figure 4-4 Amino functionalized Si-NPs subjected to Kaiser Test, showing the Ruhemann's purple.

*4.3.5 Syntheis of Acryloyl-Functionalized Silica Nanoparticles*

Acryloyl end functionality on Si-NPs was obtained by dispersing the amine-functionalized Si-NPs in dichloromethane and treating it with acryloyl chloride in the presence of DIPEA. The acryloyl functionalized NPs were subjected to the Kaiser Test producing a yellow color as expected for secondary amines (Figure 4-5).

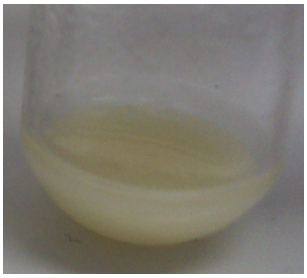

Figure 4-5 Acryloyl functionalized Si-NPs subjected to Kaiser Test.

*4.3.5 Gold Electrode Derivatization*

Figure 4-6 shows the gold electrode derivatization process to obtain amino end functionality by treating it with cysteamine ydrochloride.

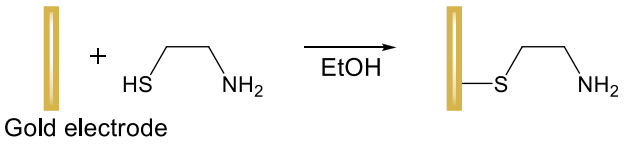


Figure 4-6 Schematic representation of electrode modification with amine functionality.

The main steps for the functionalization of the gold electrode to immobilize Q343(3-$NH_2$Tyr ) P450cam are highlited in Figure 4-7. The gold electrode was pretreated with cysteamine hydrochloride and further derivatized with tetraethylene glycol diacrylate (TEGDA) that leave the C=C bond exposed on the surface of the electrode.

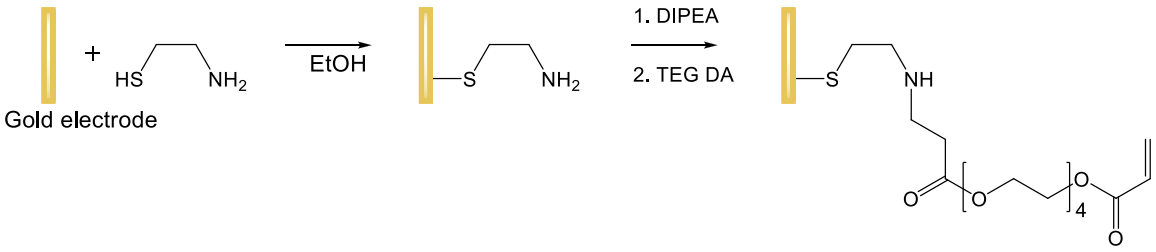


Figure 4-7 Schematic representation of electrode modification with acryloyl end functionality.

## 4.4 Conclusion

In this chapter, Si-MNPs and MNPs were successfully synthesized. Different chemical methods were utilized to surface functionalized NPs and other supports like glass and gold surfaces. These supports either contain amine or acryloyl end functionality, and may or may not have a pegylated like linker provided by tetraethylene glycol. The choice of the support and reactive end functionality has been based on future applications (as will be seen in next chapter) to covalently immobilize protein on them to be used as reusable catalysts that can be recovered with simple filtration methods, or isolated with the aid of a magnet. The supports provide a microenvironment to the protein and the functionalities present in these will play a crucial role in the stability of the protein and the reaction conditions necessary for the immobilization. As subsequent experiments will show later, the supports are effective to attach a protein and also to keep it in active form.

Chapter 5

# Covalent Immobilization of Cytochrome P450cam and P450 BM3 Proteins

Part of this work has been published on *Anal. Biochem.* **2012**, *424,* 114–123

All the experiments in this chapter were done by Leticia Loredo in the laboratory of Dr.Roshan Perera.

Electrochemistry masurements were done by Dr. Sriparna Ray.

## 5.1 Introduction

Attachment of proteins to solid supports have been carried out extensively using different approaches, regarding the nature of the support and the method in which immobilization of the protein takes place. However, these methods generally suffer from weak attachment of the protein, which causes it to leach out from the support, deformation of the protein due to unfavorable interactions with the support, coagulation of the protein on the surface, obstruction of the active site, problems with mass transfer of substrate in case of entrapped proteins and possible inactivation due to accumulation of product. These problems have led us to look for a method that overcomes these deficiencies in protein immobilization.

Chapter 5, therefore, aims to develop a method in which water soluble cytochrome P450s are covalently bound to a solid support properly functionalized for site-specific immobilization through the unique amino acid 3-$NH_2$Tyr while retaining their natural conformation and activity via a hetero Diels-Alder bioconjugation reaction in water. Fully active and covalently immobilized enzymes with control over their orientation have been attained by developing this method, which can be extended to any recombinant protein. In addition, the random covalent immobilization of P450cam via an amide bioconjugation reaction is also addressed.

Proper immobilization of proteins on solid supports can lead to the generation of cost effective bioreactors for industrial applications since these can be easily isolated after the reaction and reused. However, this process requires an innovative approach. Metalloenzymes can be immobilized on supports like Si-NPs or Si-MNPs.[51-55] This type of immobilization is promising to produce a reusable biocatalyst. The catalyst can be recovered from the reaction medium by simple filtration in the case of Si-NPs or by magnetization with an external magnet in the case of MNPs. Considerations have to be taken regarding the magnetic iron oxide NPs as there is the possibility for the development of the unfavorable Fenton chemistry in the presence of hydrogen peroxide.[56,57] This possibility can be minimized by encapsulating the MNPs with silica coating and further protected by a layer of PEG.[58]

There are important aspects that have to be taken into consideration for the development of functional immobilized enzyme on solid supports. There must be a permanent linkage between the protein and the substrate to avoid leaching of the enzyme from the solid support. Additionally, the attachment of the protein to the solid support should be uniform to prevent coagulation of unbound proteins and possible obstruction of the active site. The orientation of the immobilized protein is essential so that the active site is available to the substrate. Equally important is the retention of the native conformation so that the protein is stable and activity is preserved.[25] Therefore, it is crucial to achieve proper functionalization of the support, as it will provide the microenvironment required for protein activity. Many proteins are unstable *in vitro*, and the proper immobilization methods are required in order to satisfy those requirements.[58,59] Although this is a challenging task, if the requirements are met, fully active, stable and recyclable catalysts can be produced.

In this study, immobilization of protein has been carried out on glass slides as a proof of concept. AFM analysis of these slides reveals that the development of the following methods is successful for the intended purpose. WT protein immobilization via amide bioconjugation reaction in presence of EDC is an alternative to site-specific immobilization when incorporation of the unnatural amino acid in the protein is not desirable, or when mutant protein expression is not feasible compared to that of the WT. This process takes advantage of the functional groups that the protein has already present on its surface, such as the amine and the carboxyl groups which can react in presence of EDC to form amide bonds. Early reports of the use of water soluble carbodiimides for amide bond formations are those of Hoare and Koshland providing milder conditions for these types of reactions.[66,67] This chapter focuses on the immobilization of WT P450cam on different surfaces via amide bond bioconjugation in presence of EDC. At the same time, it investigates the electrochemistry of randomly immobilized WT P450cam proteins on a gold electrode as well as that of mutant Q343(3-$NH_2$Tyr) P450cam immobilized via Diels Alder reaction.

## 5.2 Experimental Section

### *5.2.1 Chemicals*

Chemicals used were of analytical grade or higher quality, and were used as received unless stated otherwise. Sodium Periodate and 1-Ethyl-3-(3-Dimethylaminopropyl)Carbodiimide Hydrochloride were purchased from Sigma-Aldrich, Mes (2-(N-morpholino)ethanesulfonic acid) Hydrate was obtained from Acros Organics

### *5.2.2 Instrumentation*

#### 5.2.2.1 UV–Vis Measurements

UV–Vis spectroscopic measurements were conducted on a Cary 50 Bio UV-visible spectrophotometer.

#### 5.2.2.2 AFM Measurements

The experiments were performed with a commercially available Veeco MultiMode V SPM. The cantilevers used in this experiment were Phosphorus doped n-type Si cantilevers. The cantilever was oscillated in the constant excitation mode. Tapping mode-AFM images were acquired in the constant frequency shift mode using a frequency modulation (FM) detection method. The bias voltage of both the cantilever and the sample were kept at zero during the AFM imaging. Data analysis of the surfaces was done with the diNanoscope software 7.0.

#### 5.2.2.3 Electrochemical Instrumentation

Cyclic voltammetry (CV) was carried out using a three-electrode cell at 22 °C on a CHI720C electrochemical analyzer (CH Instruments, Austin, TX). The working electrode was polycrystalline gold (2 $cm^2$ in area, Alfa Aesar), the counter electrode was a platinum wire, and the reference electrode was Ag/AgCl (3.5 M KCl). The counter electrode and reference electrode were obtained from CH Instruments. All potential values below are reported with respect to the Ag/AgCl (3.5 M KCl) reference electrode. The working electrode surface was first polished on

microcloth (Buehler No. 40-7212) with alumina slurry suspension (0.05 μm), then sonicated in ethanol, and finally rinsed thoroughly with Milli-Q water. The electrolyte solution was 0.1 M potassium phosphate buffer with 10 mM KCl solutions at pH 7.0. The solutions were deoxygenated by bubbling nitrogen prior to each experiment. The CV measurements were recorded at potential scan rates ranging from 2 $mVs^{-1}$ to 5 $mVs^{-1}$.

*5.2.3 Oriented Immobilization of CYP P450s*

Methods followed for functionalization of supports was given in the synthesis of nanoparticle and surface derivatization chapter.

5.2.3.1 Immobilizaton of Q343(3-$NH_2$Tyr) P450cam

Q343(3-$NH_2$Tyr) P450cam in 50 mM potassium phosphate buffer pH 7.4 was deposited on the acryloyl end functionalized glass surface in presence of 100 μM $NaIO_4$. Incubation was allowed for 2 h at room temperature. After incubation, the slide was thoroughly washed with 100 mM potassium phosphate buffer pH 7.4.

5.2.3.2 Au/Cysteamine/TEGDA/Q343(3-$NH_2$Tyr) P450cam.

Immobilization of Q343(3-$NH_2$Tyr) P450cam on electrode was done following a reported procedure.[68] The Q343(3-$NH_2$Tyr) P450cam was taken in a phosphate buffer solution and an aqueous solution of 40 μM $NaIO_4$ was added to it. The chemically modified gold electrode with acryloyl end group was washed thoroughly to remove the traces of unreacted molecules and incubated in the mutant protein solution overnight at 4 °C. The electrode was then removed, rinsed with Milli-Q water and allowed to dry under nitrogen flow before use.

5.2.3.3 Immobilization of T365(3-$NH_2$Tyr) P450 BM3

T365(3-$NH_2$Tyr) P450 BM3 in 50 mM potassium phosphate buffer pH 7.4 was deposited on the acryloyl end functionalized glass surface with a pegylated linker in presence of 100 μM

$NaIO_4$. Incubation was allowed for 2 h at room temperature. After incubation, the slide was thoroughly washed with 100 mM potassium phosphate buffer pH 7.4.

For AFM analysis, slides were further washed with water and dried under a gentle stream of nitrogen.

*5.2.4 Microarray Development*

A microarray of five proteins was prepared with 3-$NH_2$Tyr mutated proteins. The proteins were mixed with 0.1 mM $NaIO_4$ for 10 min prior to printing in a solution of 100 mM potassium phosphate buffer (pH 6.0). Printing was performed using a BioRobotics Micro- Grid II 600 with an internal chamber humidity of 70%. After printing, mutant proteins were allowed to bind for 4 h at room temperature before being transferred to phosphate-buffered saline (PBS) buffer (pH 7.5) for 48 h of washing. Binding of HiLyte 647 fluorophore- tagged anti-6xHis tag rabbit IgG was performed with a 1:500 dilution in PBS buffer containing 1% bovine serum albumin (BSA) and 0.1% Tween 20 for 1 h over the top of the entire slide, followed by washing in PBS buffer containing 0.1% Tween for 5 min twice. Coomassie staining was done using Coomassie bromophenol blue staining solution for 10 min, followed by 24 h of washing in water

*5.2.5 Random Immobilization of WT P450cam*

5.2.5.1 WT P450cam Immobilization on Glass Surface

The amino-functionalized glass support was immersed in a solution of WT P450cam protein (5 μM final concentration) in MES buffer (0.1 M, pH 5.0). To this mixture, a freshly prepared aqueous solution of EDC was added and the protein was allowed to bind for 3 h at room temperature. The glass support containing bound P450cam was removed from the mixture and rinsed thoroughly with KPi buffer (0.50 mM, pH 7.4). Finally the bound protein support was stored for a short period of time in KPi buffer (0.50 mM, pH 7.4) before its use.

A control was done with the exact same conditions for the WT P450cam immobilization on the amine-functionalized support but EDC was omitted.

5.2.5.2 WT P450cam Immobilized on Amino Functionalized Si-MNPs

The procedure for the amino functionalization of Si-MNPs was given previously in chapter 4.The dried amino-functionalized NPs were immediately used to immobilize the WT P450cam protein. 0.8 mL of the derivatized NPs was added to a solution of 40 μM WT P450cam in MES buffer (0.1 M, pH 5.0, supplemented with 0.5 mM camphor). To this mixture, a freshly prepared aqueous solution of EDC was added and the protein was allowed to bind for 2 hours at room temperature. The silica bound P450cam was isolated and rinsed thoroughly with several washing with KPi buffer (0.50 mM, pH 7.4) and centrifugation rounds. Finally, the volume of the silica was suspended to a final volume of 1.5 mL with KPi buffer (0.50 mM, pH 7.4).

5.2.5.3 Au/Cysteamine/WT P450cam

Immobilization of WT P450cam on the electrode was done following a reported procedure.[68] Briefly, the pretreated gold electrode was immediately immersed in a 400 mM ethanolic solution of cysteamine hydrochloride for 8 h. It was washed thoroughly and immersed in the 5 μM WT P450cam solution in MES buffer at pH 5.0. To this solution, freshly prepared aqueous solution of EDC was added and the electrode was dipped in it overnight at 4 °C. The electrode was then removed, rinsed with Milli-Q water and allowed to dry under a gentle stream of nitrogen before use.

*5.2.6 Preliminary Electrochemical Studies of Immobilized P450cam Proteins*

Cyclic voltammetry (CV) was used to investigate the reduction potential ($E^o$) of immobilized WT and Q343(3-$NH_2$Tyr) P450cam on a gold electrode in 100 mM phosphate buffer, pH 7.0 with 10 mM KCl at room temperature in nitrogen saturated conditions and at potential scan rates of 2-5 and 2-6 mV $s^{-1}$ respectively.

## 5.3 Results and Discussion

### *5.3.1 Immobilization of 3-$NH_2$Tyr Incorporated CYPs via the Diels-Alder Reaction in Water*

#### 5.3.1.1 Protein immobilization on derivatized glass surface

The 3-$NH_2$Tyr in the mutated protein provides a new functionality that can be selectively oxidized to *o*-imino-quinone via $NaIO_4$. [69] This quinone is highly reactive and can conjugate to the carbon-carbon double bond of the acryloyl group present in the solid support via the Diels-Alder reaction. Taking the advantage of these reactive functionalities, the Diels-Alder reaction was carried out by spreading buffer containing the unnatural amino acid incorporated cytochrome P450 onto the acryloyl functionalized surface, and incubating it in the presence of 100 μM $NaIO_4$ for 2 h. Breslow and Rideout have reported an increase in the rate of the Diels-Alder reaction in water which has been attributed to hydrophobic effects.[60] This makes the immobilization process even milder for the protein.

The reaction can be done at room temperature or at 4 °C. No effect on the reaction by temperature was observed. The product is a benzoxazine ring that leaves the protein covalently attached to the support with a yield higher than 90%. The support bound protein was thoroughly washed with phosphate buffer and water to remove any non-covalently bound protein from the support. A representation of the main steps used for the functionalization of the support and covalent immobilization of cytochrome P450cam is depicted in Figure 5-1. Activation of the support with amino end group and further modification with acryloyl chloride allowed the immobilization of the mutated protein via Diels-Alder bioconjugation reaction between the carbon-carbon double bond of the support and the *o*-imino-quinone of the oxidized unnatural amino acid. The support containing the P450cam protein was washed, dried under a stream of nitrogen, and analyzed with AFM.

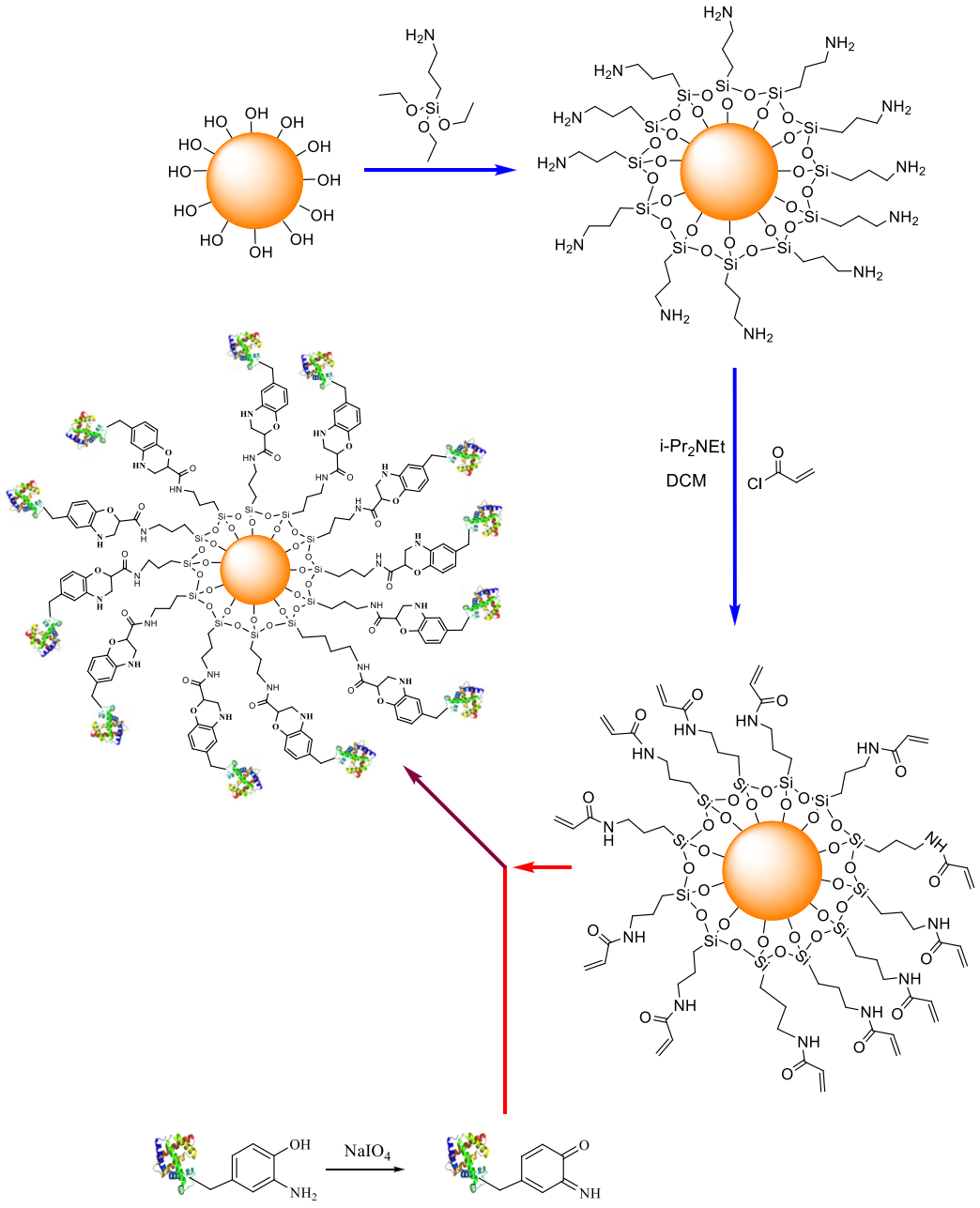


Figure 5-1 Solid support derivatization and immobilization of mutant Q343(3-$NH_2$Tyr) P450cam. The supports were first silanized with APTES and derivatized with acryloyl chloride. Covalent immobilization of the protein resulted by Diels Alder reaction reaction between the carbon-carbon double bond of the support and the oxidized unnatural amino acid by forming *o*-iminoquinone.

In this immobilization method, sodium periodate catalyzes the reaction in mild conditions and it is not detrimental to the protein's activity as it does not normally react with them. It is possible for periodate to react with some amino acids present in the protein at high concentration. These include methionine and cysteine which may be attacked at the sulfur group, tryptophan and histidine where the heterocycle as well as the side chain are involved in the oxidation, tyrosine where the phenolic group substituted at the para position is relevant for oxidation to take place, and N-terminal serine and threonine (as for these last two, the amino and hydroxyl groups must be unsubstituted).[70] There are reports where the composition of the peptide remained qualitatively unchanged upon oxidation with a 15 M excess for 10 days at room temperature.[71]

Generally, reaction of periodate with peptide residues takes place when the oxidant is in large excess and the oxidation is carried out for a prolonged time, 120-250 M in more than 15 hours.[72,73] The amount of over-oxidation will be even less when the amino acids susceptible to it are not exposed on the surface.[74] Furthermore, the oxidation of different amino acids is highly affected by the conditions used. At a certain pH, the oxidation of a residue may be favored, but at a different pH the residue oxidized may be a different one.[75]

Also, oxidation depends on the nature of the compound to be oxidized; for example, some residues are more readily oxidized than others, which may render selectivity in the process. High oxidizability of a residue over others like 3,4-dihydroxyphenylalanine (DOPA)-containing peptides renders selectivity during oxidation with periodate.[76,77] This property is expected for the incorporated 3-$NH_2$Tyr in this work.

T365(3-$NH_2$Tyr) P450 BM3 was immobilized in the same way as the mutated P450cam. Nevertheless, the tagging process was not as good as when tetraethylene glycol was used as the linker. Attempts to attach the protein in a non-pegylated surface were not fully successful, but a monolayer of protein was obtained when the pegylated surface was used. This is most likely due to the properties that the PEG-like linker provides. PEG renders protein stability, prevents aggregation of proteins, especially for hydrophobic ones by providing a lipid-like environment, or because of its hydrophilicity by increasing the water content around the protein and providing a

more like cell environment for water soluble proteins. For example, water soluble gold and FePt MNPs have been produced when functionalized with PEG ligands.[78] It is biocompatible, inert to the protein and to the reaction conditions used. Pegylated surfaces are also important in preventing or minimizing protein adsorption[79,80] which may change the 3D shape of the protein which can lead to denaturation[81] This is most likely because the protein is no longer in solution so its hydrophilic interactions are gone after the adsorption and the hydrophobic ones may change as well on the support. Another property that the pegylated surface provides is the flexibility of the linker and the minimization of steric hindrance resulting in a more orderly attachment of protein and without deformations of its 3D shape. It may be possible that both adsorption of the protein as well as the size of the protein is more appropriate for the pegylated surface. But on non-pegylated surfaces the protein attaches in a more sporadically way resulting in some places containing more protein than other spaces as the support is cleaned of the adsorbed protein during the washing process by leaching out. It may also be possible that the surface area of the pegylated support increases with the flexibility of the linker as compared to the non-pegylated one.

*5.3.2 AFM Characterization of Immobilized CYP P450s with Controlled Orientation*

AFM topography was done to monitor the immobilization of the mutated protein (Figure 5-2). It can be observed from these AFM images that the morphology of the support has changed considerably along the process of functionalization and protein immobilization. Figure 5-2 (A) shows an average height of 7 nm for the Q343(3-$NH_2$Tyr) P450cam which is consistent with the size of the linker and the protein based on the crystal structure of the WT P450cam. Figure 5-2 (B) corresponds to the acryloyl derivatized glass slide. The irregularities on its surface are due to the presence of the functional groups. However, the 15 nm feature height clearly allows for the difference once the protein has been attached confirming therefore, that the protein has been successfully immobilized in an almost uniform monolayer.

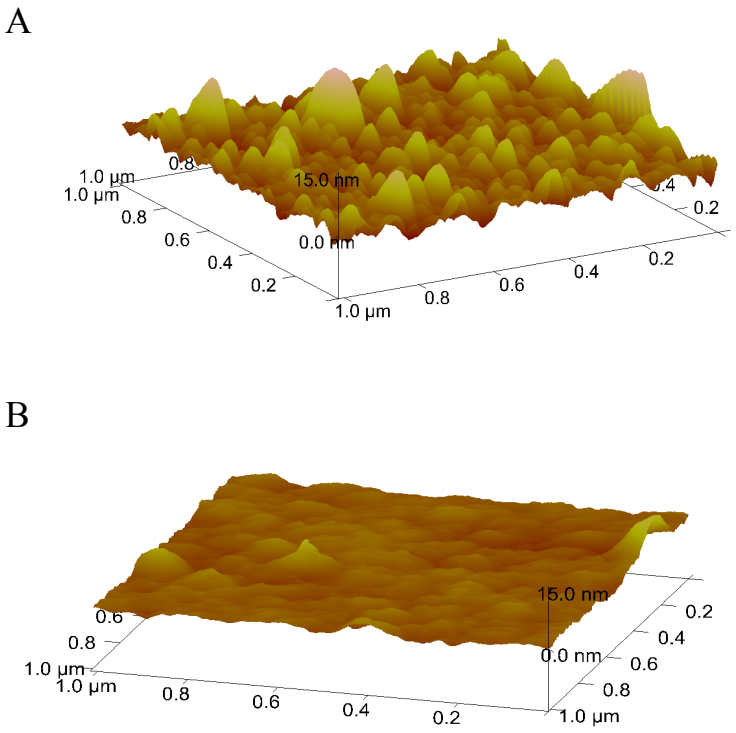


Figure 5-2 Three-dimensional representation of the AFM topographic image for (A) Q343(3-$NH_2$Tyr) P450cam immobilized onto acryloyl functionalized glass surface. (B) Blank acryloyl derivatized glass surface.

Figure 5-3 shows AFM topographic images of immobilized T365(3-$NH_2$Tyr) P450 BM3 on glass surface. Figure 5-3 (B) shows a homogeneous monolayer of proteins evenly spaced on the support and presenting an average height of 15 nm, which is in agreement with the length of the modified linker and the size of the protein based on the crystal structure of the WT P450 BM3. On the other hand, Figure 5-3(C) shows the topographic image of the support with PEG linker and acryloyl end functionality which provide irregularities to the morphology of the glass derivatized glass surface, but these are minimal even at a of 10 nm feature height. Additionally, Figure 5-3(D) shows that the WT P450 BM3 does not attach in the presence of $NaIO_4$ further confirming the efficiency of the method to immobilize proteins with full control over their orientation. These results are comparable to those obtained for P450cam proteins described above.

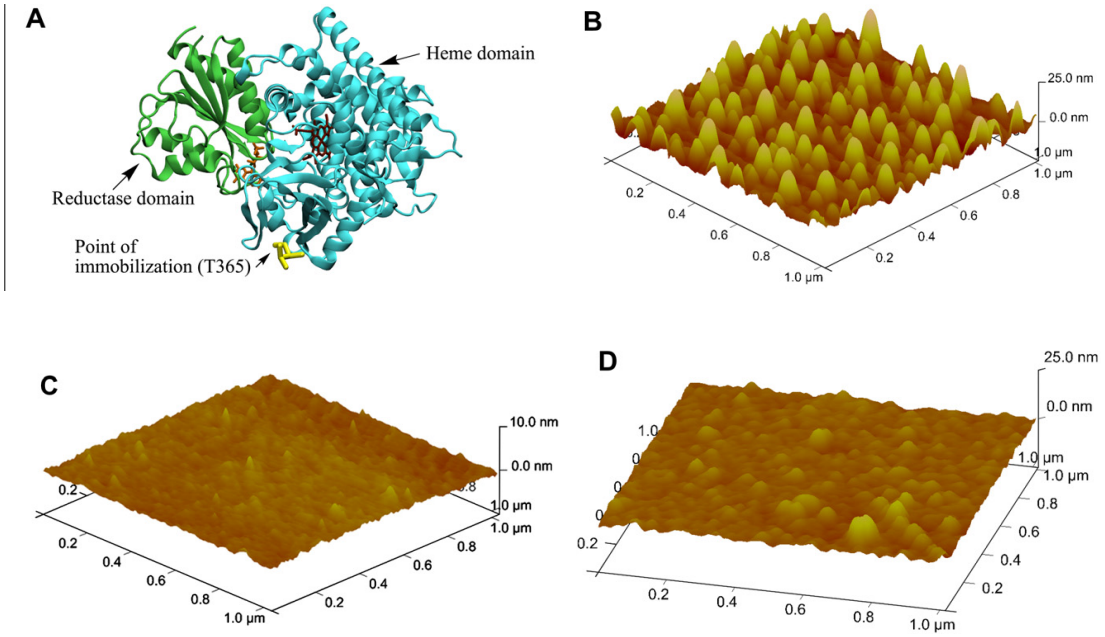


Figure 5-3 AFM topographic image of solid support attachment of P450 BM3. (A) 3-$NH_2$Tyr mutation at Thr365 position inP450 BM3 provides the site of attachment leaving the active site fully accessible. P450 BM3 image was prepared by Visual Molecular Dynamics (VMD) program and Protein Data Bank (PDB) accession number 1BVY. (B) Three-dimensional representations of the AFM topographical data for T365 (3-$NH_2$Tyr) mutant P450 BM3 immobilized onto acryloyl functionalized glass surface. (C) The blank polyethylene glycol (PEG)-acryloyl derivatized glass surface.(D)WT P450 BM3 attachment onto PEG–acryloyl surface in the presence of NaIO4 (100 µM).

These results were obtained based on a method with potential for the generation of protein microarrays. Therefore, the investigation regarding the effectiveness of this method was addressed by generating a microarray where five mutants were printed on a single functionalized glass slide (Figure 5-4). Figure 5-4 (Column 1) shows the presence of Coomassie bromophenol blue stained proteins after the slide had been thoroughly washed to remove any unbound protein. Figure 5-4 (Column 1 B) proves that protein is bound only in the presence of $NaIO_4$, which reassures that proteins are immobilized through covalent bonds. Studies related to the orientation of the protein arrays and protein-protein interactions were done by allowing HiLyte 647 fluorophore-conjugated anti-6xHis tag rabbit IgG to interact with the proteins spotted on the glass surface in column 2. Results clearly show the controlled orientation of the protein and the specific

interaction with IgG provided that only T365(3-$NH_2$Tyr) P450 BM3 and S3(3-$NH_2$Tyr) MB have the surface-exposed 6-His-tag chains are the only proteins that show efficient binding with IgG.

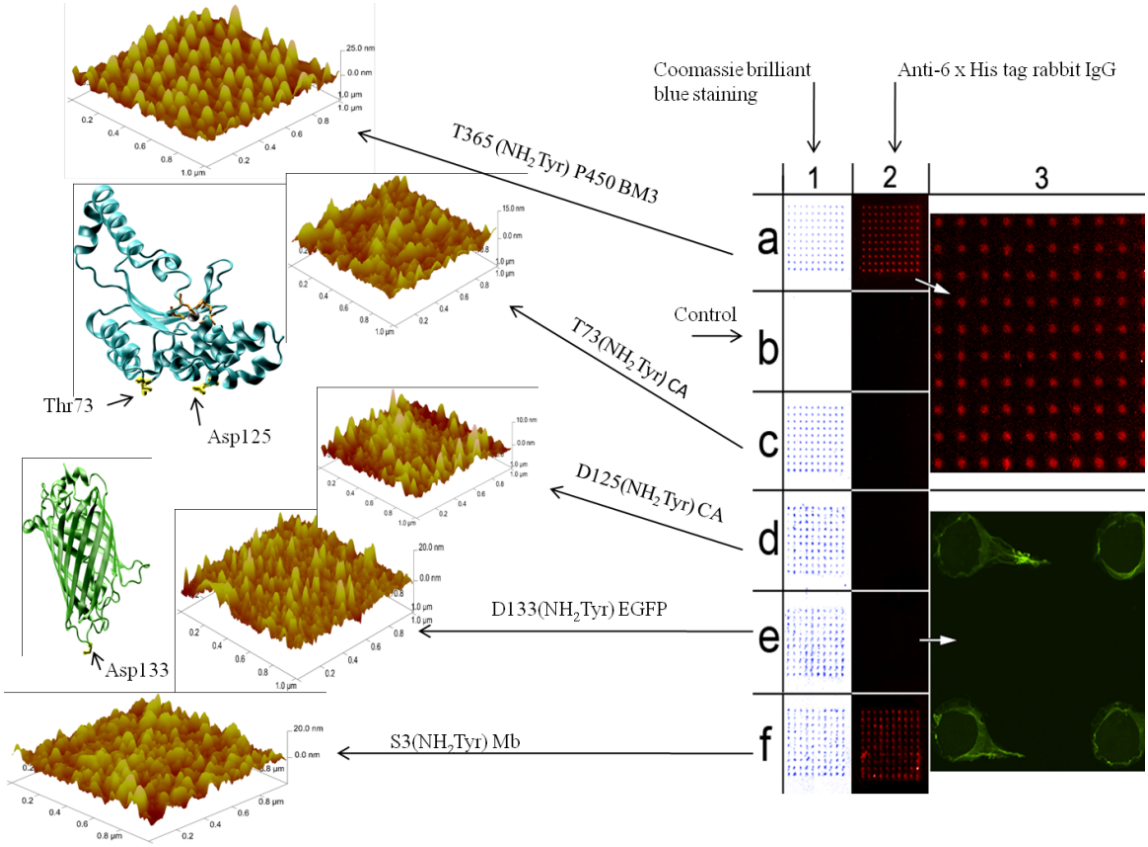


Figure 5-4 A microarray of five proteins on a single slide displays Coomassie brilliant blue staining and binding of HiLyte-conjugated anti-6-His-tagged rabbit IgG and EGFP (495 nm excitation). Column 1 displays a Coomassie bromophenol blue- stained protein slide showing five separate proteins printed onto an acryloyl- functionalized slide after the addition of 0.1 mM $NaIO_4$ (BioRobotics MicroGrid II 600). The printed slide was washed for more than 48 h using 100 mM potassium phosphate buffer at pH 6.0. (A) T365(3-$NH_2$Tyr) P450 BM3. (B) P450 BM3 control without $NaIO_4$ (control shows that printed proteins were detached from the surface after washing). (C) T73(3-$NH_2$Tyr) CA. (D) D125(3-$NH_2$Tyr) CA. (E) D133(3-$NH_2$Tyr) EGFP. (F) S3(3-$NH_2$Tyr) Mb. Column 2 displays an image of excitation at 649 nm and emission at 666 nm (GenePix 4200a) after binding of HiLyte 647 fluorophore- labeled anti-6xHis-tagged rabbit IgG (Anaspec), showing availability of the 6-His tag to only T365(3-$NH_2$Tyr) P450 BM3 and S3(3-$NH_2$Tyr) Mb mutants. Column 3 displays row A zoomed in, showing an ordered array interacting with the C-terminal His tag of the P450 BM3 and rabbit IgG, and displays a row E image of printed D133(3-$NH_2$Tyr) mutant EGFP on the surface after washing (but not binding with rabbit IgG) taken with a Nikon microscope using excitation at 488 nm with emission at 510 nm with a 10x objective lens.

The concept of covalent immobilization following the method described was proved. Consequently, it was expanded for the immobilization of the protein onto other supports such as gold electrodes. Furthermore, random immobilization of P450cam via amide bioconjugation reaction was explored in such supports

*5.3.3 WT P450cam Immobilization on Glass surface*

Figure 5-5 describes the main steps carried out for support functionalization and immobilization of the WT protein. Protein tagging on the amino functionalized support takes place by amide bond formation between the carboxyl groups available on the surface of the protein and the amino groups of the support aided by EDC under acidic conditions. This was achieved by simply incubating the amino-functionalized glass support in a solution of WT protein in presence of EDC for 3 h. After the immobilization, the support was thoroughly washed with KPi buffer (0.50 mM, pH 7.4) to remove any unbound protein. The carboxyl groups are provided by Asp, Glu and carboxyl end residues on the periphery of the protein, which are shown in red in Figure 5-6. These carboxyl groups can be activated by carbodiimides, which form the presumptive highly reactive o-acylisourea intermediates that undergo nucleophilic substitutions with amines. While the nature of the amine has been found to influence the type of reaction at the carboxylic carbon where substitution is not always the main product, the nature of the carbodiimide seems not to affect amide bond formation. However, any side reaction or by-product must be taken into consideration while deciding which carbodiimide to use.[67]

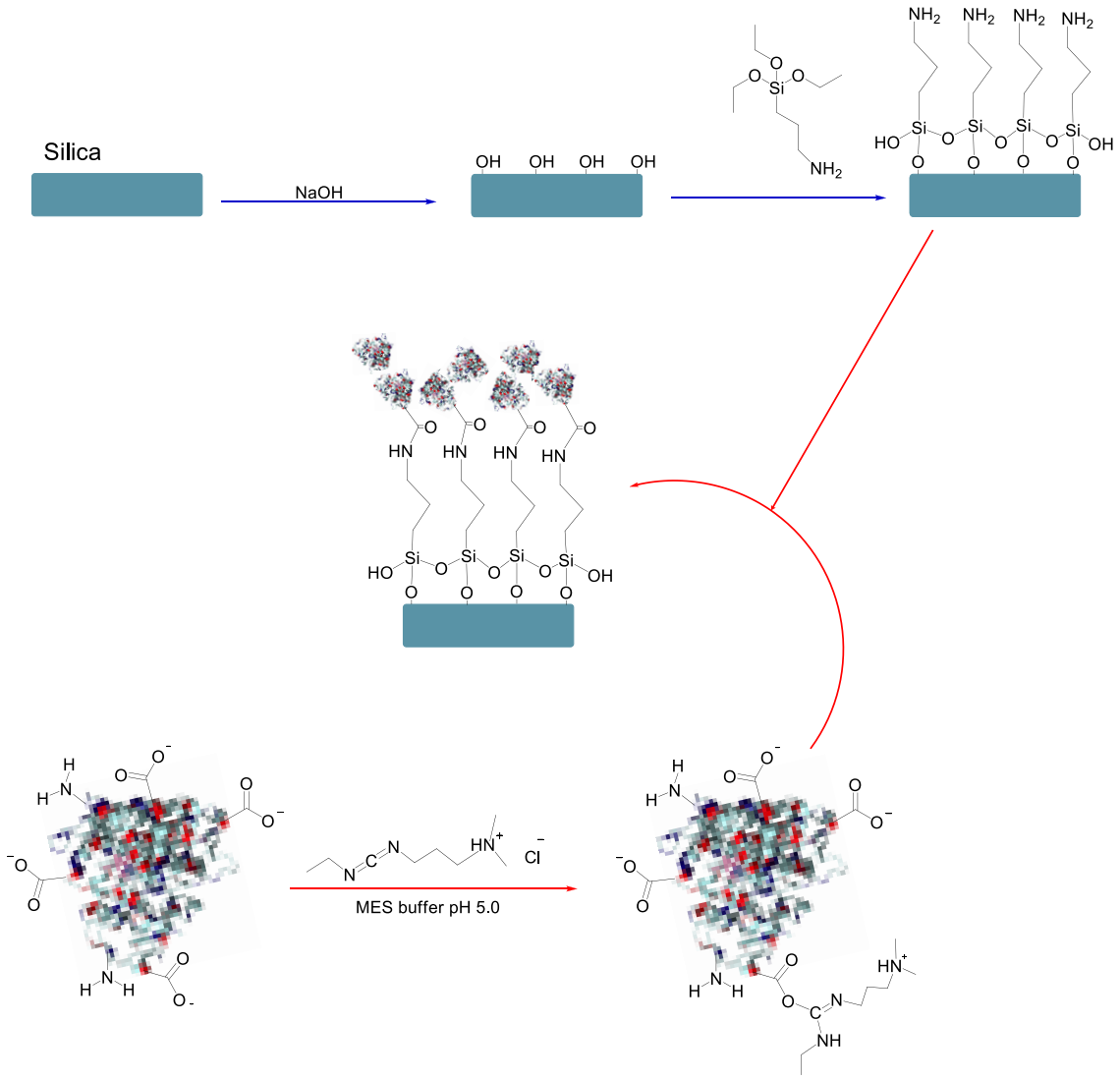


Figure 5-5 Schematic representation of silica dervatization and immobilization of WT P450cam.

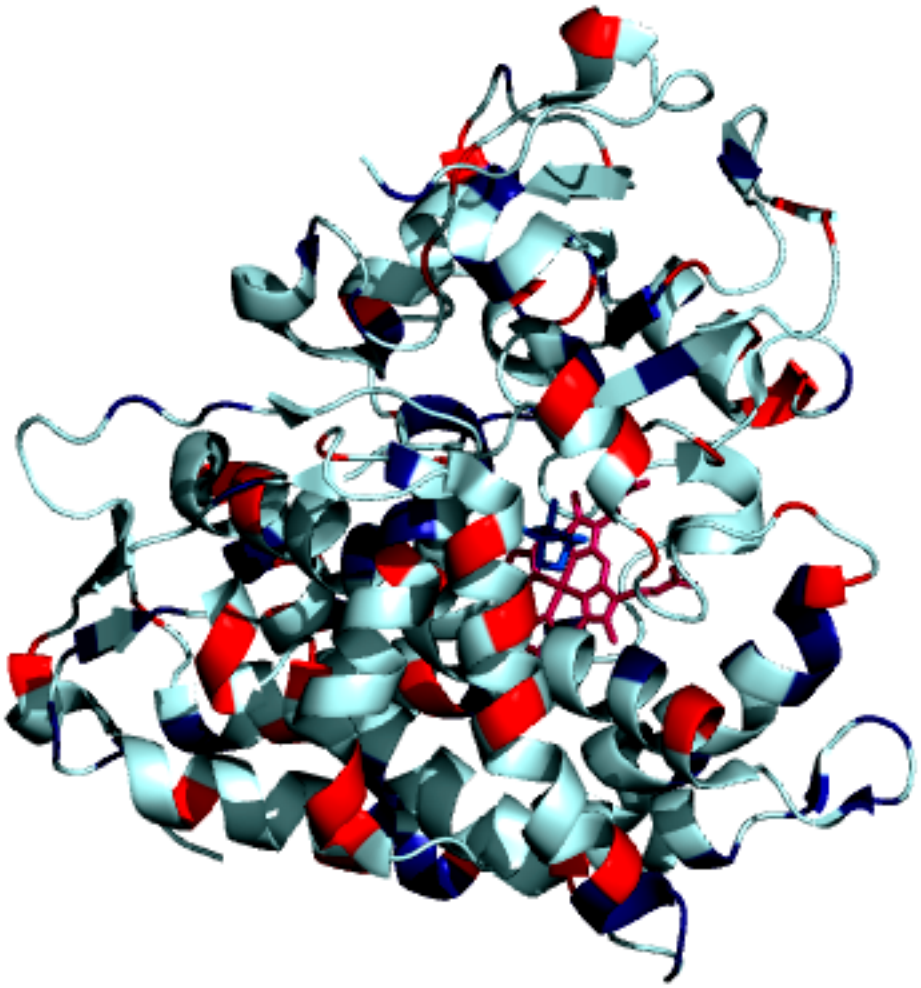

Figure 5-6 Graphical representation of WT P40cam showing acidic (red) and basic (blue) amino acid residues. The WT P450cam image was prepared by the PyMol Molecular Graphics System program and PDB accession number 1DZ8.

*5.3.4 AFM Characterization*

AFM topography (Figure 5-7) demonstrates the covalent immobilization of WT protein via amide bioconjugation reaction. Figure 5-7 (A) shows a layer with thickness varying from 15-30 nm. It is clear evidence that a large amount of protein has been immobilized when compared to the site specifically immobilized mutant protein (Figure 5-2 A). This result is not surprising as the protein has numerous amino groups exposed in its periphery (Lys, Arg and amino end) indicated

in blue (Figure 5-6) that can participate in amide bioconjugation with the carboxyl groups of other proteins forming a multiprotein layer on the chemically modified surface.

To ensure that WT protein on the glass surface was covalently bound and not just adsorbed and coagulated on the surface, a control sample was prepared with the protein in absence of EDC (Figure 5-7 C) This topographic image shows that the morphology of the support has been changed as the surface shows irregularities when compared to the blank amino functionalized chip (Figure 5-7 B) which clearly shows a flat surface at 30 nm feature. These irregularities are most likely the result of coagulated protein on the support. Nevertheless, the irregularities are minimal at 30 nm feature and consequently provides evidence that the WT protein has been covalently bound only in presence of EDC (Figure 5-7 A). It also reveals that bioconjugation reaction provides a protein multilayer on the chemically modified support.

Sriparna *et al*.[68] have recently reported a WT myoglobin multilayer immobilized onto gold electrode via EDC bioconjugation vs. a single protein monolayer generated by immobilized S3-$NH_2$Tyr Mb onto acryloyl derivatized gold electrode via Diels Alder reaction. They observed a multilayer of 175 nm height feature topography image compared to a single mutant myoglobin monolayer with 5 nm height feature topography. This is a 35-time layer increment in height. In the case of immobilized WT P450cam in this study reveals a 2-time layer increment. It may be possible that not all the carboxylate and amino groups on the periphery of the protein have the same reactivity towards crosslinking with EDC, as was observed in the case of WT myoglobin. Timkovich has observed that EDC may have preference for some residues or even carboxylic acid side chains. [82] It is also possible that the reaction time may have an effect on the observed results.[83,84]

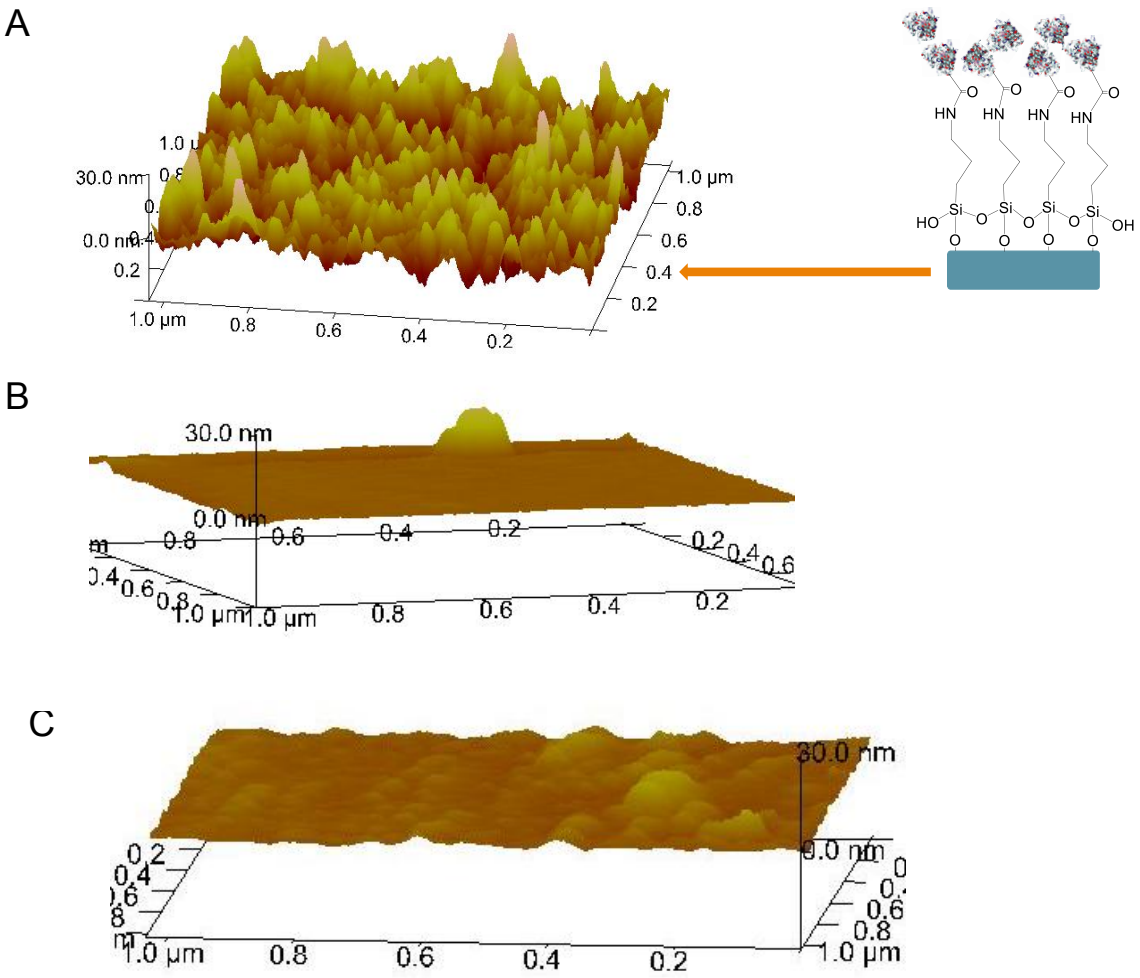


Figure 5-7 Three-dimensional representation of the AFM topographic image for (A) WT P450cam immobilized onto amine functionalized surface. (B) Blank amine derivatized glass surface. (C) WT P450cam immobilization amine functionalized surface in absence of EDC.

Immobilization of WT P450cam following the method described above was successful. Consequently, it was expanded for the immobilization of the protein to other supports, such as Si-NPs, gold electrodes, polypropylene surfaces, etc.

*5.3.5 Random Immobilization of P450cam on Amine-Functionalized Silica Nanoparticles*

Protein immobilization onto silica followed the same principles for the immobilization on glass support. The amino-functionalized NPs were added to a protein solution in MES buffer (pH

5) containing camphor to prevent protein denaturation followed by addition of EDC. A 3 h time incubation was enough to tag the protein on the silica NPs surface. The tagging process was monitored using UV-Vis. At the end of the reaction, the silica bound protein was thoroughly washed to eliminate any unbound protein. The washings were collected and checked for unbound protein. The concentration of the protein in the washings was very low indicating that the load of the protein on silica following this method is highly efficient. Although it is probable that some of the protein has been adsorbed, the washings were not extended for very long periods to prevent any possible denaturation of the protein. Furthermore, as it was mentioned, the concentration of the protein in the first washing was extremely low, and protein was not detected in subsequent washes. Figure 5-8 shows the bound WT P450cam silica NPs with a reddish colored due to the presence of the bound P450cam.


Figure 5-8 Silica bound WT P450cam in potassium phosphate buffer (50 mM, pH 7.4)

Preliminary studies related to the electrochemistry of the protein were carried out to investigate the effect on the redox properties when the protein is immobilized.

*5.3.6 Electrochemical Studies*

To investigate the electrochemistry of WT P450cam proteins, the bioconjugation reaction via amide bond formation was used to immobilize cytochrome P450 proteins on gold electrode surface. In this case, the gold surface was cleaned and functionalized by incubating it in a cysteamine solution. The protein was immobilized onto the derivatized gold surface in the presence of EDC. This process is represented in Figure 5-9.

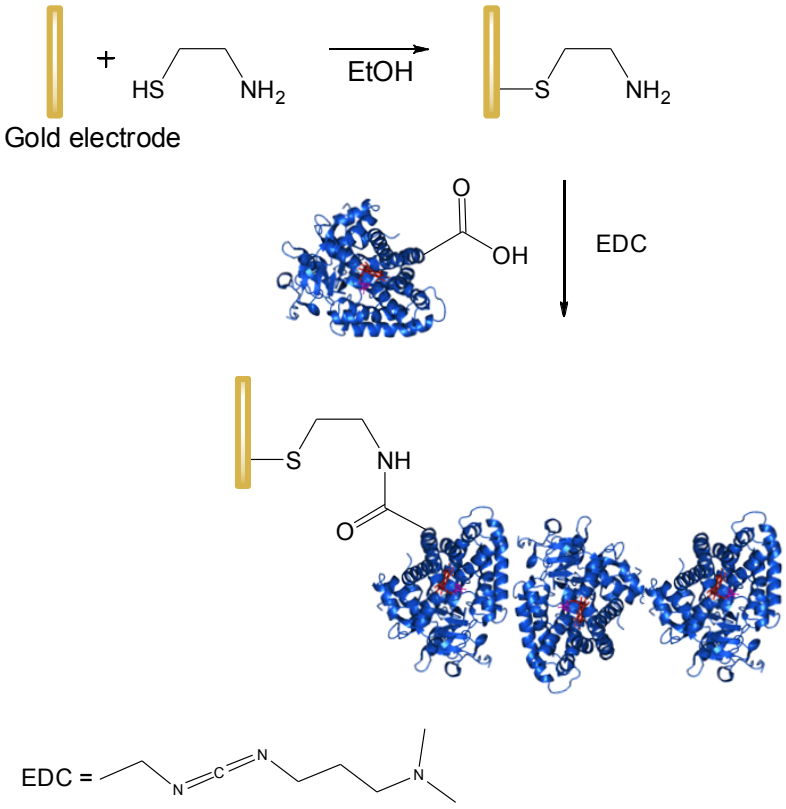


Figure 5-9 Schematic representation of electrode modification and immobilization of WT P450cam.

The main steps for the Q343(3-$NH_2$Tyr) mutant P450cam immobilization are highlighted in Figure 5-10, where the mutant protein was immobilized on a gold electrode pretreated with cysteamine hydrochloride and further derivatized with tetraethylene glycol diacrylate (TEGDA)

that leave an unsaturated C=C bond exposed on the surface of the electrode. Protein tagging was achieved by Diels-Alder bioconjugation between the unsaturated functional group on the electrode surface and the oxidized unnatural amino acid of the protein in presence of 40 μM $NaIO_4$.

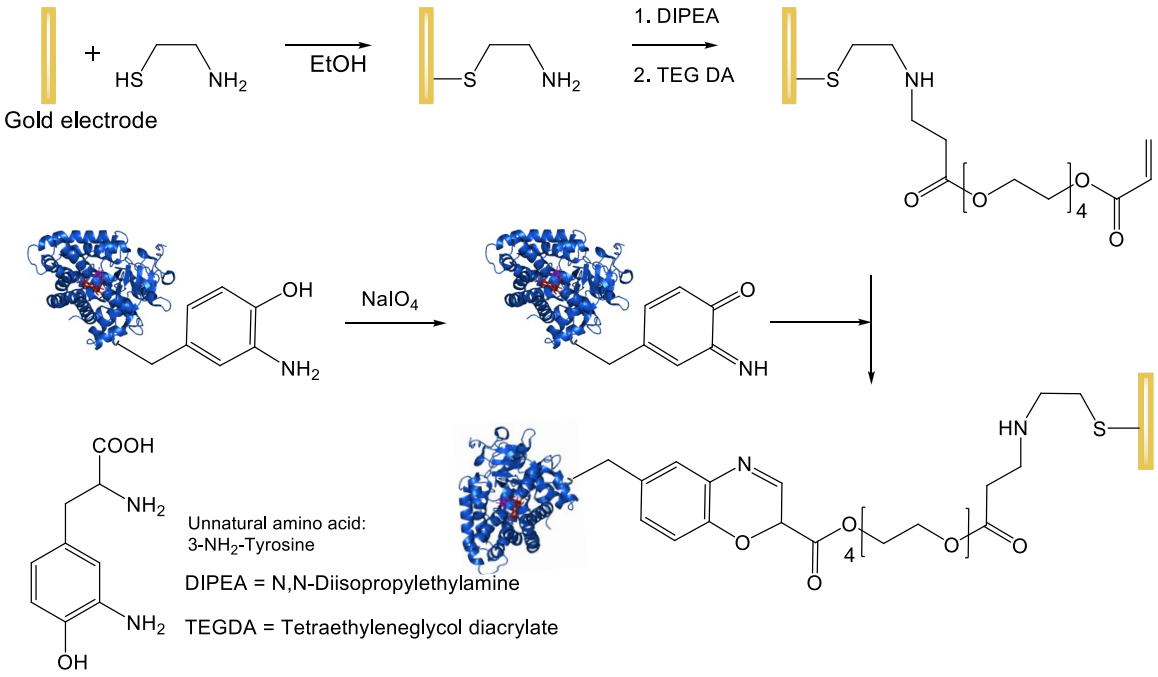


Figure 5-10 Schematic representation of electrode modification and immobilization of mutant Q343(3-$NH_2$Tyr) P450cam

Figure 5-11 shows a cyclic voltamogram of WT P450cam immobilized on the gold electrode. It was found that the redox potential (E°) is -350 mV compared to -375 mV (literature value) [85] The immobilization of the protein resulted in a slight decrease of the protein's redox potential, such variations often occur when electrodes are modified with different substances. The linker is different for both proteins. Therefore, this may be a factor, as the nature of the linker has been found to affect electron transfer from the electrode to the protein.[86,87]

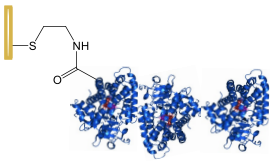


WT P450cam *vs* Ag/AgCl

$E^o$ = - 350 mV
$E^o$ = - 375 mV (literature value)

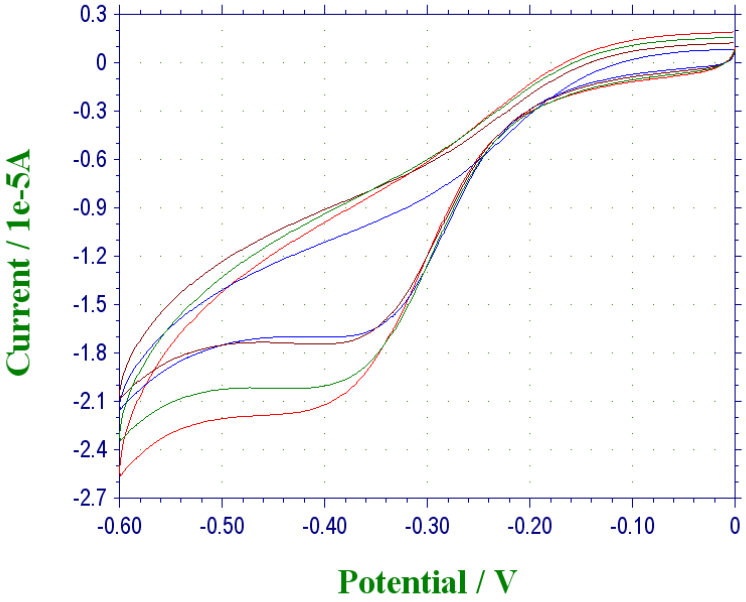


Figure 5-11 Electrochemical response of WT P450cam-immobilized gold electrode in 100 mM phosphate buffer, pH 7.0, 10 mM KCl at room temperature in nitrogen saturated conditions and at potential scan rates of 2-5 mV $s^{-1}$. The electrode area is 2 $cm^2$.

Figure 5-12 shows the electrochemical response of mutant Q343(3-$NH_2$Tyr) P450cam immobilized on the gold electrode. The results indicate an E° value of -400 mV for the mutant, compared to -350 mV for the WT protein as indicated in the above studies.

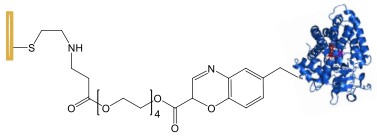

Mutant P450cam *vs* Ag/AgCl

$E^o$ = - 400 mV

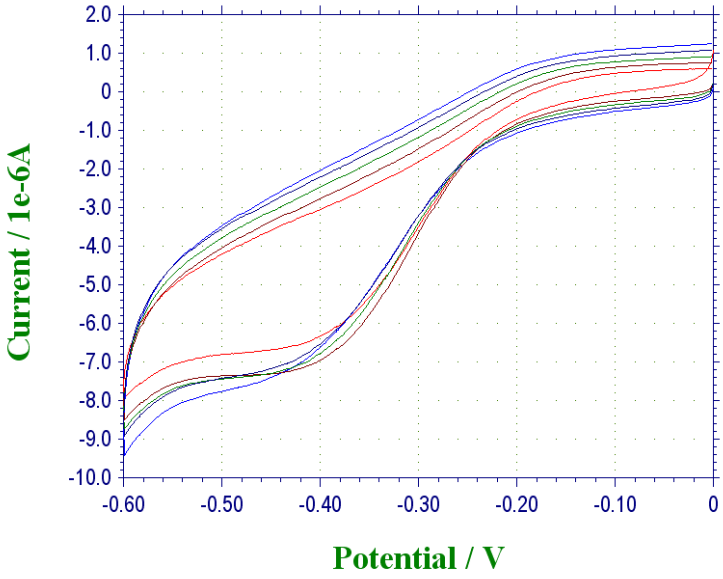


Figure 5-12 Electrochemical response of mutant Q343(3-$NH_2$Tyr) P450cam-immobilized gold electrode in 100 mM phosphate buffer, pH 7.0, 10 mM KCl at room temperature in nitrogen saturated conditions and at potential scan rates of 2-6 mV $s^{-1}$. The electrode area is 2 $cm^2$.

To ensure that the protein was immobilized and that it was transferring electrons, electrochemistry was done in the presence of potassium ferricyanide for the bare gold electrode, cysteamine functionalized gold electrode and WT P450cam immobilized on gold electrode for comparison as it can be seen in Figure 5-13 the voltammogram reveals that the functionalized gold electrode is equally efficient as the bare gold electrode during electron transfer, indicating that the presence of the cysteamine causes no effect during the process. However, the change in electron transfer can be observed for the protein immobilized electrode voltamogram. This effect is clearly due to electron uptake by the P450 protein on the gold electrode confirming that protein was immobilized on the electrode.

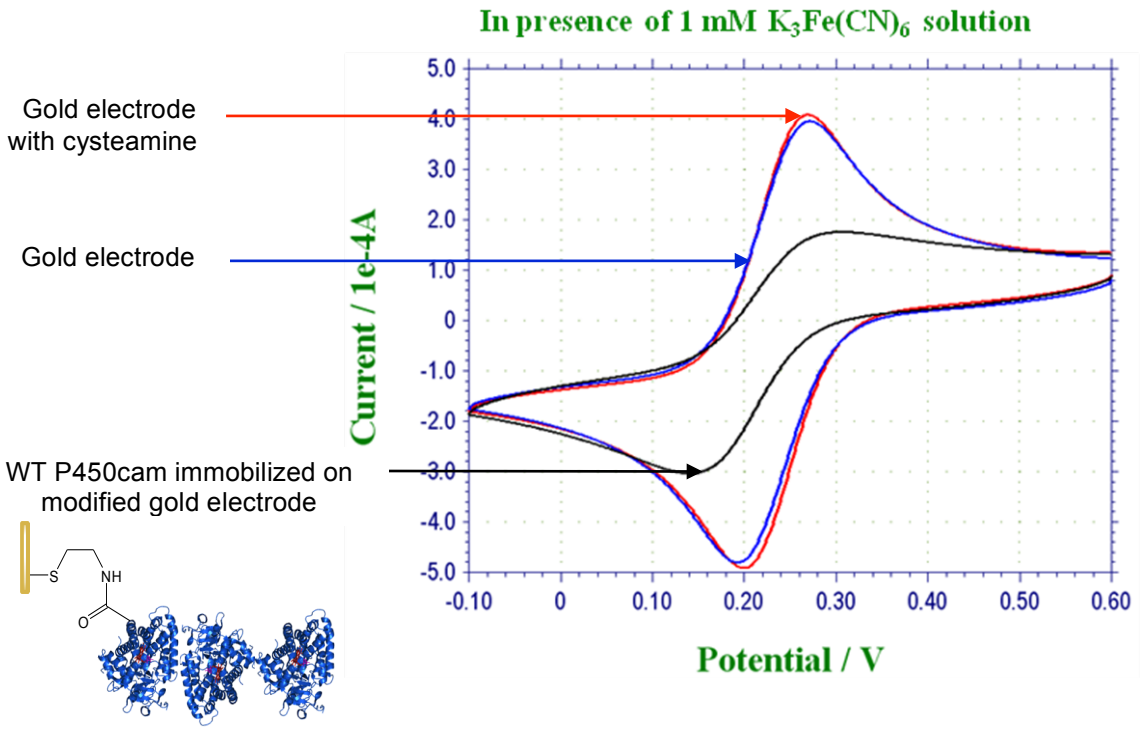


Figure 5-13 CV voltammograms of bare, modified and WT protein-immobilized gold electrode in presence of 1 mM $K_3Fe(CN)_6$ solution in 100 mM phosphate buffer, pH 7.0, 10 mM KCl at room temperature in nitrogen saturated conditions. The electrode area is 2 $cm^2$.

As mentioned before, these studies were done to investigate the redox potential and the electron transfer of immobilized P450cam proteins onto gold electrodes. Although the electrochemical catalysis was not investigated, it would be interesting to see the electro-catalytic activity of the protein when immobilized onto the modified gold electrode. While some studies have reported redox processes for protein immobilized on electrodes, there are other reports which revealed inactivation of immobilized proteins.[88] Todorovic *et al*. were unable to immobilize active P450cam on a silver electrode via EDC bioconjugation reaction as they found that immobilized protein was in the P420 form either in presence or absence of camphor.[87] Consequently, through the electrochemistry studies reported herein, it is not conclusive whether the immobilized P450 protein on the gold electrodes is active or not. But the immobilization method reported here was based on the work by Sriparna *et al.* with immobilized myoglobin

which exhibited active electrocatalytic oxidation of thioanisole.[68] Hence, more experimental evidence is required to show the electrocatalytic activity of immobilized P450cam. Furthermore, as it will be seen in chapter 6, silica immobilized P450cam via EDC amide bond formation was effectively used for cyclohexane oxidation, demonstrating that protein was active after immobilization with this method.

## 5.4 Conclusion

A method to site-specifically bind proteins to support has been developed successfully in this study. The method takes advantage of a genetically incorporated 3-$NH_2$Tyr amino acid in P450cam and P450 BM3, which reacts with the acryloyl end group present in the functionalized support in presence of $NaIO_4$ via the Diels-Alder reaction in water. The strategy followed resulted in the respective protein monolayer covalently attached to the support as AFM studies revealed. Furthermore, the position of the unnatural amino acid on the proteins provides the opportunity to control its orientation; consequently, the anchored proteins have a particular orientation that provides availability of the active site to incoming substrates. This method has proven effective for the generation of oriented protein microarrays with potential to be exploited in drug discovery, bioremediation, biosensing, etc. A different approach for protein attachment consisted of an amide bioconjugation reaction which can be used to covalently immobilize protein on a functionalized support. The process takes advantage of the carboxyl groups present on the surface of the protein and the amino groups present on the support. AFM analysis reveled a multilayer attached on the support. P450cam protein has been efficiently immobilized in different supports including Si-NPs and gold electrodes. These methods for protein immobilization offer the possibility to generate fully active, stable and recyclable catalysts as the support carrying the protein can be recovered from the reaction medium which has also the advantage of reducing purification requirements as the reaction is not contaminated with the catalyst.

# Chapter 6

## Alkane Oxidation by P450cam and P450 BM3

All the experiments in this chapter were done by Leticia Loredo in the laboratory of Dr. Roshan Perera.

## 6.1 Introduction

The studies on this group of protein have allowed for a better understanding of the structure and function of immobilized as well as free (in solution) P450. P450cam catalyzes the oxidation of camphor to 5-exohydroxycamphor by the incorporation of an oxygen atom from molecular oxygen to the unreactive C-H bond, as a carbon source for *Pseudomonas putida*. To carryout its catalytic activity, the protein requires a two one-electron reduction at different stages of the catalytic cycle. NADH provides the electrons via redox patterns, PdR, and Pdx, where Pdx enables the ultimate electron transfer to the P450cam. The importance of Pdx goes beyond that of electron transfer, as it has been regarded as an effector important for the oxidation of the substrate.[89-91] The absence of this effector leads to auto oxidation of the oxygen bound to ferrous P450 substrate complex.[91]

The ability of P450s to efficiently activate stereospecifically and selectively C-H bonds has attracted much attention so as to exploit their catalytic properties to carry out the oxidation of un-reactive C-H bonds, which remains a challenge in organic synthesis. Protein engineering is very helpful for this purpose. It has been used to broaden substrate specificity as well as to improve the catalytic rate of these proteins.[92]

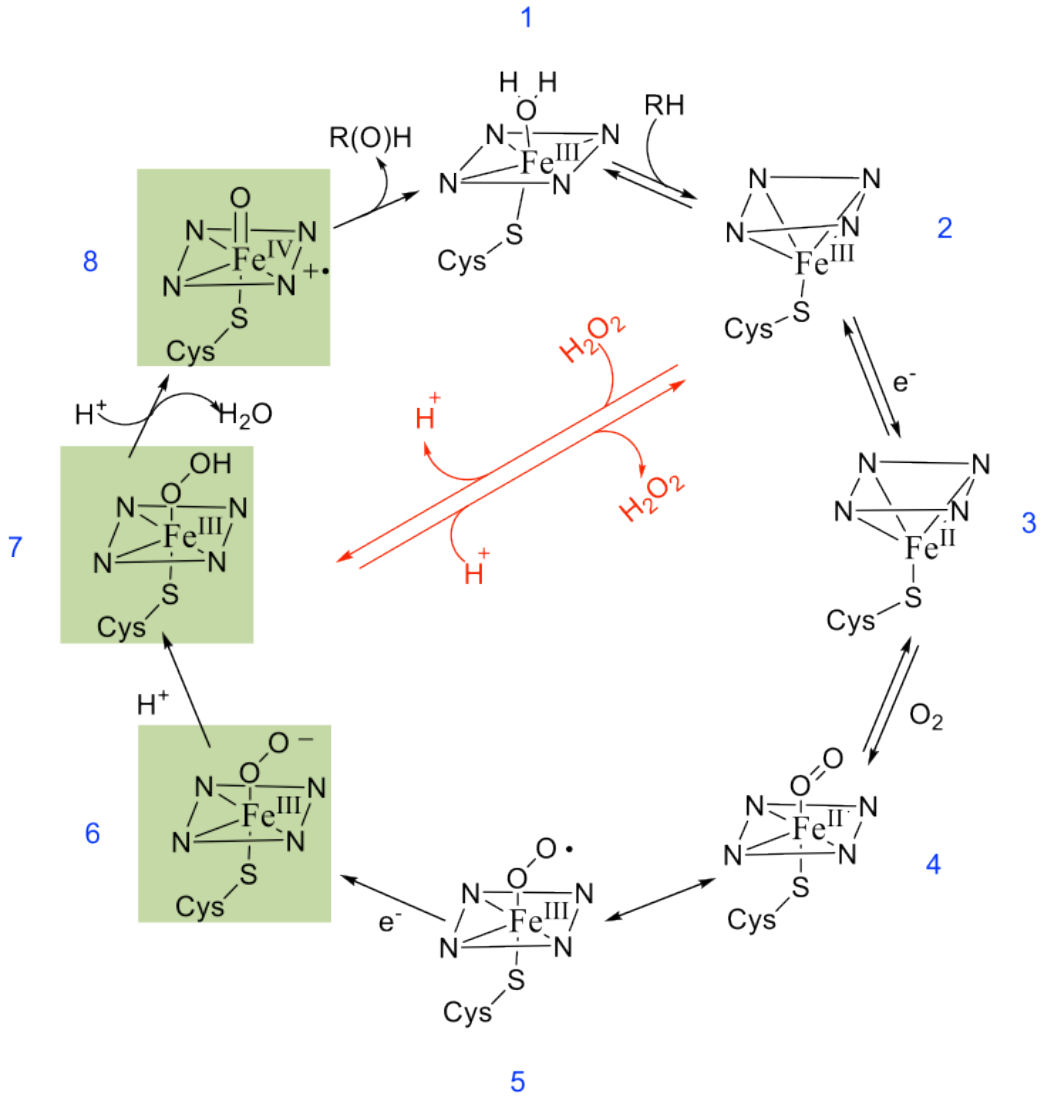


Figure 6-1 Catalytic cycle of cytochrome P450

P450 cytochromes catalyze the insertion of oxygen into a wide variety of compounds (Rxn 1). The proposed catalytic cycle of P450s (Figure 6-1)[85] starts with substrate binding to the resting state of the enzyme **1** which is found mainly in a low-spin hexacoordinate ferric form to give a high-spin pentacoordinate complex **2** by displacement of the axial ligand water. This change in spin is accompanied by a change in redox potential that makes possible the reduction [by NAD(P)H via flavoprotein/FeS proteins] to produce the high-spin ferrous state **3**. This is a good dioxygen binder and binds $O_2$ to give **4**, which is in equilibrium with the superoxide species

**5**. A second electron transfer takes place forming the iron(III)-peroxo complex **6**. Protonation of the distal oxygen in this complex aided by Thr 252 via water molecules leads to formation of iron(III)-hydroperoxo complex **7**. A second protonation of the distal oxygen in **7** gives $H_2O$ and oxygenated product, likely via **8**. This oxo-ferryl ($O=Fe^{IV}$) porphyrin cation radical called compound I is held responsible for hydroxylation reactions. Peroxide addition to **2** results in formation of **7** in a path known as the shunt pathway.

Given that the second electron transfer is the rate-determining step (r.d.s) and the subsequent steps highlighted in green in the catalytic cycle take place very fast, it has been difficult to characterize some of these reactive species, especially 6,7,and8. Nevertheless, these different reactive oxygen species (ROS) have been held responsible for carrying out diversity of reactions as well as the broad range of substrates that these proteins can act on. These properties of P450s have been attributed to the different oxidation states that the P450 heme center can acquire and the nature of its proximal ligand.[93] Figure 6-2 illustrates different reactions catalized by CYP P450s.

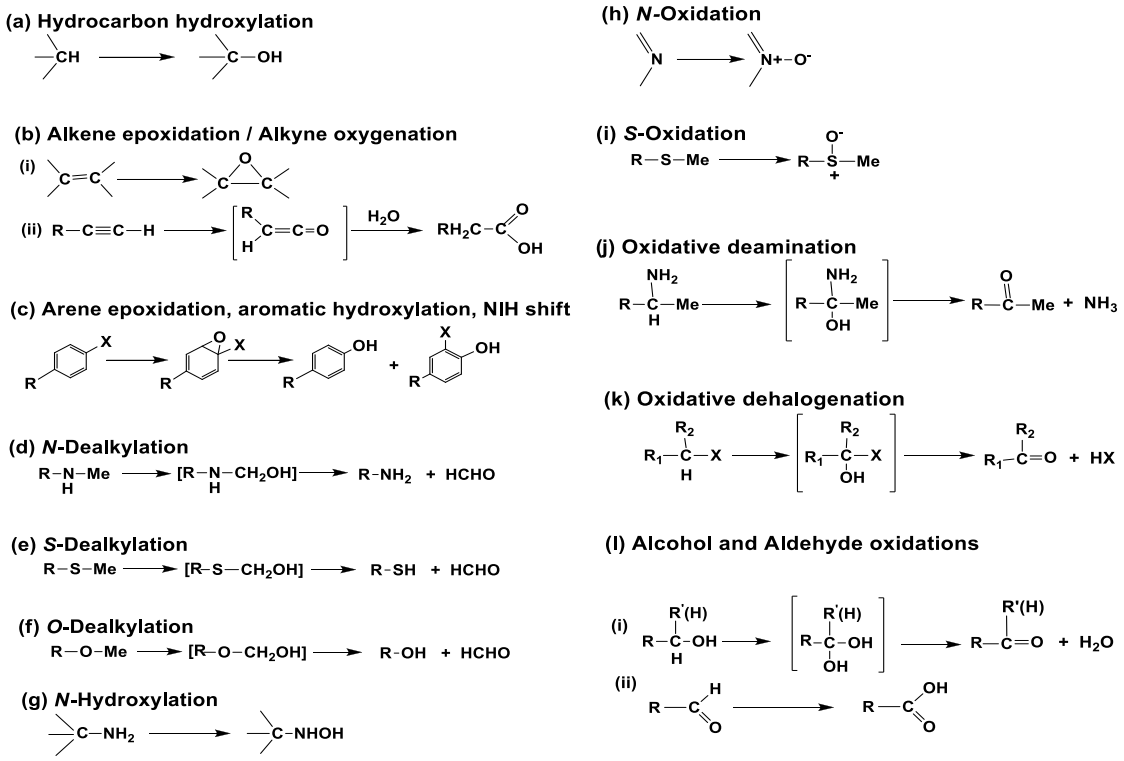


Figure 6-2 Schematic summary of the diverse P450 catalyzed reactions (Sono et al. 1996)[85]

The oxidation of camphor by P450cam is tightly bound to the ultimate electron donor of P450cam, the putidaredoxin coenzyme, which has been regarded as a protein necessary for the oxidation process of the P450cam. Studies on the binding of Pdx to P450cam have been crucial for the understanding of how these two proteins interact, and the possible pathway the electron transfer follows. These studies usually imply mutations that diminish the activity of the P450cam**.** Herein, we report the enhanced activity that results from the single mutation of P450cam at position Q343 with the unnatural amino acid 3-$NH_2$Tyr for the oxidation of camphor. This mutation is located next to an amino acid found to be important in the electron transfer from Pdx to P450cam. Mutation of P450cam at position Q343 has shown enhancement of the protein activity for the oxidation of camphor about four fold increments relative to the rate of the WT protein. This leads us to conclude that the position of the mutation and the redox properties of the 3-$NH_2$Tyr

may facilitate the electron transfer from the putidaredoxin to the P450cam protein as it is probably in the electron transfer pathway of these proteins.

## 6.2 Experimental Section

### *6.2.1 Chemicals*

3-(N-morpholino)propanesulfonic acid (MOPS) was obtained from Alfa Aesar, β-Nicotinamide adenine dinucleotide, reduced form disodium salt was from Acros Organics, β-Nicotinamide adenine dinucleotide 2′-phosphate reduced tetrasodium salt hydrate was from Sigma-Aldrich.

### *6.2.2 Instrumentation*

UV–Vis spectroscopy was taken using Cary 50 Bio UV-visible spectrophotometer.

Gas chromatography was performed on GCMS-QP2010 Shimadzu System, with a column SHRXI-5MS 30.0 m, diameter 0.25 mm, thickness 0.15 µm; carrier gas He, total flow 44.4 mL/min, column flow 1.34 mL/min, and linear velocity 41.7 cm/s.

### *6.2.3 Recombinant Proteins: Expression and Purification*

Experimental details for protein expression and purification of WT P450cam, Q343(3-$NH_2$Tyr) P450cam, non-His-tagged Pdx and PdR, WT P450 BM3 and T365(3-$NH_2$Tyr) P450 BM3 were given in chapter 3.

### *6.2.4 Catalytic Activities of WT and Mutant P450cam*

Catalytic activities were determined by spectrophotometrically monitoring the NADH consumption at 340nm following a literature procedure. [94] Briefly, reactions were carried out at 25 °C with the following composition: Protein (0.05 µM), PdR (4.0 µM), Pd (10 µM), D-(+)-camphor (1.0 mM), NADH (0.5 mM), and KCl (100 mM) in 20 mM phosphate buffer pH 7.4. The reaction was initiated by the addition of NADH. The activity was determined from the initial linear portion of

the graphs using the molar absorptivity with $\varepsilon_{340}$ = 6.22 $(mM.cm)^{-1}$ for NADH. Reactions were terminated and extracted with dichloromethane. The extracts were concentrated and analyzed via GC-MS.

*6.2.5 Cyclohexane to Cyclohexanol Conversion by Free WT P450cam*

Reactions were carried out at 25 °C in 1 mL volume with the following composition: WT P450cam (1.3 μM), cyclohexane (300 μL), PdR (4.0 μM), Pd (10 μM), D-(+)-camphor (1.0 ,mM), NADH (2 mM), KPi buffer (50 mM, pH 7.4). Reactions were allowed to run overnight, the cyclohexane layer and the extracts from aqueous layer with dichloromethane were analyzed via GC-MS, following the temperature program in Figure 6-3. Control reactions contained all components except protein.

| Rate (°C/min) | Final Temperature (°C) | Hold Time (min) |
|---|---|---|
| - | 40 | 2.00 |
| 20 | 200 | 2.00 |

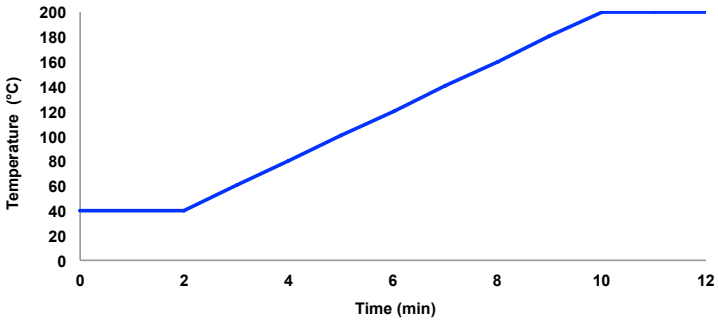


Figure 6-3 GC-MS temperature program conditions for conversion of cyclohexanol analysis.

*6.2.6 Cyclohexane to Cyclohexanol Conversion by WT P450cam Bound Si-NPs*

Reactions were carried out at 25 °C in 1 mL volume with the following composition: WT P450cam bound silica NPs, cyclohexane (1 mM), $H_2O_2$ (50 mM), KPi buffer (50 mM, pH 7.4). The reaction was initiated by addition of $H_2O_2$, which was added in aliquot portions over a period of 2 h. Reactions were allowed to run overnight. The reaction was centrifuged at 1000 rpm to isolate the protein bound NPs; the liquid portion was decanted and extracted with dichloromethane. The organic extracts were analyzed via GC-MS following the temperature conditions in Figure 6-3. Control reactions were carried out containing all components including amino-derivatized silica NPs except protein.

*6.2.7 Catalytic Activities of WT and Mutant P450 BM3*

Catalytic activities were determined by spectrophotometrically monitoring the NADH consumption at 340nm following a literature procedure. Briefly, the reactions were run in 0.5 mL. To P450 BM3 protein (25 nM) in MOPS buffer (50 mM, pH 7.4) was added arachidonic acid (100 μM). The mixture was incubated for 5 minutes followed by addition of NADPH (1 mM).

## 6.3 Results and Discussion

Activity measurement assays for camphor hydroxylation were carried out to determine the proper monooxygenation functionality of both WT P450cam and the mutant protein. The activity assays were carried out under the normal catalytic pathway of the protein, thereby using the reconstituted system containing Pdx and PdR, as well as the cofactor NADH. The catalytic process was monitored using UV-Vis spectrophotometry (Figure 6-4). This is possible due to the absorption of the cofactor at 340 nm, which can be correlated to the concentration of the consumed NADH and hence to the oxidation of camphor as the consumption of NADH is tightly coupled to the substrate oxidation in a 1:1 mol ratio. The WT P450cam showed activity of 1171 (nmol $min^{-1}$) similar to that of literature reported values, while the mutant Q343(3-$NH_2$Tyr) P450cam produced by site directed mutagenesis, showed enhanced activity compared to that of WT 4150 (nmol $min^{-1}$). Nevertheless, this value would increase even more, if the time between the mixing process and the first reading was taken in to consideration. It is clearly evident from Figure 6-4 that the consumption of NADH is higher for the reaction with the mutant protein than that of the WT. While NADH concentration is about 240 nmol for the reaction with WT that of the mutant protein is already about 130 nmol in the first reading. Additionally, for the mutant protein, it keeps decreasing to near complete consumption, while for the WT protein the process is much slower. Products were analyzed by GC-MS.

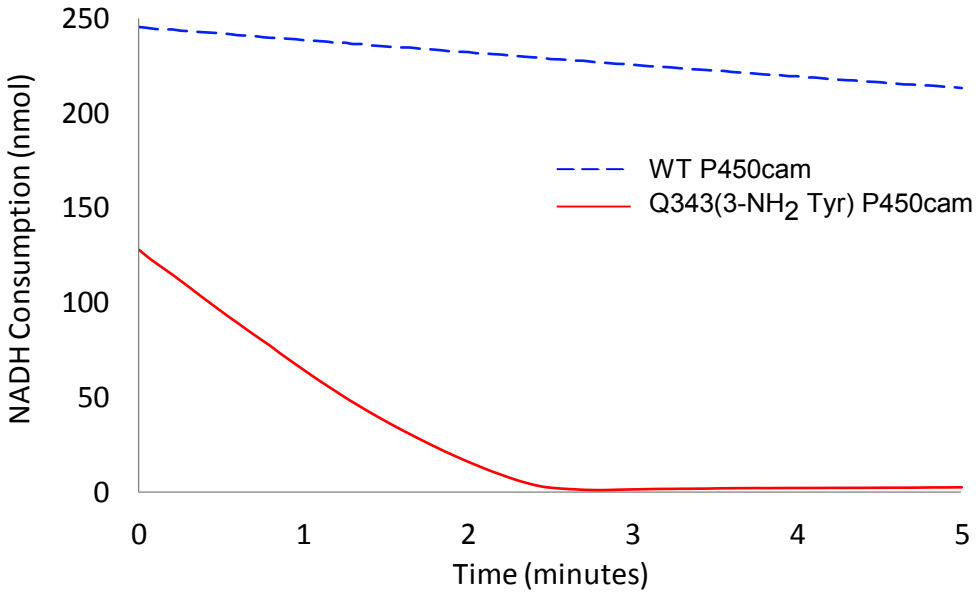


Figure 6-4 NADH consumption catalyzed by WT P450cam (dashed line) and Q343(3-$NH_2$Tyr) mutant P450cam (solid line) during the metabolism of camphor.

It has been concluded that the mutation at position Q343(3-$NH_2$Tyr) had no detrimental effects on the structure of the protein. From the results obtained, a possible explanation for the increased rate for camphor oxidation seems to be that the redox properties introduced by the unnatural amino acid and its position, which may facilitate the electron transfer from Pdx to the cytochrome. It is possible that Pdx interacts with Q343, which seems level with the R112, an important residue in the binding of Pdx[95] if the Pdx interactions extend over all this area. It may be particularly relevant if one takes into consideration that K344 residue interaction with Pdx has been reported[96] and is next to the mutation of the protein in this study (Figure 6.5).

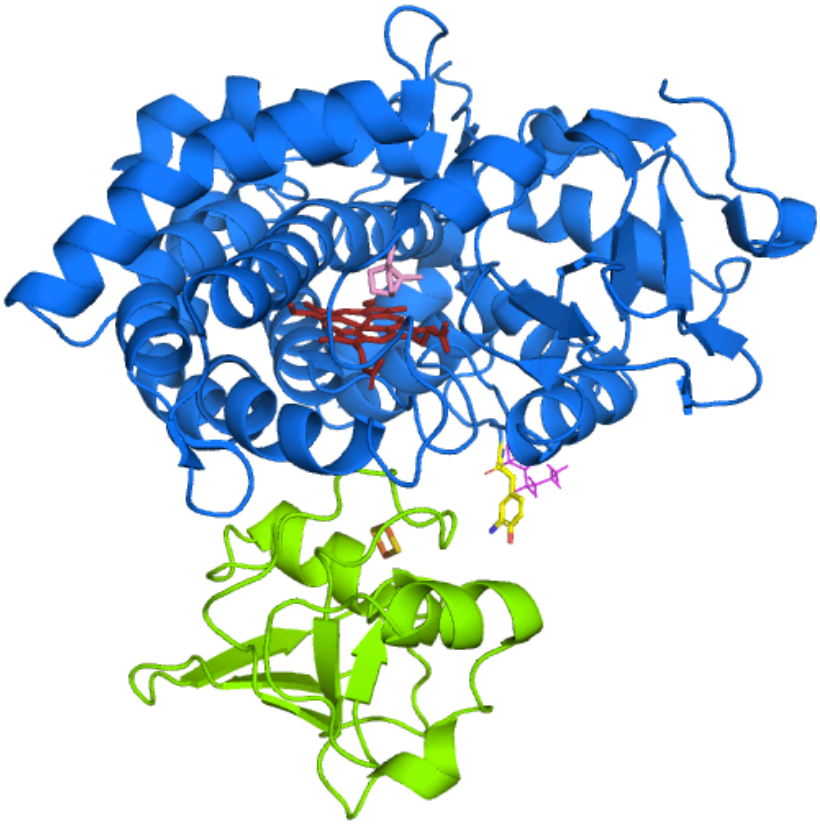

Figure 6-5 Graphical representation of Q343(3-$NH_2$Tyr) P40cam bound to Pdx showing K344 residue (magenta) next to the unnatural amino acid. The WT P450cam image was prepared by the PyMol Molecular Graphics System program and PDB accession number 2M56.

Given that the proteins were active, the next step was to investigate the potential of these CYP proteins to carry out the conversion of cyclohexane to cyclohexanol. In this context, the starting point was the use of free WT P450cam in its reconstituted system. Maurer *et al*. have used a biphasic system for the oxidation of cyclohexane[97] and in this study we applied this system to P450cam with its coenzymes, Pdx and PdR, and NADH cofactor. At the end of the reaction, the organic phase and combined extracts were analyzed by GC-MS.

Figure 6-6 presents the GC-MS analysis of the cyclohexanol produced by P450cam in its natural pathway. The gas chromatogram presents a peak with 5.14 min retention time identified for cyclohexanol through the EI-MS. As can be seen, no conversion of cyclohexanol took place in absence of proteins.

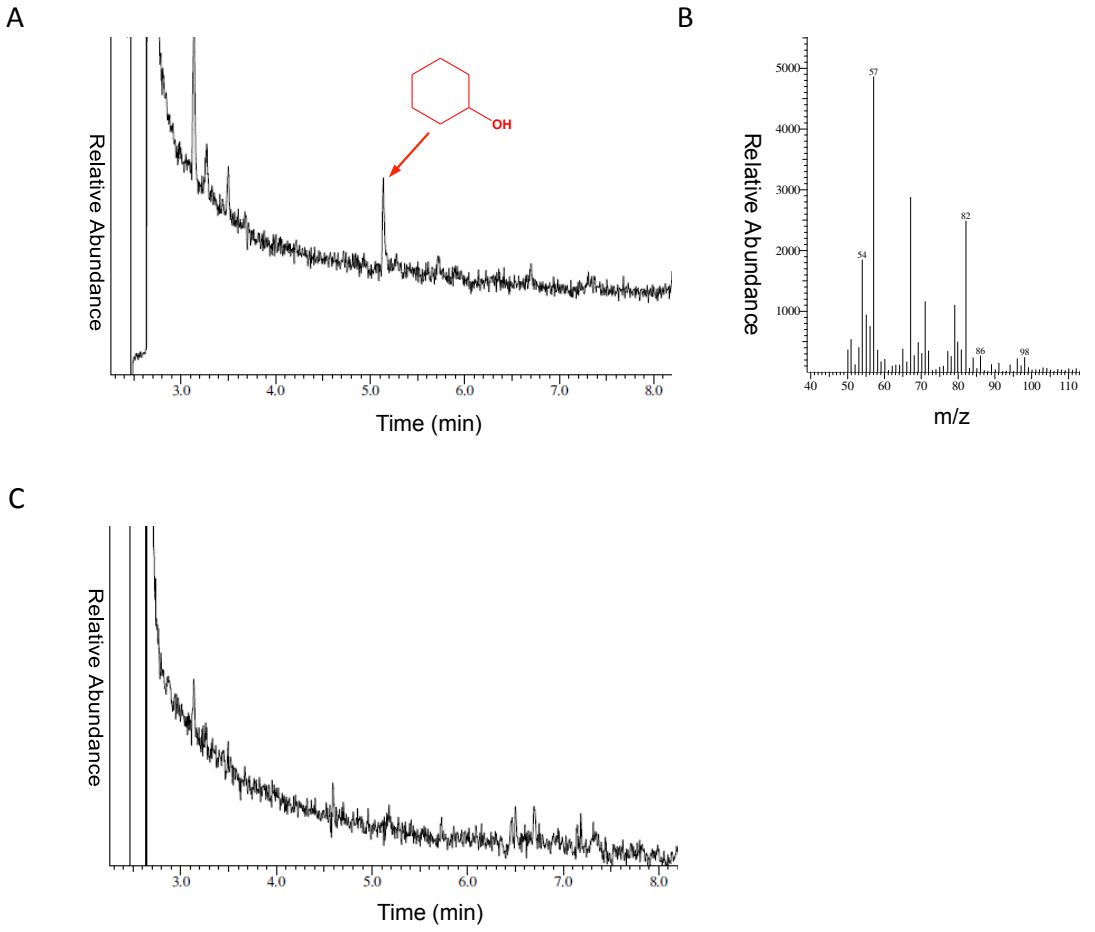


Figure 6-6 GC-MS analysis of cyclohexane layer and organic extracts from the cyclohexane to cyclohexanol conversion in biphasic system: (A) Gas chromatogram of the organic phase for cyclohexane to cyclohexanol conversion by WT P450cam. (B) Mass Spectrum of the cyclohexanol produced from the conversion of cyclohexane free WT P450cam as identified by comparing the spectra to the NIST database and to the authentic standard. (C) Gas chromatogram of the control from the biphasic system cyclohexane to cyclohexanol conversion. Conditions given under instrumentation and in Figure 6-3.

P450cam was able to carry out the oxidation of cyclohexane in solution. Nevertheless the goal has been to use immobilized protein to make a nanobioreactor where the catalyst can be recovered and reused for this type of hydrocarbon oxidation reactions. Furthermore, as mentioned earlier P450 proteins are capable of catalyzing oxidation reactions via the shunt pathway, eliminating coenzymes and cofactor requirements, which account for the limitations regarding the use of enzymes in synthetic lab reactions. Therefore, to take advantage of

immobilized enzymes and their catalytic activity in presence of peroxides the strategy presented in Figure 6-7 was developed. It consists of the C-H activation of cyclohexane by P450cam bound NPs using hydrogen peroxide as the oxidant; the hydroxylation can take place either in a batch reactor or in a continuous flow reactor mode. In this case, the batch reactor mode was used.

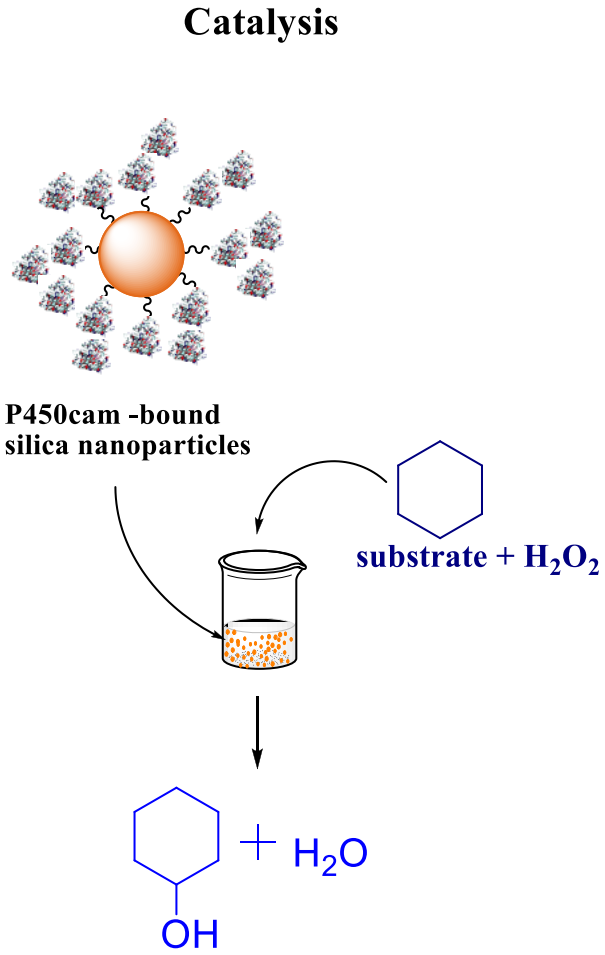


Figure 6-7 Strategy for the utilization of immobilized protein in the catalysis of cyclohexanol from cyclohexane in the presence of hydrogen peroxide

In this context, WT P450cam bound silica NPs were used in a batch reactor containing buffer, and cyclohexane. The reaction was initiated with aliquot additions of hydrogen peroxide. The reaction was allowed to take place under stirring conditions at 25 °C. At the end of the

reaction, the nano-biocatalyst was isolated from the reaction medium by centrifugation. The catalytic products were extracted from the reaction medium with dichloromethane and analyzed using GC-MS.

Figure 6-8 shows the GC-MS analysis of the cyclohexane to cyclohexanol conversion by P450cam in a batch reactor. The mass spectrum of the reaction shows a peak at 5.14 min, which corresponds to cyclohexanol (Figure 6-8 A). The ESI-MS of said peak is in agreement with that of cyclohexanol (Figure 6-8 B). Figure 6-8 (C) demonstrates that no cyclohexanol conversion takes place in absence of protein. The yield of cyclohexanol in this reaction was of 30%, which is relatively high if compared to the 10% yield of industrial processes. It is true that the reaction still needs optimization, but one thing to keep in mind is that the proteins in these studies were camphor bound. Camphor being their natural substrate, there is a higher affinity towards camphor by the protein than for cyclohexane, and consequently the efficiency of cyclohexane hydroxylation by the protein may be reduced.

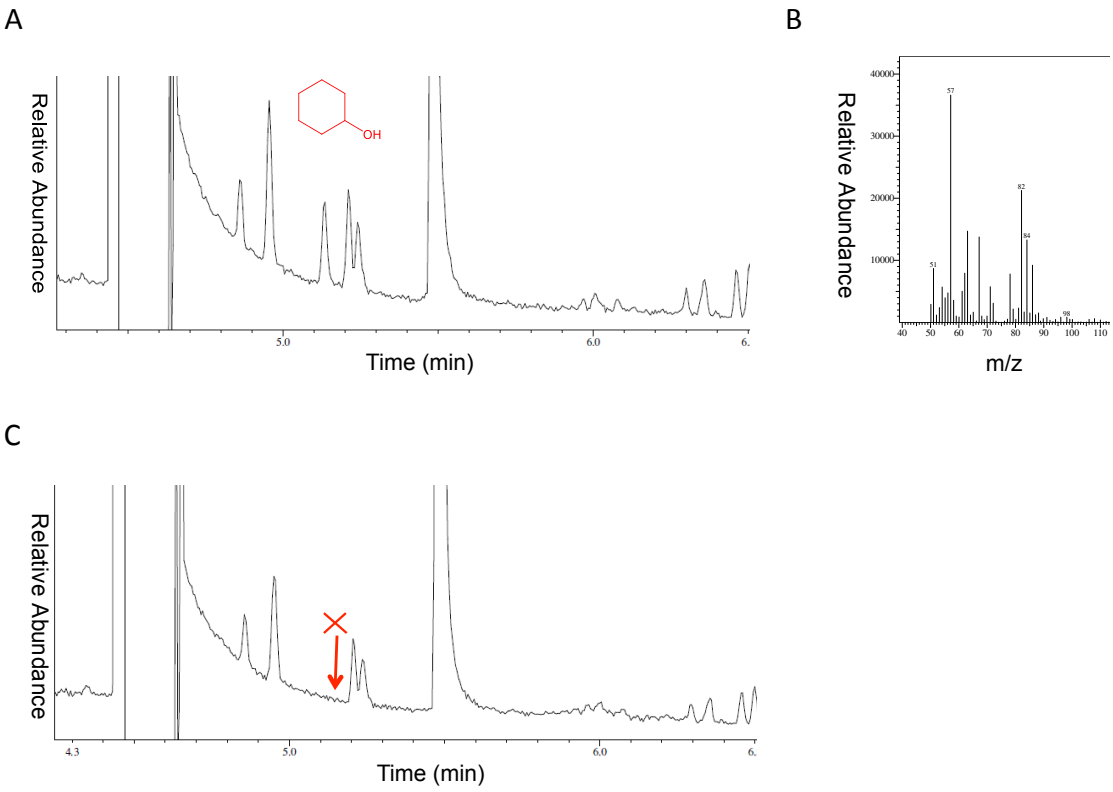


Figure 6-8 GC-MS analysis of dichloromethane extracts from the cyclohexane to cyclohexanol conversion in a batch reactor: (A) Gas chromatogram of the extract from cyclohexane to cyclohexanol conversion by immobilized WT onto amine derivatized silica. (B) Mass Spectrum of the cyclohexanol produced from the conversion of cyclohexane by immobilized WT onto amine-derivatized silica, as identified by comparing the spectra to the NIST database and to the authentic standard (data not shown). (C) Gas chromatogram of the control from the extract for the cyclohexane to cyclohexanol conversion in presence of amine derivatized silica without protein. Conditions given under instrumentation and in Figure 6-3.

This type of reaction can be optimized by using other organoperoxides, which have been found to be more efficient for oxidation by P450s. Nevertheless, the employment of these organoperoxides will generate waste, and it is one of the aspects in cyclohexanol production we try to minimize in order to make the bioreactor a greener alternative. An important improvement may be obtained by genetically engineering the protein to make it more resistant to the hydrogen peroxide oxidant and more active in its presence as well as to broaden the substrate range of the protein that allows for activation of inert carbon hydrogen bonds of different compounds.

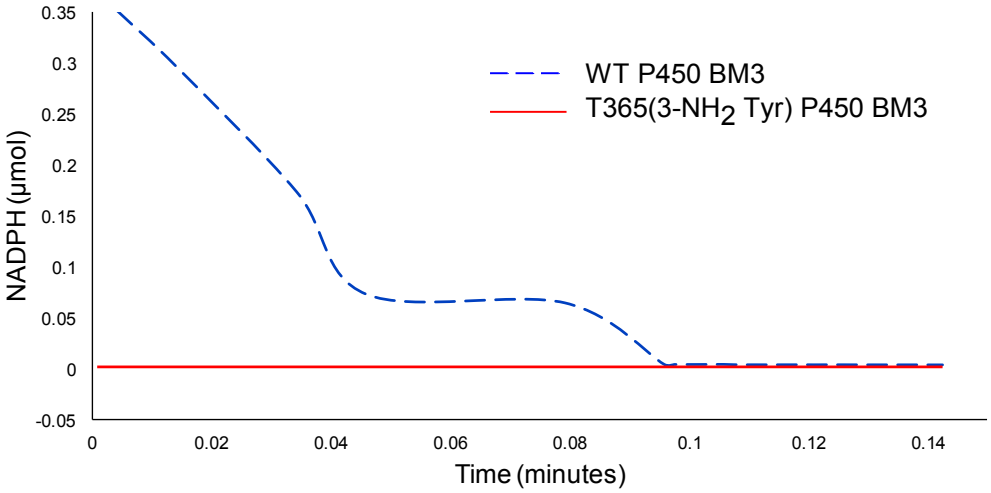


Figure 6-9 NADPH consumption catalyzed by WT P450 BM3 (dashed line) and T365(3-$NH_2$Tyr) P450 BM3 (solid line) during the metabolism of arachidonic acid.

Activity measurement assays for arachidonic acid hydroxylation were carried out to determine the proper monooxygenation functionality of both WT P450 BM3 and the mutant protein. The activity assays were carried out under the normal catalytic pathway of the protein, thereby using NADPH. The catalytic process was monitored using UV-Vis spectrophotometry (Figure 6-9). It can be concluded from the graphs that the catalytic activity of the mutant protein is faster, nevertheless mixing time may be a factor; therefore, the catalytic rates are not conclusive in this case.

## 6.4 Conclusion

Cytochrome P450cam and its reconstituted system showed activity comparable to reported values, while the Q343(3-$NH_2$Tyr) P450cam proteins have shown a four fold increase in the activity towards the natural substrate camphor. In solution, WT P450cam has been successfully used for the conversion of cyclohexane to cyclohexanol in a biphasic system composed of cyclohexane and buffer. In this case the yield of cyclohexanol can be improved by immobilizing the reconstituted system. Since the proteins will be away from the bulk of organic layer of cyclohexane, it reduces the possible denaturation. Thereby, the cyclohexane will diffuse slowly into the aqueous layer where the protein can catalyze the hydroxylation. Silica NPs bound WT P450cam have proved efficient for the oxidation of cyclohexane to give a 30% yield of cyclohexanol via shunt pathway producing water as the only byproduct. Although these results have been obtained in a bench-type reactor, it has the potential to be optimized for large-scale processes rendering the method greener and more efficient than the prevalent industrial ones. In the case of WT P450 BM3, the protein has shown activity comparable to literature values for the oxidation of arachidonic acid, while the T365(3-$NH_2$Tyr) P450 BM3 has shown increased activity towards the same substrate. Nevertheless, as mentioned previously, a different method like rapid scan stopped-flow can be used to accurately determine such fast rates and the real time difference between the activities of the mutant and the WT protein.

(1) Labinger, J. A.; Bercaw, J. E. Understanding and Exploiting C–H Bond Activation. *Nature* **2002**, *417*, 507–514.
(2) Bergman, R. G. C–H Activation. *Nature* **2007**, *446*, 391–393.
(3) Lide, D. R. *CRC Handbook of Chemistry and Physics 2004-2005: A Ready-Reference Book of Chemical and Physical Data*; CRC press, 2004.
(4) Arndtsen, B. A.; Bergman, R. G.; Mobley, T. A.; Peterson, T. H. Selective Intermolecular Carbon-Hydrogen Bond Activation by Synthetic Metal Complexes in Homogeneous Solution. *Accounts Chem. Res.* **1995**, *28*, 154–162.
(5) Chefson, A.; Auclair, K. Progress Towards the Easier Use of P450 Enzymes. *Mol. Biosyst.* **2006**, *2*, 462.
(6) Wencel-Delord, J.; Glorius, F. C–H Bond Activation Enables the Rapid Construction and Late-Stage Diversification of Functional Molecules. *Nat. Chem.* **2013**, *5*, 369–375.
(7) Suresh, A. K.; Sharma, M. M.; Sridhar, T. Engineering Aspects of Industrial Liquid-Phase Air Oxidation of Hydrocarbons. *Ind. Eng. Chem. Res.* **2000**, *39*, 3958–3997.
(8) Thoma, J. A.; Koshland, D. E. Stereochemistry of Enzyme, Substrate, and Products During β-Amylase Action. *J. Biol. Chem.* **1960**, *235*, 2511–2517.
(9) Koshland, D. E. The key–Lock Theory and the Induced Fit Theory. *Angew. Chem. Int. Ed. Engl.* **1995**, *33*, 2375–2378.
(10) Miles, C. S.; Ost, T. W.; Noble, M. A.; Munro, A. W.; Chapman, S. K. Protein Engineering of Cytochromes P-450. *Biochim. Biophys. Acta BBA-Protein Struct. Mol. Enzym.* **2000**, *1543*, 383–407.
(11) Poulos, T. L.; Finzel, B. C.; Howard, A. J. High-Resolution Crystal Structure of Cytochrome P450cam. *J. Mol. Biol.* **1987**, *195*, 687–700.
(12) Katchalski-Katzir, E. Immobilized Enzymes—Learning from Past Successes and Failures. *Trends Biotechnol.* **1993**, *11*, 471–478.
(13) Hill, C., G.; Otero, C.; Garcia, H., S. Immobilized Enzyme Technology. *Encycl. Chem. Process.* 1367–2001.
(14) Proteins at Interfaces II, Copyright, 1995 Advisory Board, Foreword: Fundamentals and Applications. In *Proteins at Interfaces II*; Horbett, T. A.; Brash, J. L., Eds.; American Chemical Society: Washington, DC, 1995; Vol. 602, pp. i–iv.
(15) Nakanishi, K.; Sakiyama, T.; Imamura, K. On the Adsorption of Proteins on Solid Surfaces, a Common but Very Complicated Phenomenon. *J. Biosci. Bioeng.* **2001**, *91*, 233–244.
(16) Wehmeyer, J. L.; Synowicki, R.; Bizios, R.; García, C. D. Dynamic Adsorption of Albumin on Nanostructured TiO2 Thin Films. *Mater. Sci. Eng. C* **2010**, *30*, 277–282.

(17) Norde, W. Driving Forces for Protein Adsorption at Solid Surfaces. In *Macromolecular Symposia*; 1996; Vol. 103, pp. 5–18.
(18) Malmsten, M. Formation of Adsorbed Protein Layers. *J. Colloid Interface Sci.* **1998**, *207*, 186–199.
(19) Haynes, C. A.; Norde, W. Structures and Stabilities of Adsorbed Proteins. *J. Colloid Interface Sci.* **1995**, *169*, 313–328.
(20) Kondo, A.; Fukuda, H. Effects of Adsorption Conditions on Kinetics of Protein Adsorption and Conformational Changes at Ultrafine Silica Particles. *J. Colloid Interface Sci.* **1998**, *198*, 34–41.
(21) Giacomelli, C. E.; Norde, W. The Adsorption–Desorption Cycle. Reversibility of the BSA–Silica System. *J. Colloid Interface Sci.* **2001**, *233*, 234–240.
(22) Santore, M. M.; Wertz, C. F. Protein Spreading Kinetics at Liquid-Solid Interfaces Via an Adsorption Probe Method. *Langmuir* **2005**, *21*, 10172–10178.
(23) Norde, W.; Anusiem, A. C. I. Adsorption, Desorption, and Re-adsorption of Proteins on Solid surfaces. *Colloids Surfaces* **1992**, *66*, 73–80.
(24) Bos, M. A.; Shervanl, Z.; Anusiem, A. C. I.; Giesbers, M.; Norde, W.; Kleijn, J. M. Influence of the Electric Potential of the Interface on the Adsorption of Proteins. *Colloids Surf. B Biointerfaces 3*, 91–100.
(25) Rusmini, F.; Zhong, Z.; Feijen, J. Protein Immobilization Strategies for Protein Biochips. *Biomacromolecules* **2007**, *8*, 1775–1789.
(26) Camarero, J. A. Recent Developments in the Site-specific Immobilization of Proteins onto Solid Supports. *Biopolymers* **2008**, *90*, 450–458.
(27) Gauthier, M. A.; Klok, H.-A. Peptide/protein–Polymer Conjugates: Synthetic Strategies and Design Concepts. *Chem. Commun.* **2008**, 2591.
(28) Köhn, M. Immobilization Strategies for Small Molecule, Peptide and Protein Microarrays. *J. Pept. Sci.* **2009**, *15*, 393–397.
(29) Gerrard, J. A. Protein–Protein Crosslinking in Food: Methods, Consequences, Applications. *Trends Food Sci. Technol.* **2002**, *13*, 391–399.
(30) Heck, T.; Faccio, G.; Richter, M.; Thöny-Meyer, L. Enzyme-catalyzed Protein Crosslinking. *Appl. Microbiol. Biotechnol.* **2012**, *97*, 461–475.
(31) Kluger, R.; Alagic, A. Chemical Cross-linking and Protein–Protein Interactions—a Review with Illustrative Protocols. *Bioorganic Chem.* **2004**, *32*, 451–472.
(32) Migneault, I.; Dartiguenave, C.; Bertrand, M. J.; Waldron, K. C. Glutaraldehyde: Behavior in Aqueous Solution, Reaction with Proteins, and Application to Enzyme Crosslinking. *Biotechniques 37*, 798–802.
(33) Singh, H. Modification of Food Proteins by Covalent Crosslinking. *Trends Food Sci. Technol.* **1991**, *2*, 196–200.

(34) Schilling, B.; Row, R. H.; Gibson, B. W.; Guo, X.; Young, M. M. MS2Assign, Automated Assignment and Nomenclature of Tandem Mass Spectra of Chemically Crosslinked Peptides. *J. Am. Soc. Mass Spectrom.* **2003**, *14*, 834–850.
(35) Hedegaard, J.; Gunsalus, I. C. Mixed Function Oxidation IV. An Induced Methylene Hydroxylase in Camphor Oxidation. *J. Biol. Chem.* **1965**, *240*, 4038–4043.
(36) Katagiri, M.; Ganguli, B. N.; Gunsalus, I. C. A Soluble Cytochrome P-450 Functional in Methylene Hydroxylation. *J. Biol. Chem.* **1968**, *243*, 3543–3546.
(37) Gunsalus, I. C.; Lipscomb, J. D.; Marshall, V.; Frauenfelder, H.; Munck, E.; Greenbaum, E. Structure and Reactions of Oxygenase Active Centres: Cytochrome P-450 and Iron-Sulphur Proteins. *Biochem J* **1971**, *125*, 5P–6P.
(38) Tsai, R.; Gunsalus, I. C.; Dus, K. Composition and Structure of Camphor Hydroxylase Components and Homology Between Putidaredoxin and Adrenoxin. *Biochem. Biophys. Res. Commun.* **1971**, *45*, 1300–1306.
(39) Wang, L.; Magliery, T. J.; Liu, D. R.; Schultz, P. G. A New Functional Suppressor tRNA/Aminoacyl-tRNA Synthetase Pair for the *in Vivo* Incorporation of Unnatural Amino Acids into Proteins. *J. Am. Chem. Soc.* **2000**, *122*, 5010–5011.
(40) Wang, L.; Schultz, P. G. A General Approach for the Generation of Orthogonal tRNAs. *Chem. Biol.* **2001**, *8*, 883–890.
(41) Wang, L.; Brock, A.; Herberich, B.; Schultz, P. G. Expanding the Genetic Code of Escherichia Coli. *Science* **2001**, *292*, 498–500.
(42) Wang, L.; Schultz, P. G. Expanding the Genetic Code. *Chem. Commun.* **2002**, 1–11.
(43) Liu, D. R.; Schultz, P. G. Progress Toward the Evolution of an Organism with an Expanded Genetic Code. *Proc. Natl. Acad. Sci.* **1999**, *96*, 4780–4785.
(44) Moore, B.; Nelson, C. C.; Persson, B. C.; Gesteland, R. F.; Atkins, J. F. Decoding of Tandem Quadruplets by Adjacent tRNAs with Eight-Base Anticodon Loops. *Nucleic Acids Res.* **2000**, *28*, 3615–3624.
(45) Wang, L.; Schultz, P. G. Expanding the Genetic Code. *Angew. Chem. Int. Ed.* **2005**, *44*, 34–66.
(46) Schultz, K. C.; Supekova, L.; Ryu, Y.; Xie, J.; Perera, R.; Schultz, P. G. A Genetically Encoded Infrared Probe. *J. Am. Chem. Soc.* **2006**, *128*, 13984–13985.
(47) Aldag, C.; Gromov, I. A.; García-Rubio, I.; von Koenig, K.; Schlichting, I.; Jaun, B.; Hilvert, D. Probing the Role of the Proximal Heme Ligand in

Cytochrome P450cam by Recombinant Incorporation of Selenocysteine. *Proc. Natl. Acad. Sci.* **2009**, *106*, 5481–5486.
(48) Maurer, S. C.; Schulze, H.; Schmid, R. D.; Urlacher, V. Immobilisation of P450 BM-3 and an NADP+ Cofactor Recycling System: Towards a Technical Application of Heme-Containing Monooxygenases in Fine Chemical Synthesis. *Adv. Synth. Catal.* **2003**, *345*, 802–810.
(49) Dawson, J. H.; Andersson, L.; Sono, M. Spectroscopic Investigations of Ferric Cytochrome P-450-CAM Ligand Complexes. Identification of the Ligand Trans to Cysteinate in the Native Enzyme. *J. Biol. Chem.* **1982**, *257*, 3606–3617.
(50) Girvan, H. M.; Seward, H. E.; Toogood, H. S.; Cheesman, M. R.; Leys, D.; Munro, A. W. Structural and Spectroscopic Characterization of P450 BM3 Mutants with Unprecedented P450 Heme Iron Ligand Sets: New Heme Ligation States Influence Conformational Equilibria in P450 BM3. *J. Biol. Chem.* **2006**, *282*, 564–572.
(51) Laurent, S.; Forge, D.; Port, M.; Roch, A.; Robic, C.; Vander Elst, L.; Muller, R. N. Magnetic Iron Oxide Nanoparticles: Synthesis, Stabilization, Vectorization, Physicochemical Characterizations, and Biological Applications. *Chem. Rev.* **2008**, *108*, 2064–2110.
(52) Lu, A.-H.; Salabas, E. L.; Schüth, F. Magnetic Nanoparticles: Synthesis, Protection, Functionalization, and Application. *Angew. Chem. Int. Ed.* **2007**, *46*, 1222–1244.
(53) Sun, Y.; Ding, X.; Zheng, Z.; Cheng, X.; Hu, X.; Peng, Y. Magnetic Separation of Polymer Hybrid Iron Oxide Nanoparticles Triggered by Temperature. *Chem. Commun.* **2006**, 2765.
(54) Louie, A. Multimodality Imaging Probes: Design and Challenges. *Chem. Rev.* **2010**, *110*, 3146–3195.
(55) Kobayashi, H.; Ogawa, M.; Alford, R.; Choyke, P. L.; Urano, Y. New Strategies for Fluorescent Probe Design in Medical Diagnostic Imaging. *Chem. Rev.* **2010**, *110*, 2620–2640.
(56) Prousek, J. Fenton Chemistry in Biology and Medicine. *Pure Appl. Chem.* **2007**, *79*, 2325–2338.
(57) Sawyer, D. T. Metal [Fe (II), Cu (I), Co (II), Mn (III)]/Hydroperoxide-Induced Activation of Dioxygen ($\cdot O_2 \cdot$) for the Ketonization of Hydrocarbons: Oxygenated Fenton Chemistry. *Coord. Chem. Rev.* **1997**, *165*, 297–313.
(58) Wan, J.; Thomas, M. S.; Guthrie, S.; Vullev, V. I. Surface-Bound Proteins with Preserved Functionality. *Ann. Biomed. Eng.* **2009**, *37*, 1190–1205.
(59) Weetall, H. H. Preparation of Immobilized Proteins Covalently Coupled Through Silane Coupling Agents to Inorganic Supports. *Appl. Biochem. Biotechnol.* **1993**, *41*, 157–188.

(60) Rideout, D. C.; Breslow, R. Hydrophobic Acceleration of Diels-Alder Reactions. *J. Am. Chem. Soc.* **1980**, *102*, 7816–7817.
(61) Razink, J. J.; Schlotter, N. E. Correction to "Preparation of Monodisperse Silica Particles: Control of Size and Mass Fraction" by G.H. Bogush, M.A. Tracy and C.F. Zukoski IV, Journal of Non-Crystalline Solids 104 (1988) 95–106. *J. Non-Cryst. Solids* **2007**, *353*, 2932–2933.
(62) Aslam, M.; Fu, L.; Li, S.; Dravid, V. P. Silica Encapsulation and Magnetic Properties of FePt Nanoparticles. *J. Colloid Interface Sci.* **2005**, *290*, 444–449.
(63) Phon, R. T. Solid-Phase Supports for Oligonucleotide Synthesis. In *Methods in Molecular Biology*; Humana Press Inc: Totowa NJ, 1993; Vol. 20, pp. 465–496.
(64) Hiramatsu, H.; Osterloh, F. E. pH-Controlled Assembly and Disassembly of Electrostatically Linked CdSe−$SiO_2$ and Au−$SiO_2$ Nanoparticle Clusters. *Langmuir* **2003**, *19*, 7003–7011.
(65) Beier, M.; Hoheisel, J. D. Derivatization of Glass and Polypropylene Surfaces. *Curr. Protoc. Nucleic Acid Chem.* **2004**, 12–4.
(66) Hoare, D. G.; Koshland Jr, D. E. A Procedure for the Selective Modification of Carboxyl Groups in Proteins. *J. Am. Chem. Soc.* **1966**, *88*, 2057–2058.
(67) Hoare, D. t; Koshland, D. E. A Method for the Quantitative Modification and Estimation of Carboxylic Acid Groups in Proteins. *J. Biol. Chem.* **1967**, *242*, 2447–2453.
(68) Ray, S.; Chand, S.; Zhang, Y.; Nussbaum, S.; Rajeshwar, K.; Perera, R. Implications of Active Site Orientation in Myoglobin for Direct Electron Transfer and Electrocatalysis Based on Monolayer and Multilayer Covalent Immobilization on Gold Electrodes. *Electrochimica Acta* **2013**, *99*, 85–93.
(69) Hooker, J. M.; Kovacs, E. W.; Francis, M. B. Interior Surface Modification of Bacteriophage MS2. *J. Am. Chem. Soc.* **2004**, *126*, 3718–3719.
(70) Clamp, J. R.; Hough, L. The periodate Oxidation of Amino Acids with Reference to Studies on Glycoproteins. *Biochem J* **1965**, *94*, 17–24.
(71) Willard, J. J. Structure of the Carbohydrate Moiety of Orosomucoid. *Nature* **1962**, 1278.
(72) Eylar, E. H.; Jeanloz, R. W. Periodate Oxidation of the α1 Acid Glycoprotein of Human Plasma. *J. Biol. Chem 237*, 1021–1025.
(73) Eylar, E. H.; Jeanloz, R. W. Sequential Periodate Oxidation of the α1-Acid Glycoprotein of Human Plasma. *Biochemistry (Mosc.)* **1966**, *5*, 253–258.
(74) Krotoski, W. A.; Weimer, H. E. Peptide-Associated and Antigenic Changes Accompanying Periodic Acid Oxidation of Human Plasma Orosomucoid. *Arch. Biochem. Biophys.* **1966**, *115*, 337–344.

(75) Geoghegan, K. F.; Stroh, J. G. Site-directed Conjugation of Nonpeptide Groups to Peptides and Proteins via Periodate Oxidation of a 2-Amino Alcohol. Application to Modification at N-terminal Serine. *Bioconjug. Chem.* **1992**, *3*, 138–146.
(76) Burdine, L.; Gillette, T. G.; Lin, H.-J.; Kodadek, T. Periodate-Triggered Cross-Linking of DOPA-Containing Peptide−Protein Complexes. *J. Am. Chem. Soc.* **2004**, *126*, 11442–11443.
(77) Liu, B.; Burdine, L.; Kodadek, T. Chemistry of Periodate-Mediated Cross-Linking of 3,4-Dihydroxylphenylalanine-Containing Molecules to Proteins. *J. Am. Chem. Soc.* **2006**, *128*, 15228–15235.
(78) Latham, A. H.; Williams, M. E. Versatile Routes Toward Functional, Water-Soluble Nanoparticles via Trifluoroethylester−PEG−Thiol Ligands. *Langmuir* **2006**, *22*, 4319–4326.
(79) Pale-Grosdemange, C.; Simon, E. S.; Prime, K. L.; Whitesides, G. M. Formation of Self-Assembled Monolayers by Chemisorption of Derivatives of Oligo(Ethylene Glycol) of Structure HS $(CH_2)_{11}$ $(OCH_2CH_2)_mOH$ on Gold. *J. Am. Chem. Soc.* **1991**, *113*, 12–20.
(80) Prime, K. L.; Whitesides, G. M. Adsorption of Proteins onto Surfaces Containing End-Attached Oligo(Ethylene Oxide): a Model System using Self-Assembled Monolayers. *J. Am. Chem. Soc.* **1993**, *115*, 10714–10721.
(81) Elbert, D. L.; Hubbell, J. A. Surface Treatments of Polymers for Biocompatibility. *Annu. Rev. Mater. Sci.* **1996**, *26*, 365–294.
(82) Timkovich, R. Detection of the Stable Addition of Carbodiimide to Proteins. *Anal. Biochem.* **1977**, *79*, 135–143.
(83) Tengvall, P.; Jansson, E.; Askendal, A.; Thomsen, P.; Gretzer, C. Preparation of Multilayer Plasma Protein Films on Silicon by EDC/NHS Coupling Chemistry. *Colloids Surf. B Biointerfaces* **2003**, *28*, 261–272.
(84) Thakur, G.; Prashanthi, K.; Thundat, T. Directed Self-Assembly of Proteins into Discrete Radial Patterns. *Sci. Reports* **2013**, *3*.
(85) Sono, M.; Roach, M. P.; Coulter, E. D.; Dawson, J. H. Heme-Containing Oxygenases. *Chem. Rev.* **1996**, *96*, 2841–2888.
(86) Murgida, D. H.; Hildebrandt, P. Heterogeneous Electron Transfer of Cytochrome *c* on Coated Silver Electrodes. Electric Field Effects on Structure and Redox Potential. *J. Phys. Chem. B* **2001**, *105*, 1578–1586.
(87) Todorovic, S.; Jung, C.; Hildebrandt, P.; Murgida, D. H. Conformational Transitions and Redox Potential Shifts of Cytochrome P450 Induced by Immobilization. *JBIC J. Biol. Inorg. Chem.* **2005**, *11*, 119–127.
(88) Schneider, E.; Clark, D. S. Cytochrome P450 (CYP) Enzymes and the Development of CYP Biosensors. *Biosens. Bioelectron.* **2013**, *39*, 1–13.

(89) Tyson, C. A.; Lipscomb, J. D.; Gunsalus, I. C. The Roles of Putidaredoxin and P450cam in Methylene Hydroxylation. *J. Biol. Chem.* **1972**, *247*, 5777–5784.
(90) Tyson, C. A.; Lipscomb, J. D.; Gunsalus, I. C. The Roles of Putidaredoxin and P450cam in Methylene Hydroxylation. *J. Biol. Chem.* **1972**, *247*, 5777–5784.
(91) Pochapsky, S. S.; Pochapsky, T. C.; Wei, J. W. A Model for Effector Activity in a Highly Specific Biological Electron Transfer Complex: The Cytochrome P450cam-Putidaredoxin Couple. *Biochemistry (Mosc.)* **2003**, *42*, 5649–5656.
(92) Gillam, E. M. J. Engineering Cytochrome P450 Enzymes. *Chem. Res. Toxicol.* **2008**, *21*, 220–231.
(93) Mansuy, D. The Great Diversity of Reactions Catalyzed by Cytochromes P450. *Comp. Biochem. Physiol. C Pharmacol. Toxicol. Endocrinol.* **1998**, *121*, 5–14.
(94) Kadkhodayan, S.; Coulter, E. D.; Maryniak, D. M.; Bryson, T. A.; Dawson, J. H. Uncoupling Oxygen Transfer and Electron Transfer in the Oxygenation of Camphor Analogues by Cytochrome P450-cam Direct Observation of an Intermolecular Isotope Effect for Substrate CH Activation. *J. Biol. Chem.* **1995**, *270*, 28042–28048.
(95) Unno, M.; Shimada, H.; Toba, Y.; Makino, R.; Ishimura, Y. Role of Arg112 of Cytochrome P450cam in the Electron Transfer from Reduced Putidaredoxin Analyses with Site-Directed Mutants. *J. Biol. Chem.* **1996**, *271*, 17869–17874.
(96) Stayton, P. S.; Sligar, S. G. Cytochrome P-450cam Binding Surface Defined by Site-Directed Mutagenesis and Electrostatic Modeling. *Biochemistry (Mosc.)* **1990**, *29*, 7381–7386.
(97) Maurer, S. C.; Kühnel, K.; Kaysser, L. A.; Eiben, S.; Schmid, R. D.; Urlacher, V. B. Catalytic Hydroxylation in Biphasic Systems using CYP102A1 Mutants. *Adv. Synth. Catal.* **2005**, *347*, 1090–1098.

## Biographical Information

Leticia Loredo was born in Mexico, D.F. She received her Bachelor's degree in Biochemistry at the University of Texas at Arlington. In 2008 she continued at the University of Texas at Arlington for her doctoral of philosophy in chemistry under the supervision of Dr. Roshan Perera. Her main project was based on the development of CYP protein microarrays and their biotechnological applications.